Design of an Energy Recovery Concept for a Small-scale Renewable-driven Reverse Osmosis Desalination System

Faculty of Applied Sciences
MSc Sustainable Energy Technology

Master of Science Thesis

Dimitrios Michas

October 2013

TU Delft Delft University of Technology

Challenge the future

Design of an Energy Recovery Concept for a Small-scale Renewable-driven Reverse Osmosis Desalination System

THESIS

submitted in partial fulfilment of the requirements for the degree of

MASTER OF SCIENCE
in
SUSTAINABLE ENERGY TECHNOLOGY

by

Dimitrios Michas
born in Athens, Greece

Committee members
Responsible instructor: Prof.dr.ir. B.J. Boersma, 3mE, TU Delft
Second reviewer: Prof.dr.ir. C.A. Infante Ferreira, 3mE, TU Delft
Third reviewer: Dr.ir H. Spanjers, CEG, TU Delft
External supervisor: R. Feenstra, MSc., Elemental Water Makers B.V.

E.T. number: 2599

Energy Technology Section
Process & Energy Department
Faculty Mechanical, Maritime and Materials Engineering
Delft University of Technology

Acknowledgments

I would like to express my gratitude to those who contributed to the completion of this thesis. First, I would like to thank my supervisor Dr. B.J. Boersma for his constructive comments and guidance throughout this project. My gratitude also goes to the reviewers of my thesis, Dr. C.A. Infante Ferreira and Dr. H. Spanjers.

In addition, I would like to thank R. Feenstra and S. Vollebregt from Elemental Water Makers for their valuable feedback and support throughout the project, as well as for giving me the opportunity to work on an interesting and challenging research topic and collaborate in an inspiring environment.

Last but not least, I would like to thank my parents for their support throughout my studies.

Dimitrios Michas
October 20, 2013
Delft, The Netherlands

Executive Summary

The desalination industry has grown exponentially the last four decades as countries seek solutions to water scarcity caused by population growth, climate change, pollution and industrial development. All source water types included, reverse osmosis is the prevalent desalination process, accounting for more than half of the global capacity. However, reverse osmosis desalination is an energy intensive process. The energy demand and, hence, the cost of reverse osmosis systems can be significantly reduced by using energy recovery. In addition, renewable energy is incorporated at newly developed systems aiming at reducing the environmental impact of the process.

In the context of this thesis, an efficient energy recovery concept for a small-scale autonomous renewable-driven reverse osmosis desalination system is designed. First, the energy recovery technologies currently available on the market and their characteristics have been identified. Taking into account the constraints defined by the examined desalination system, five energy recovery designs have been suggested. The proposed energy recovery concepts are Pelton-driven generator with centrifugal pump or piston pump, Pelton-driven centrifugal pump or piston pump with gearbox, optimized pressure exchanger with two combined double acting cylinders, optimized pressure exchanger with three combined double acting cylinders and APM-driven piston pump. Their evaluation was based on energy efficiency, power and pressure requirements, energy autonomy, operational stability, cost effectiveness and manufacturing complexity for the examined operating range and revealed that the optimised pressure exchanger with two combined double-acting cylinders is the most applicable energy recovery concept for the examined desalination system.

In order to deliver the required power output, the optimised pressure exchanger with two combined double-acting cylinders is scaled accordingly for the examined flow rates. In addition, the proposed switching mechanism of the energy recovery device (ERD) involves the use the feed stream through grooves within the rod and the centre block of the ERD in order to direct the brine stream to the required cylinder.

In more detail, the optimised pressure exchanger with two combined double-acting cylinders is the most efficient energy recovery concept, for both brackish and seawater desalination and for all examined flow rates, delivering significantly high for all cases of the examined operational range.

As a result of the high efficiency provided, the optimised pressure exchanger with two combined double-acting cylinders requires the lowest inlet feed pressure for both brackish and seawater desalination and all examined flow rates among the suggested ERDs.

In terms of energy autonomy, pressure exchangers rely on the principle of positive displacement and therefore provide constant recovery ratio and do not require additional energy. However, additional power supply may be required in order to control electronically the switching of the ERD in case the suggested mechanical switching proves to be inefficient.

Regarding the operational stability, the recovery ratio is fixed, the operation of the ERD is self-regulated and only in case leakage or switching problems occur external steering of the operation and, hence, additional power supply may be needed.

Due to the scale up of the optimised pressure exchanger with two combined double-acting cylinders required for high feed flow rates its price exceeds the price of the other ERDs, especially for seawater desalination, while for brackish water desalination and especially for low flow rate it remains competitive. Finally, the optimised pressure exchangers require the manufacturing and assembly of resized components which may be more complex and time consuming than the assembly of the main components required for the other ERDs.

Table of Contents

List of Figures

List of Tables

1. Introduction

The desalination industry has grown exponentially the last four decades as countries seek solutions to water scarcity caused by population growth, climate change, pollution and industrial development. According to the International Desalination Association (IDA), the worldwide installed capacity has grown at a compound average rate of 12.3% per year over the past 5 years and the rate of capacity growth is expected to increase even further (Figure 1). The worldwide installed capacity has reached 66.5 million cubic meters per day in 2011 and is expected to reach 120 Mm^3/day by 2020 (IDA, 2012).

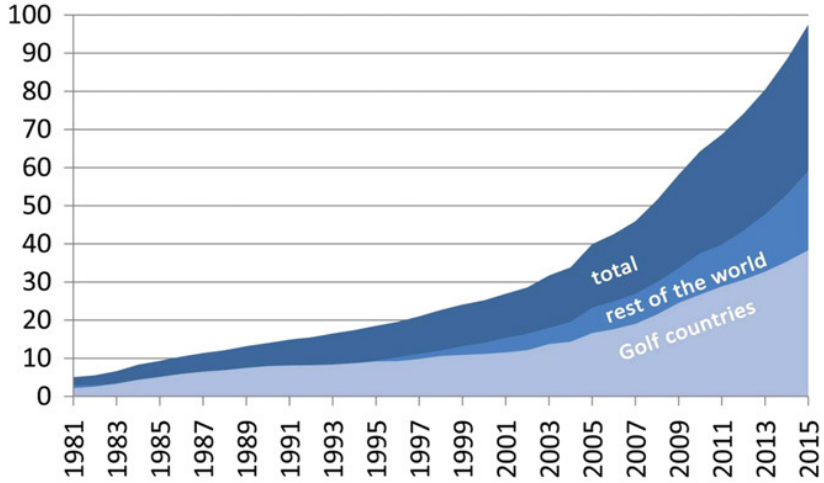

Figure 1: Projected growth of the desalination market in million cubic meters per day (including seawater, brackish water, river water, wastewater, brine, and pure water desalination processes) (Lattemann, et al., 2010)

Much of the expected growth of the desalination market will take place in the seawater sector, although brackish water and wastewater desalination processes will presumably become more important in the future. Only 5% of the total capacity of 68 Mm^3/day comes from wastewater sources, 19% is produced from brackish water sources, and 63% from seawater (Lattemann, et al., 2010).

All source water types included, reverse osmosis is the prevalent desalination process, accounting for more than half of the global capacity. Currently, reverse osmosis (RO) accounts for nearly 60% of installed capacity, followed by the thermal processes multi-stage flash (MSF) at 26% and multi-effect distillation (MED) at 8.2%. Other processes include electrodialysis (ED) at 3.4%, hybrid technologies combining membrane and thermal processes at 0.7%, and electrodeionization (EDI) at 0.4%.

In terms of regional distribution of the desalination capacity, 48% of the global desalination production takes place in the Middle East, mainly in the Gulf country states, 19% of the desalinated water is produced in Americas, 14% in Europe, 14% in the Asia-Pacific region and 6% in Africa (Figure 2). Seawater desalination is the prevalent process in all regions except for North America, where brackish water desalination is the dominating process.

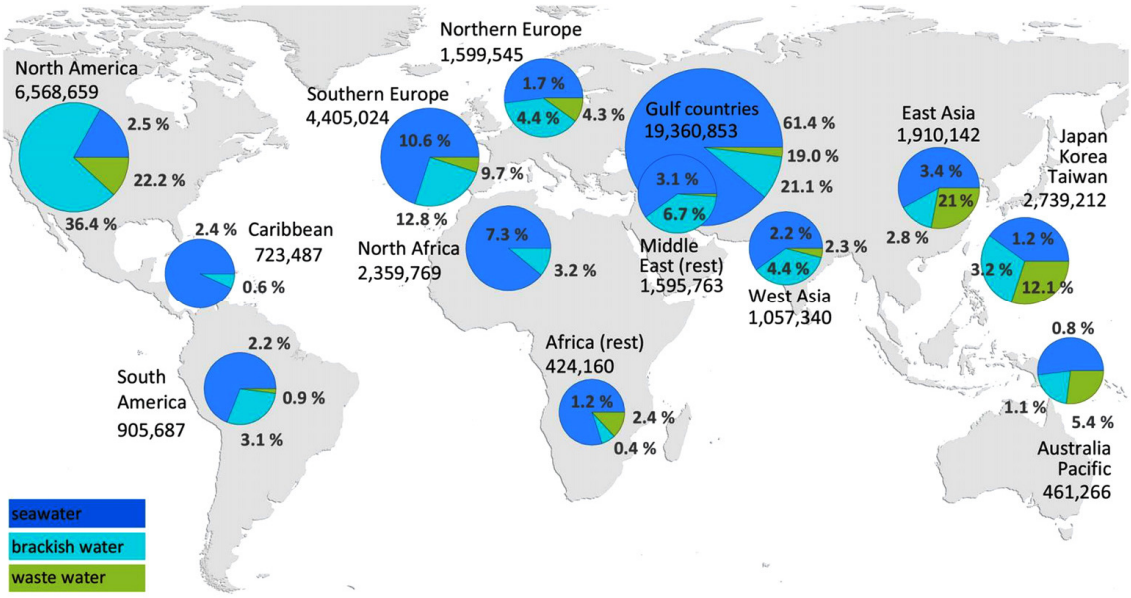

Figure 2: Global desalination capacities in cubic meters per day (Lattemann, et al., 2010)

Developments in desalination technologies are specifically aimed at reducing energy consumption and cost, as well as minimizing environmental impacts. Renewable energy is incorporated at newly developed systems.

The costs of RO desalination can be high because of its intensive use of energy (Al-Karaghouli, et al., 2009). The energy demand of RO systems depends on the process design and equipment used. The use of energy recovery can significantly reduce the specific energy demand of the system (kWh/m^3). While RO systems without energy recovery require about 5 kWh/m^3, RO systems with energy recovery achieve a total energy demand of 3–4 kWh/m^3.

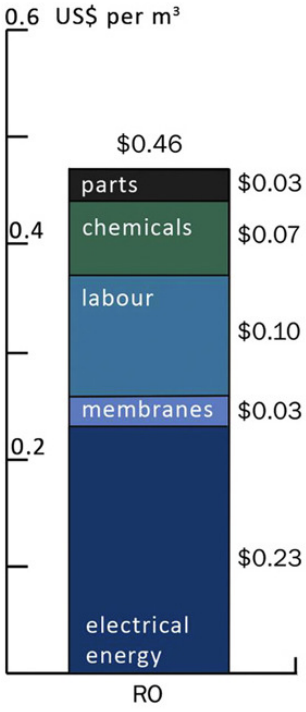

Figure 3: Operation costs in US$ of reverse osmosis (RO) desalination process (Lattemann, et al., 2010)

1.1. Research objective

The aim of this project is to design an efficient energy recovery concept for a small-scale autonomous renewable-driven reverse osmosis desalination system. To tackle this problem, the following subquestions are examined:

1. Which are the energy recovery technologies currently available and what are their characteristics?
2. Which are the constraints set by the examined renewable-driven RO desalination system and which energy recovery technologies meet these requirements?
3. Which energy recovery concepts are suggested for these requirements and how do they comply with the criteria set?
4. Which is the most applicable energy recovery concept according to the criteria set?

Thus, in Chapter 2, the theoretical background required for the study of energy recovery technologies is explained. In Chapter 3, the energy recovery technologies currently available are analysed based on their characteristics. In Chapter 4, the constraints defined by the examined RO desalination system are described and the energy recovery technologies that meet these requirements are listed. In Chapter 5, energy recovery concepts applicable for the examined RO system are designed. Based on the criteria set, the energy recovery concepts are evaluated. In Chapter 6, the energy recovery concept that fulfils most adequately the criteria set is selected. In Chapters 7 and 8, conclusions and recommendations are drawn.

2. Theoretical background

In this chapter the theoretical background required for the study and the evaluation of energy recovery technologies used in RO desalination systems is provided.

2.1. Water Salinity

Desalination refers to the physical separation of salts and water in a saline solution to produce freshwater (Contreras, 2009). In the desalination field water is classified according to its salinity. Salinity refers to the concentration of dissolved salts in water. It is defined by total dissolved solids (TDS) measured in mg/L or parts per million (ppm). Based on salinity measured by TDS, water is classified into three groups: Fresh water contains less than 1,000 mg/L, brackish water between 1,000 and 25,000 mg/L and seawater consists of more than 25,000 mg/L. Most of the brackish water available on earth has salinity up to 10,000 mg/L, whereas seawater normally has salinity in the range of 35,000-45,000 mg/l in the form of TDS (Gkeredaki, 2011).

2.2. Reverse Osmosis Desalination Process

Osmosis is a physical process that occurs when two solutions of different concentrations are separated by a semi-permeable membrane (Figure 4a). During osmosis, the tendency of the system is to reach equilibrium by equalising the concentration of the two solutions. Thus, the less saline solution flows towards the more saline solution, through the membrane, until the hydrostatic pressure difference developed due to volume difference equals to the osmotic pressure of the more saline solution and equilibrium is reached (Figure 4b).

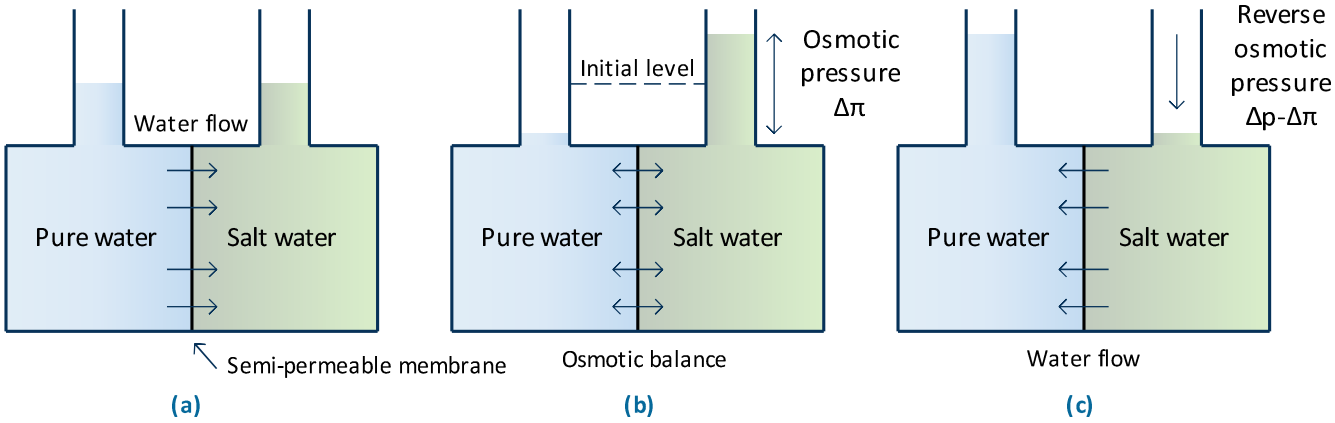

Figure 4: Osmosis and Reverse Osmosis Process

Reverse osmosis (RO) is the opposite process, where the pressure applied must exceed the osmotic pressure in order to push the more saline solution through the membrane (Figure 4c). Thus, the energy required for the separation of salts and water is supplied in the form of pressure. RO desalination is most commonly applied elements of membranes in spiral wound configuration (Figure 5). In order to withstand the high operating pressures, pressure

vessels (membrane modules) are used. Typically, one pressure vessel contains six membrane elements (Verberk, et al., 2009).

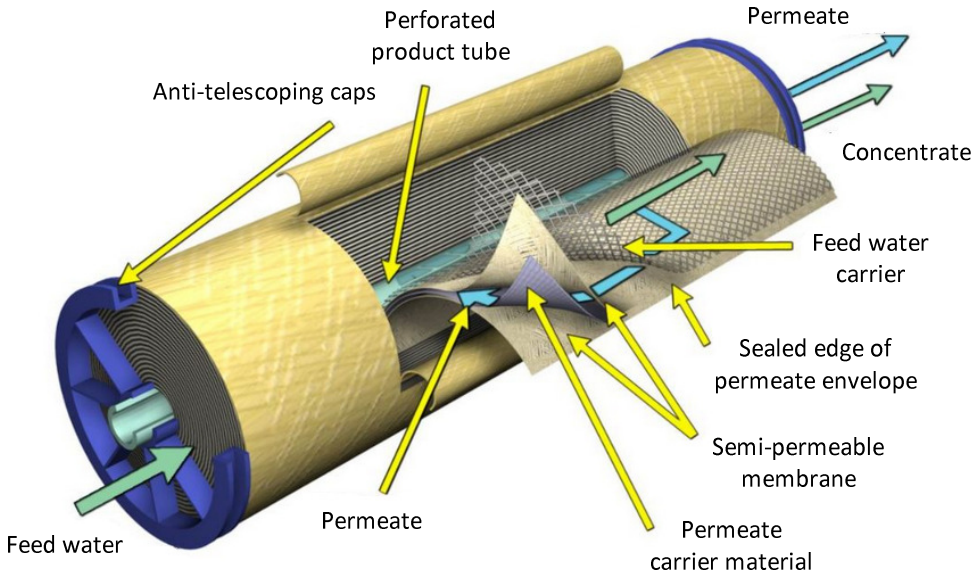

Figure 5: Spiral wound element design

RO membranes allow the passage of water but reject salts and all particulate and colloidal matter, bacteria, viruses and dissolved organic matter (Contreras, 2009). In order to prevent the accumulation of salts on the membrane surface, RO process is a cross-flow filtration during which part of the feed flow is used to remove salts from the membrane. This part of the feed flow is called concentrate, reject or brine stream, while the amount recovered to freshwater is referred to as permeate or product flow (Figure 6).

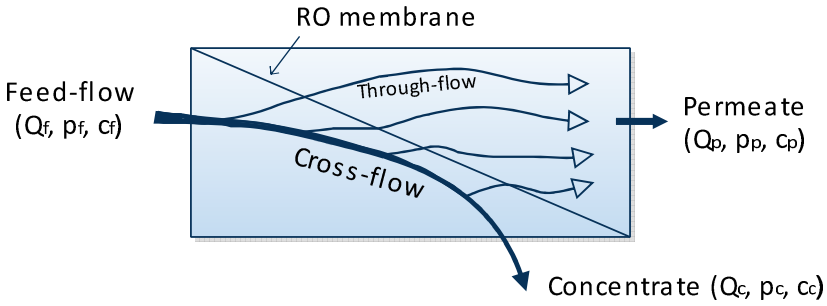

Figure 6: Reverse Osmosis Schematic

According to the mass balance for water: $$Q_f = Q_p + Q_c$$ **[1]**

Where Q_f is the flow rate of the feed flow, Q_p is the flow rate of the permeate and Q_c is the flow rate of the concentrate. The ratio between the permeate flow rate (Q_p) and the feed flow rate (Q_f) is defined as recovery ratio (RR) (Contreras, 2009):

$$RR = Q_p/Q_f$$ **[2]**

The mass balance for salt delivers: $$Q_f \cdot c_f = Q_p \cdot c_p + Q_c \cdot c_c$$ **[3]**

Where c_f is the salt concentration of the feed flow, c_p is the salt concentration of the permeate and c_c is the salt concentration of the concentrate.

By assuming $c_p \approx 0$ and using equation 2 and 3 we get: $c_c = c_f/(1 - RR)$ **[4]**

According to equation 4, for recovery ratio of 80%, the concentrate is 5 times more concentrated compared to the feed flow. Therefore, a low recovery ratio is very important to prevent scaling (Heijman, et al., 2010).

In addition, retention is calculated: $Ret = 1 - c_p/c_f$ **[5]**

Furthermore, since RO membranes are not ideal, they present some resistance to the water flowing through them. As a result, apart from the energy required for the separation of water and salt, additional pressure is needed to force water trough the membranes. The flow of water is proportional to the net pressure applied above the osmotic pressure:

$$Q_p = K_w \cdot A_m \cdot [(p_f - p_p) - (\pi_{avg} - \pi_p)] \quad \textbf{[6]}$$

where K_w is the water permeability coefficient of the membrane, A_m is the area of the membrane, Pf and Pp are the feed flow and permeate pressures, respectively, π_{avg} is the osmotic pressure in the feed-brine channel, and π_p is the osmotic pressure of the permeate. The term in square brackets is known as the net driving pressure (Figure 4c).

Equation 6 shows that increasing the feed pressure would result in higher product flow rate and, hence, higher recovery ratios. However, the relationship between the applied pressure and the recovery ratio is not straightforward since increasing the recovery ratio increases the concentration of the brine, and hence its osmotic pressure, affecting also the net driving pressure (Contreras, 2009).

A typical configuration of RO desalination system includes a high pressure pump which provides feed water with the required pressure for the RO process and the pressure vessels which include the RO membranes. As already described part of the feed flow is going to the permeate flow and the remaining to the concentrate flow, while a regulated valve is used in order to control the concentrate flow.

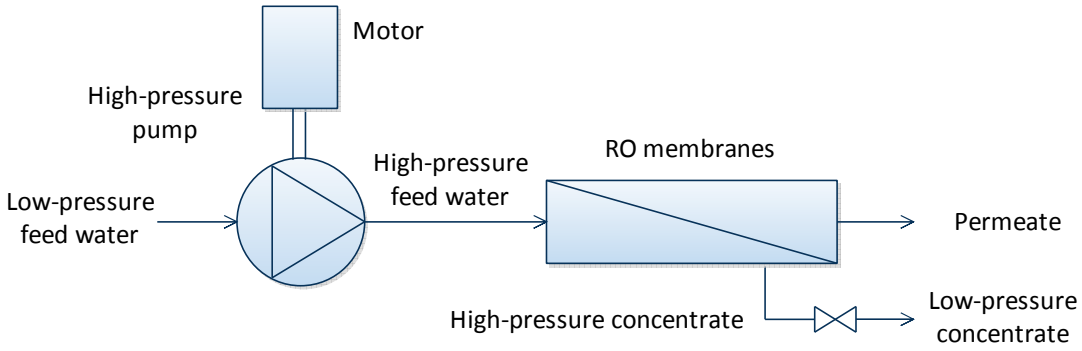

Figure 7: RO desalination system

2.3. Energy recovery Process

The pressure drop across the feed-brine channel of the RO membranes is small (up to 2 bar). Thus, depending on the recovery ratio, concentrate stream carries a large share of the energy in feed flow. Recycling this energy back into the process improves the overall efficiency of the operation. The recovery of energy in RO desalination systems is a major factor in the reduction of the energy consumption of the system and the cost of desalinated

water. Amongst the mainstream seawater desalination technologies, reverse osmosis with energy recovery has the lowest energy requirements per unit of freshwater produced (El-Dessouky, et al., 2002). This energy is known as the specific energy consumption (SEC) and is used to measure the efficiency of RO operations (Contreras, 2009).

The operating pressure for brackish water RO desalination ranges from 10-30 bar, while for seawater from 40-80 bar (Charcosset, 2009). For brackish water desalination the recovery ratio can reach the value of 95%, while for seawater the maximum value is about 50% due to the possibility of scaling, caused by high salt concentrations (Verberk, et al., 2009). Due to high recovery ratios and low pressures observed in brackish water RO desalination systems, the amount of energy that can be recovered is much less than in seawater systems and thus energy recovery is rarely used (Contreras, 2009).

3. Energy recovery technologies

In Chapter 3 the energy recovery technologies developed for RO desalination are presented and evaluated according to their characteristics.

The energy recovery is conducted through a mechanical system, which intensifies the feed pressure of the RO process by recycling the energy found in the waste stream of the RO process. This system is called energy recovery device (ERD). Currently several approaches of ERDs exist, depending on the scale and the capacity of the RO system. Subsequently, energy recovery devices are classified according to their working principle and each type is described. Examples for each technology, available on the market, are identified.

3.1. Centrifugal Energy Recovery Devices

Centrifugal ERDs convert the hydraulic energy found in the concentrate stream into rotational energy using a turbine, which either serves as a shaft assist mechanism for the main high-pressure pump of the desalination system or is directly coupled to a centrifugal pump (MacHarg, 2002). Thus, centrifugal ERDs can be classified as hydraulic to mechanical-assisted pumping and hydraulically driven pumping in series (Guirguis, 2011).

3.1.1. Hydraulic to mechanical-assisted pumping

In this configuration, the turbine is coupled to the main high-pressure pump that supplies the feed water to the RO membranes (Figure 8). The energy required by the high pressure pump is provided by the motor and the turbine, which is applied as an add-on package in the form of a shaft assist mechanism (MacHarg, 2002).

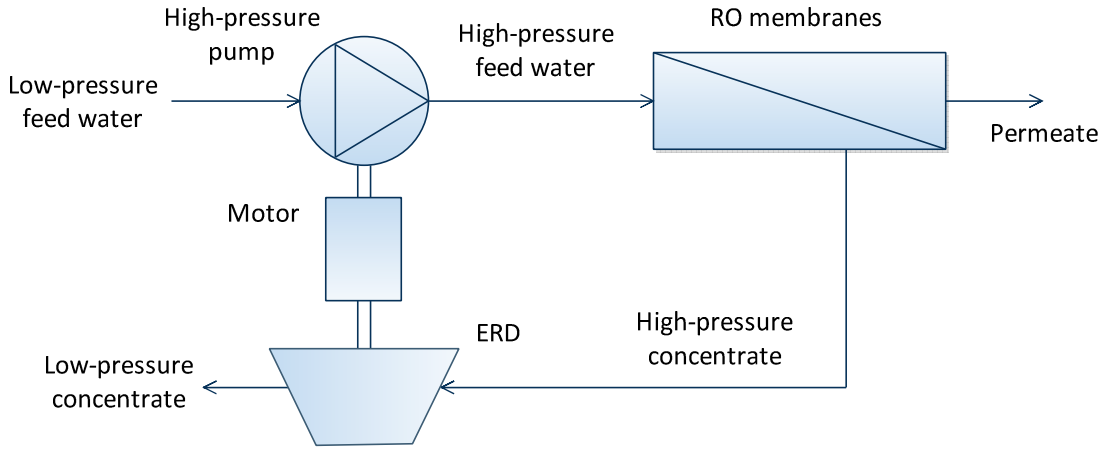

Figure 8: RO desalination system including turbine-driven shaft assist mechanism

Francis turbines and Pelton turbines are typically used for this type of configuration. The configuration operates at its peak efficiency in a narrow range of pressure and flow (Contreras, 2009).

Francis turbine, also known as reverse running pump, was the first turbine to be employed in seawater RO municipal scale desalination plants. Francis turbines recover the hydraulic energy from the brine stream which is then mechanically transferred to the main feed pump

motor. In most applications of Francis turbines the turbine drives an alternator and its speed must be maintained constant (Figure 9). Other installations involve a clutch between the turbine and a pump.

Figure 9: Francis turbine with generator (Guirguis, 2011)

Francis turbines are reaction turbines. The flow path followed is from a radial direction to an axial direction. Water enters via a spiral casing; called volute or scroll, which surrounds the runner (Figure 10); at pressure higher than the atmospheric pressure and reaches the turbine blades containing kinetic energy and pressure energy, which the turbine then transforms into mechanical energy. The area of cross-section of the volute decreases along the flow path in such a way that the flow velocity remains constant. From the volute the flow enters a ring of stationary guide vanes which direct it onto the runner at the most appropriate angle, depending on the energy requirements. Different shaft speeds can be obtained for specific head and flow, depending on the design of the blades (Rodriguez, et al., 2011).

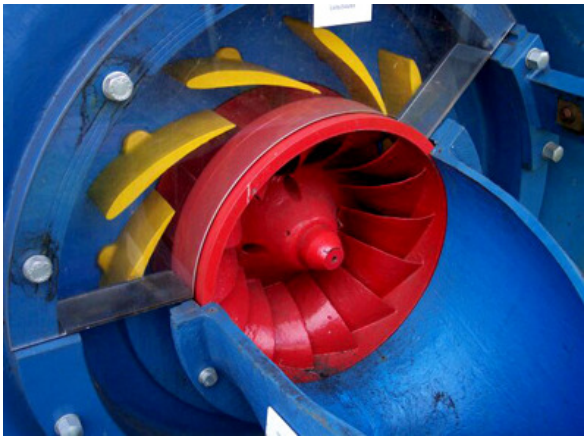

Figure 10: Horizontal axis Francis turbine

Francis turbines handle high to medium flow and low to medium head (<650 m), which can be expressed in pressure (<64 bar) using the following equation:

$$H = p/\gamma \qquad [7]$$

The earliest identified disadvantage of Francis Turbines was that the flow range and pressure required for achieving maximum efficiency of operation was narrow and limited. In addition, these energy recovery devices did not generate energy until the design condition reached about 40% (Farooque, et al., 2008). They are also difficult to control and pose a significant challenge in maintenance. Francis turbines are sized to specific characteristics and the flow or pressure changes need to be bypassed resulting to losses in their efficiency. Furthermore, operation at part load causes a whirl velocity component to be set up downstream of the runner, resulting to reduced efficiency. The strength of the vortex can be such that cavitation can occur along the axis of the draft tube. Manufacturers of Francis turbines are Sulzer Ltd. (Sulzer Ltd., 2013), Wasserkraft Volk AG (Wasserkraft Volk AG, 2010) and Tamar (Tamar, 2012).

The overall efficiency of the energy recovery system including a turbine coupled to the main high pressure pump can be quantified as the hydraulic energy out minus the motor shaft power in all divided by the hydraulic energy in (MacHarg, 2002). For the Francis turbine, the efficiency can reach 69%.

In case of a Francis-driven generator which supplies electricity to the motor of the pump the overall efficiency is calculated as the product of the efficiency of the Francis turbine, the efficiency of the alternator and the efficiency of the motor and the pump. The maximum overall efficiency of the Francis turbine is 75%-80% (Guirguis, 2011). Peak efficiencies of alternators at full output vary from 55% to almost 80% (Bradfield, 2008). The efficiency of the motor is assumed to be 94% (at feed flow of 20 m^3/h). The peak efficiency of the pump, achieved at specific speed of 3000 and flow rate greater than 2,300 m^3/h (10,000 gpm), is 89% (Stover, 2006). Thus, the peak overall efficiency of the Francis-driven generator energy recovery system is estimated:

$$\eta_{\text{Francis}} = 80\% \cdot 80\% \cdot 94\% \cdot 89\% = 53\% \qquad \textbf{[8]}$$

Pelton turbines replaced Francis turbines used for RO desalination applications, in 1980s, due to their higher efficiency (Stover, 2007). The Pelton turbine recovery system includes a tangential flow impulse turbine that converts the hydraulic energy of the concentrate stream into rotary power. The concentrate stream is directed to the centre of the blades (spoon-shaped buckets) mounted around the circular disc through one or more nozzles that convert the kinetic energy of the water into mechanical energy. Each bucket splits the oncoming jet into two equal streams, using the ridge at its centre and reverses their flow, leaving them with diminished energy. The resulting impulse produces the required torque in order to spin the turbine. The buckets are mounted in pairs to keep the forces on the wheel balanced as well as to ensure smooth, efficient momentum transfer of the fluid jet to the wheel.

Since the Pelton turbine is an impulse turbine the shaft speed depends only on the diameter of the wheel and the head delivered to the nozzle.

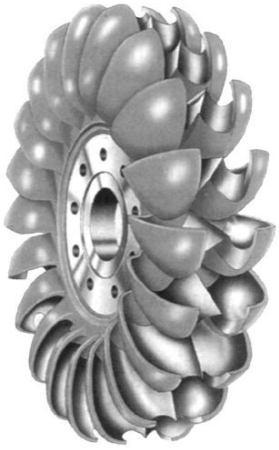

Figure 11: Pelton turbine runner (Dixon, 2005)

Pelton turbines are preferred because of their familiarity, proven liability, ease in operation and low capital cost (Stover, 2006). Unlike the majority of models, Pelton turbines are characterised for their high efficiency when working with partial flows. Over a large range of loading (20% up to 100%), Pelton turbines deliver almost constant overall efficiency as a result of the hydraulic losses reducing in proportion to the power output (Dixon, 2005). A disadvantage of Pelton turbines is the formation of a foamy stream that can only be evacuated by gravity, or re-pumped after it has settled (Liberman, 2010).

Pelton turbines are designed for high to medium head and low to medium flow rate. Thus, Pelton turbines are preferred when the available water source has relatively high hydraulic head at low flow rates, where the Pelton wheel is most efficient. More power can be extracted from a water source with high-pressure and low-flow than from a source with low-pressure and high-flow, even when the two flows theoretically contain the same power. Depending on water flow and design, Pelton wheels operate best with heads from 15 meters to 1,800 meters, although there is no theoretical limit. Using equation 7 and the specific weight of water $\gamma = 9.8\ \mathrm{kN/m^3}$, the brine pressure required is calculated 1.47-176.4 bar.

The overall efficiency of the energy recovery system including a Pelton turbine coupled to the main high pressure pump, taking into account the shaft power provided by the motor, can reach 76%.

In case of a Pelton-driven generator which supplies electricity to the motor of the pump the overall efficiency is calculated as in equation 8. The maximum overall efficiency of the Pelton turbine is 80%-85% (Guirguis, 2011), hence the efficiency is calculated:

$$\eta_{\mathrm{Pelton}} = 85\% \cdot 80\% \cdot 94\% \cdot 89\% = 57\% \qquad \textbf{[9]}$$

Manufacturers of Pelton-driven shaft assist mechanisms include Calder (ERT), Sulzer Ltd. (TUP). Energy Recovery Turbine (ERT), developed by Calder, consists of Pelton turbine coupled to a shaft, covered by stainless steel casing. ERT handles brine flow from 15 up to 1,200 m^3/h, pressures up to 80 bar and rotational speeds up to 3,600 rpm while having a relatively low capital cost. Calder ERT is claimed to reach efficiencies up to 90% and deliver power up to 1500 kW (Calder, 2013). However, its efficiency declines in accordance with the efficiencies of the impeller, the nozzle and the turbine and as the flow rate or pressure of the reject stream diverges from optimal. Its recovery ratio ranges from 20% to 50%. The

maximum overall efficiency of Calder ERT is 90% (Guirguis, 2011). Hence, as in equation 8, the peak overall efficiency of the ERT driven generator energy recovery system is estimated:

$$\eta_{\mathrm{ERT}} = 90\% \cdot 80\% \cdot 94\% \cdot 89\% = 60\% \qquad \textbf{[10]}$$

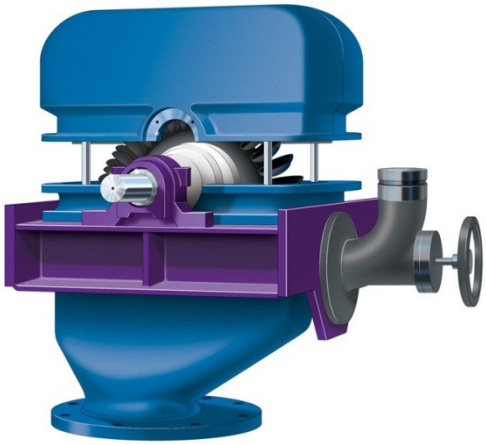

Figure 12: Calder Energy Recovery Turbine (Calder, 2013)

3.1.2. Hydraulically driven pumping in series

Hydraulically driven pumping in series devices are commonly referred to as turbochargers (MacHarg, 2002). Turbochargers consist of a turbine and a centrifugal pump impeller connected on the same shaft with no motor. The concentrate stream is directed to the turbine rotor where its hydraulic energy is converted to mechanical energy. Then, the pump impeller converts the mechanical energy produced by the turbine rotor back to pressure energy by raising medium-pressure feed stream to high pressure prior to entering the RO membranes (Contreras, 2009). Thus, turbochargers are entirely powered by the concentrate stream, having no electrical, external lubrication or pneumatic requirements (Shaligram, 2011). An energy saving is achieved because the main pump's required discharge pressure is reduced (MacHarg, 2002).

Since the turbocharger is independent of the motor speed, its own speed can be selected so as to obtain its best efficiency (Contreras, 2009). Turbochargers are manufactured at various scales according to the capacity required. However, at smaller capacities the peak efficiency diminishes considerably. Turbocharger systems consume slightly less energy than shaft assist mechanism systems because the high-pressure pump in the latter operates at higher pressure and therefore lower efficiency (Stover, 2006).

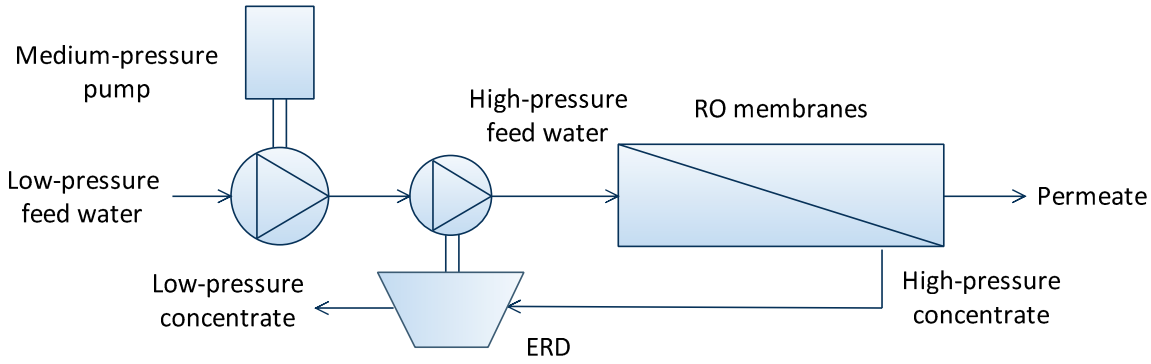

Figure 13: RO desalination system including hydraulically driven pumping in series

Manufactures of turbochargers are Energy Recovery Inc. (ERI), Fluid Equipment Development Company (FEDCO) Grundfos A/S.

ERI has developed two types of hydraulic turbochargers. ERI TurboCharger (LPT) (Figure 14) is designed for low-pressure applications (multi-stage brackish RO water treatment), since it delivers pressures up to 45 bar and handles flows from 6.8 to 908 m^3/h. Its materials of construction include rotor AL6XN, bearings Graphitar 39 and casings SS304, 316, Duplex 2205 (for max. feed pressure of 41.4 bar). At the following table the capacities of the existing models are defined at 17.2 bar.

TurboCharger Model	Feed flow rate (m^3/h)
LPT-32	> 6.8
LPT-63	10.2 - 20.4
LPT-125	20.6 - 34.1
LPT-250	34.3 - 68.1
LPT-500	68.4 - 136.3
LPT-1000	136.5 - 272.5
LPT-2000	272.3 - 545.1
LPT-4000	< 908

Figure 14: ERI LPT TurboCharger models and capacities (ERI, 2013)

ERI AT TurboCharger (Figure 15) is designed for high-pressure applications (small to medium seawater RO systems), handling pressures from 45 up to 80 bar and flows from 11 to 2,272 m^3/h (ERI, 2013). Its materials of construction include rotor AL6XN, bearings Graphitar 39 and casing Duplex SS 2205. At the following table the capacities of the existing models are defined at 69 bar.

Figure 15: ERI AT TurboCharger (ERI, 2013)

FEDCO has developed Hydraulic Pressure Booster (HPB) which exists in 16 models. The table below summarises their characteristics (FEDCO, 2013). The operating temperature is $0 - 70.0℃$ and the maximum storage temperature is 85℃. The minimum brine outlet pressure is 0.5 bar and the maximum operating pressure is 80 bar (82 bar only for HPB-10).

Hydraulic Pressure Booster Model	Pump-side flow (m^3/h)	Turbine-side flow (m^3/h)	Peak Efficiency (%)
HPB-10	3.5 – 15	-	-
HPB-20	15 – 25	8 – 20	64
HPB-30	23 – 38	13 – 30	66
HPB-40	30 – 50	17 – 40	67
HPB-60	45 – 75	25 – 60	71
HPB-80	60 – 100	33 – 80	72
HPB-120	90 – 150	50 – 120	73
HPB-160	120 – 200	66 – 160	74
HPB-250	188 – 313	103 – 250	76
HPB-350	263 – 438	145 – 351	77
HPB-500	375 – 626	206 – 501	78
HPB-700	525 – 875	289 – 700	79
HPB-1000	750 – 1,250	413 – 1,000	80
HPB-1400	1,050 – 1,750	578 – 1,400	81
HPB-2000	1,500 – 2,500	825 – 2,000	82
HPB-2800	2,100 – 3,500	1,155 – 2,800	85

Table 1: FEDCO HPB operating parameters

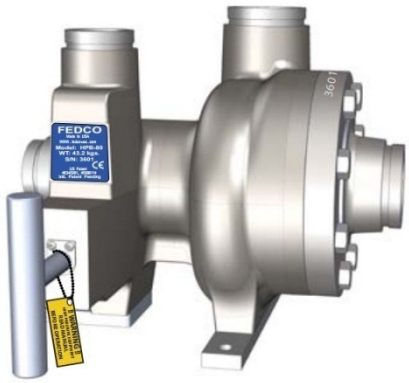

Figure 16: FEDCO Hydraulic Pressure Booster (HPB) (FEDCO, 2013)

Another commercial example of hydraulically driven pumping in series is the BMET booster module, developed by Grundfos, which consists of a high pressure pump (BME booster module) connected in series with a Pelton-driven pump (Figure 17). The energy from the resulting high-pressure concentrate stream of the RO process is recovered by the Pelton turbine. This configuration results in energy savings up to 34% compared to conventional systems. BMET booster module handles flow range of 4 to 130 m^3/hr and pressure up to 80 bar. Using the following equation and recovery ratio of 35%, the inlet brine flow rate range is calculated 2.64-85.8 m^3/h.

$$Q_b = Q_f - Q_p = (1 - RR) \cdot Q_f$$

The Pelton-driven pump requires feed pressure between 2-5 bar and delivers to the high pressure pump pressure up to 30 bar. BMET booster module comes in 50 Hz and 60 Hz. All turbine and pump parts are water lubricated and thus maintenance-free.

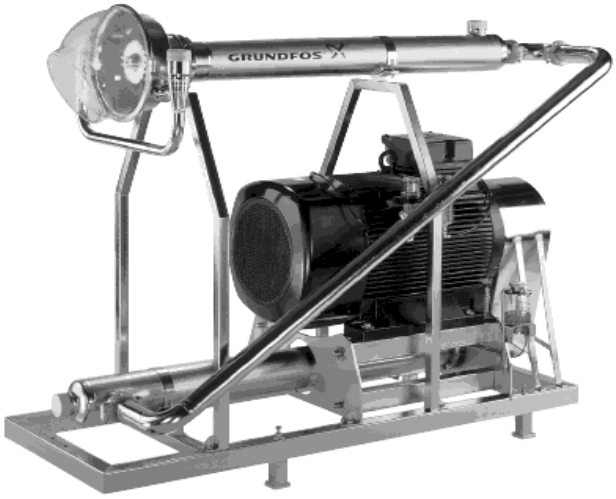

Figure 17: Grundfos BMET booster module (Grundfos A/S, 2013)

The high pressure pump is powered by an electric standard motor via the V-belt pulley, which is geared 2:1 (max. speed approx. 6,000 rpm). Motor bearings are grease-lubricated, while the ball bearings of the V-belt pulley are lubricated and cooled by an oil lubrication system. The shaft seal is made of carbon/silicon carbide. Both pumps have a water lubricated axial thrust bearing build in, to absorb the axial thrust from the pump. However, in this system configuration the high pressure pump is interposed between the energy recovery device and the RO membranes (Figure 18).

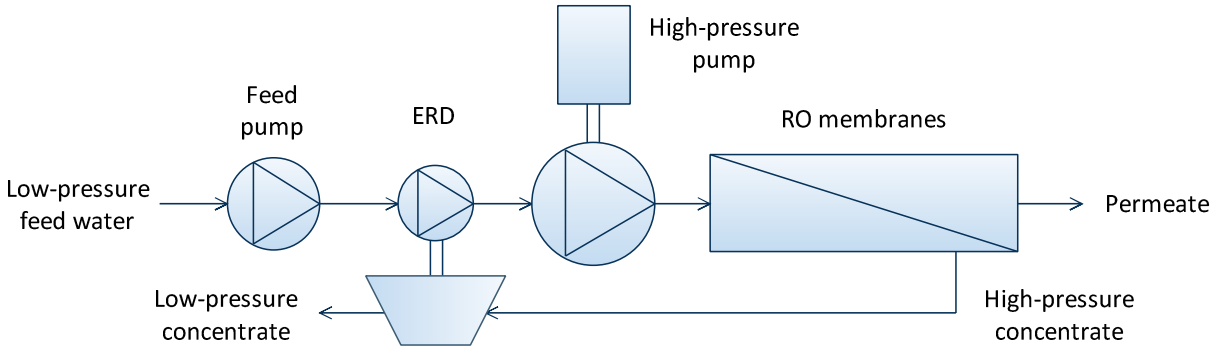

Figure 18: System configuration including the BMET booster module (Grundfos A/S, 2013)

3.2. Pressure Exchangers

3.2.1. Piston Isobaric Energy Recovery Devices

Piston isobaric energy recovery devices use the principle of positive displacement. These devices transfer the energy in the reject stream directly to the feed water stream with the use of valves and pistons. Energy saving is achieved by reducing the volumetric output required by the main high-pressure pump (MacHarg, 2002). Piston isobaric devices require dynamic control to operate their valves and to limit piston movement. Each ERD must be operated individually and in conjunction with the other devices in the array to minimise overflush/bypass and to prevent excessive pulsations and water hammer. In configurations without piston, the long contact time (20 to 60 seconds) between the brine and seawater in

the isobaric chambers results in some intermixing, resulting and an increase in the membrane feed salinity of up to 1.5%. However, piston isobaric devices operate at an efficiency that is limited only by the energy loss in moving the pistons and valves and can exceed 95%. Their efficiency is claimed to be relatively constant despite flow and pressure variations and is independent of device capacity. Multiple isobaric devices operate in parallel in arrays with no loss of efficiency. Piston isobaric energy recovery devices are classified according to their working principle to single double-acting cylinder, two double-acting cylinders, three double-acting cylinders and two valve controlled cylinders ERDs.

3.2.1.1. Pressure exchangers with a single double-acting cylinder

The energy recovery device used at the PowerSurvivor developed by Katadyn, is the only commercial example of pressure exchanger with a single double-acting cylinder (Went, et al., 2010).

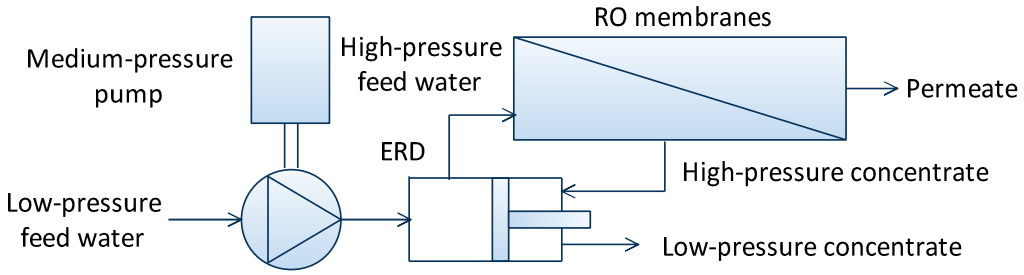

Figure 19: configuration including the pressure exchanger with a single double-acting cylinder

Two models exist, PowerSurvivor 40E and 80E. Both models have efficiency from 96-98.4% and recovery ratio 10% and deliver to the RO membranes feed pressure of 55 bar. PowerSurvivor 40E delivers permeate flow rate of 0.006 m^3/h and PowerSurvivor 80E delivers permeate flow rate of 0.013 m^3/h. Using the recovery ratio, the feed pressure required is calculated 0.06 m^3/h and 0.13 m^3/h respectively.

Figure 20: PowerSurvivor 40E and 80E, developed by Katadyn (Katadyn, 2013)

3.2.1.2. Pressure exchangers with two combined double-acting cylinders

The RO desalination system including the pressure exchanger with two combined double-acting cylinders requires a medium pressure feed pump.

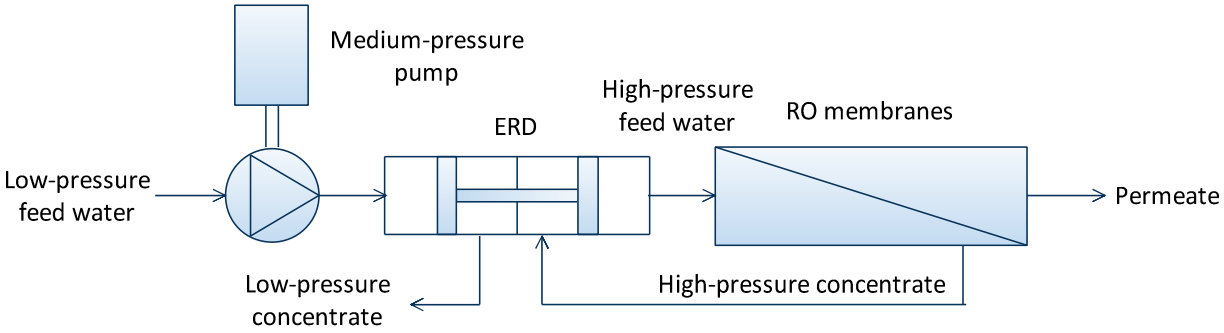

Figure 21: System configuration including the pressure exchanger with two combined double-acting cylinders

Current manufacturers of pressure exchangers with two combined double-acting cylinders include Spectra Watermakers (Clark Pump), Schenker (Schenker Energy Recovery System), Eco-Sistems Watermakers (ST-08-PRO Pump) and Sea Recovery (EfficientSea Energy Transfer Device).

The Clark Pump, developed by Spectra Watermakers, works on the principle of positive displacement and uses two opposing cylinders with pistons connected on a single rod that passes through a centre block (Figure 22). A reversing valve allows the cylinders to alternate between driving and pressurising. In the driving cylinder the feed flow pushes the outer surface of the driving piston and the piston pushes the rod through the centre block. The brine water between the inner surface of the driving piston and the centre block is discharged. At the same time the pressurising piston, which is pushed by the rod, circulates the feed water through the membranes and back to the reversing valve. The reversing valve directs it into the same cylinder between the inner surface of the piston and the centre block. Thus, a closed loop is created between the cylinder and the membrane. The rod displaces water as it enters the cylinder, and, since the displaced water has no place to go, the pressure rises until there is enough pressure for the RO to occur in the membrane, allowing the displaced water to be forced out as product. Therefore, the amount of fresh water produced on every stroke is equal to the volume of the rod entering the cylinder. When the inner surface of the driving piston reaches the centre block, a pilot valve gets mechanically actuated and inverses the process instantly by moving the reversing valve.

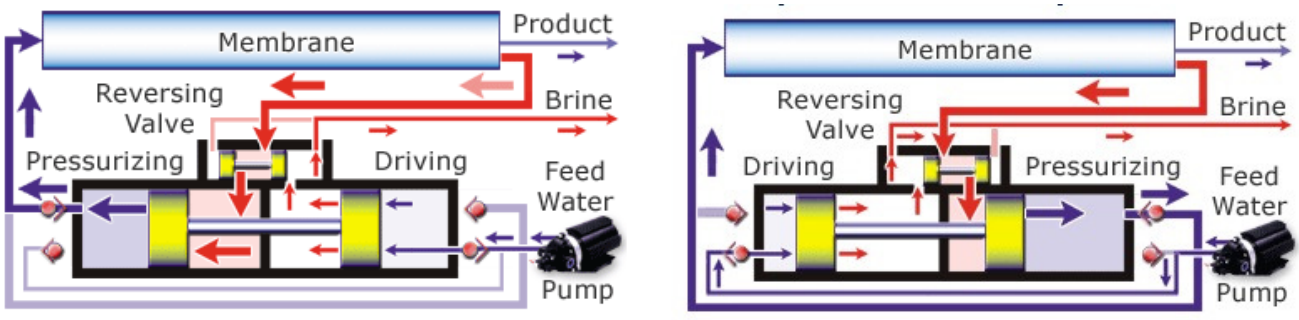

Figure 22: RO desalination system configuration including Spectra Clark Pump (Spectra Watermakers, Inc, 2013)

The RO desalination system including the Clark Pump does not require the use of a motorized high-pressure pump, since the pressure of the feed water is about 4.2 to 12.6 bar. The pressure of the feed flow provided to the membranes is claimed to reach 55 bar. The

highest efficiency achieved by the Clark Pump is 97% (Contreras, 2009). The product salinity is claimed to be less than 300 TDS.

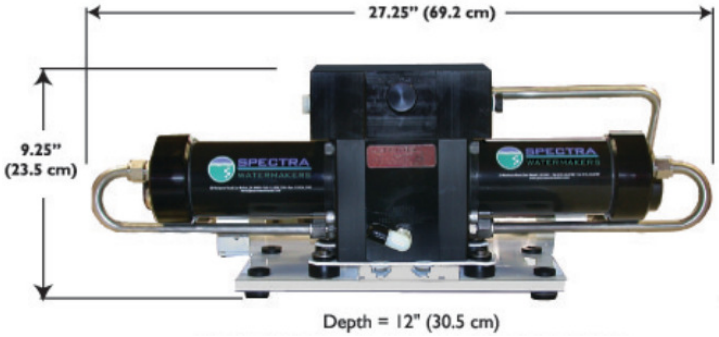

Figure 23: Spectra Clark Pump Intensifier (Spectra Watermakers, Inc, 2013)

Using a mass balance and assuming constant water density and no leakage in the system, it can be said that as the piston displacement is equal on both sides, the surfaces then determine the ratio between the volume flows. The volume of water entering and leaving the cylinder equals to the product of the area of the piston and the displacement x (Snieder, et al., 2013). The areas A and B differ because of the rod coupled to the one side of the piston.

$$V_f = A \cdot x\,, \quad V_b = B \cdot x\,, \quad V_f/V_b = A/B\,, \quad Q_f/Q_b = A/B \qquad [11]$$

Using equation 11 the recovery ratio (Equation 2) can be formulated:

$$RR = Q_p/Q_f = (Q_f - Q_b)/Q_f = 1 - Q_b/Q_f = 1 - B/A \qquad [12]$$

Thus, the recovery ratio is fixed by the surface ratio.

For the Spectra Clark Pump the diameter of the rod is $d_{rod} = 2.22\ cm$ and the diameter of the outer surface of the piston is $d = 6.98\ cm$ (Spectra Watermakers, Inc, 2013). Thus, the recovery ratio is calculated:

$$RR = 1 - \frac{B}{A} = \frac{(A-B)}{A} = \frac{A_{rod}}{A} = \frac{(\pi \cdot d_{rod}^2/4)}{(\pi \cdot d^2/4)} = \left(\frac{d_{rod}}{d}\right)^2 = 10.12\%$$

Depending on the surface ratio, the recovery ratio of the Clark Pump can be 7, 10, 15 and 20%. The Clark Pump delivers permeate flow rate of 0.02-0.15 m^3/h and requires inlet feed flow rate from 0.4-0.9 m^3/h.

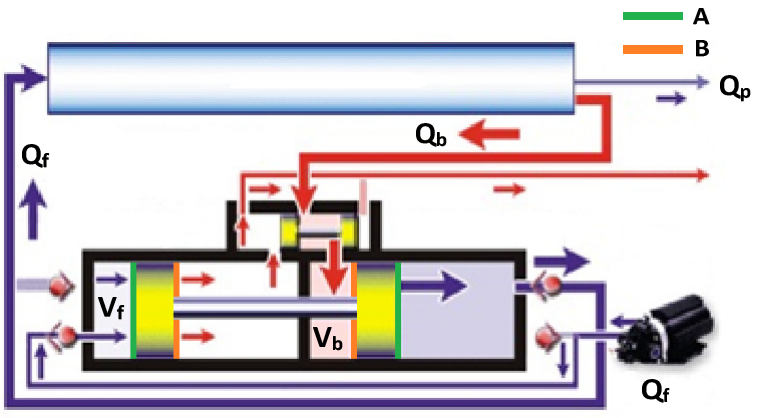

Figure 24: A schematic view of the relevant forces, pressures and surfaces of the Spectra Clark Pump (Spectra Watermakers, Inc, 2013)

The Schenker Energy Recovery System (Figure 25), developed by Schenker, works on the same principle as the Spectra Clark Pump. The area of the inner (B) and outer (A) surfaces of the pistons of the Schenker Energy Recovery System can reach $59.22\ \mathrm{cm}^2$ and $69.40\ \mathrm{cm}^2$ respectively. Thus, using equation 10, the maximum achievable recovery ratio for this system is calculated $\mathrm{RR} = 1 - \mathrm{B/A} = 14.67\%$. The minimum recovery ratio is 10%. The Schenker Energy Recovery System delivers permeate flow rate of 0.035-0.21 m^3/h and, using the range of recovery ratio of 10-14.67%, the feed flow rate is calculated 0.35-1.43 m^3/h.

Figure 25: Schenker Energy Recovery System shown as part of the 'smart watermaker' RO desalination system developed by Schenker (Schenker, 2012)

The ST-08-PRO Eco-Sistems Pump, developed by Eco-Sistems Watermakers, is a positive displacement energy recovery device with two double-acting cylinders controlled by a mechanically driven reversing valve (Figure 26). Hence, it shares the working principle and the system configuration of the Spectra Clark Pump. 0.72-2.16 The ST-08-PRO Pump handles feed water flow rate in the range of 0.03-0.89 m^3/h and inlet feed water pressure between 10-19 bar (after the medium pressure pump) and delivers outlet feed pressure of 45-60 bar and permeate flow rate from 0.03 to 0.09 m^3/h.

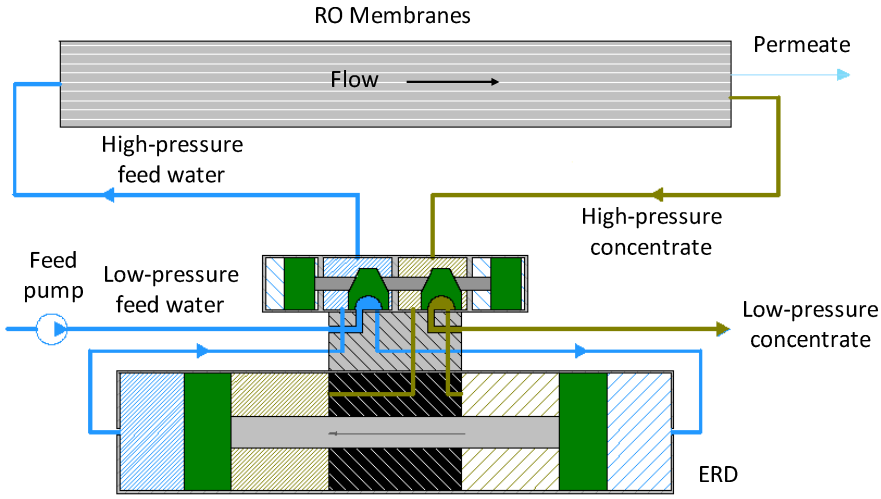

Figure 26: ST-08-PRO Pump and WATER-PRO system scheme developed by Eco-Sistems Watermakers (Eco-Sistems Watermarkers S.L., 2013)

EfficientSea Energy Transfer Device, developed by Sea Recovery, is another commercial example of pressure exchanger with two double-acting cylinders. It delivers permeate flow rate of 0.03-0.09 m^3/h and requires feed flow rate of 0.3-0.78 m^3/h. It handles inlet feed pressure of 6-15 bar and delivers to the membranes outlet feed pressure of 42-57 bar.

Figure 27: EfficientSea Energy Transfer Device developed by Sea Recovery (Sea Recovery Corp., 2013)

In addition, a different configuration of the RO desalination system including the Clark Pump was proposed by Bermudez-Contreras and Thomson (Bermudez-Contreras, et al., 2009). In the modified Clark Pump system, the Clark Pump operates in parallel with a high pressure pump realising a variable recovery ratio.

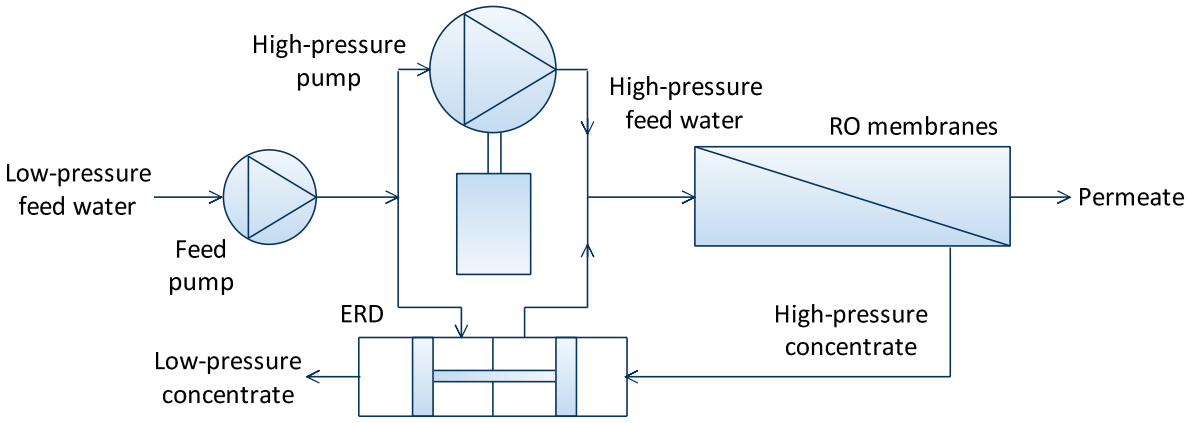

Figure 28: Modified Clark Pump RO desalination system (Bermudez-Contreras, et al., 2009)

3.2.1.3. Pressure exchangers with three double-acting cylinders

Current manufacturers of pressure exchangers with three combined double-acting cylinders include Spectra Watermakers (Pearson Pump), Enercon (PES) and VARI-RO (IPER) (Childs, et al., 1999). This type of ERD requires a low pressure pump to pressurise the feed water (Figure 29).

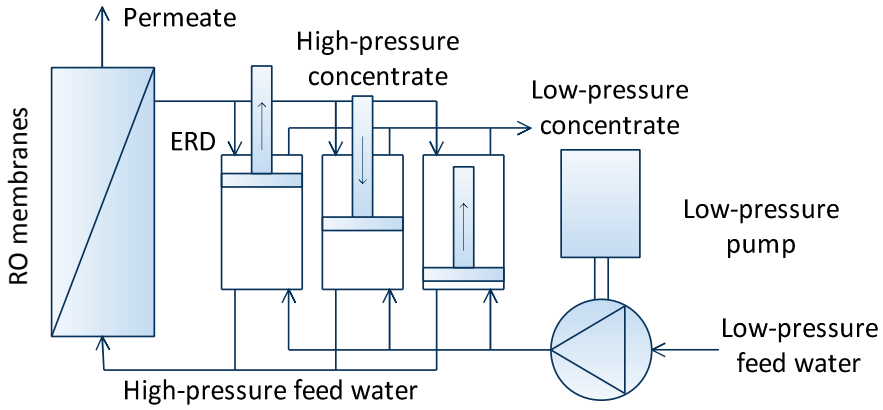

Figure 29: System configuration including the pressure exchanger with three combined double-acting cylinders

The Spectra Pearson pump, developed by Spectra Watermakers, is a positive displacement three cylinder reciprocating high pressure pump. In the Pearson pump the high pressure concentrate flows into the pump cylinders on the backside of the piston, transferring its energy to the feed water being discharged to the membranes (Figure 30). Since part of the volume of the driving cylinder is taken up by the ceramic plunger, only a portion of the water provided to the membranes will be able to return to the backside of the piston, as concentrate, creating a "hydraulic lock". The electric motor of the device forces the piston upwards resulting to pressure rise until the displaced water can flow through the membrane as permeate.

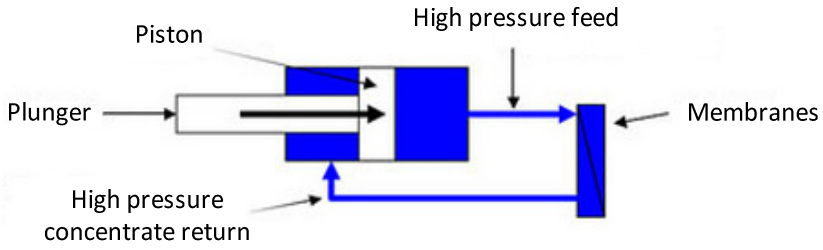

Figure 30: Spectra Pearson Pump scheme for one cylinder (Spectra Watermakers, Inc, 2013)

The amount of permeate flow is defined by the volume of the cylinder taken up by the plunger. Thus, the device provides constant recovery ratio of 20%, 30% and 50%, depending on the size of the plunger. The Pearson Pump handles feed flows from 0.79-1.58 m^3/day, product flow rate from 0.16 up to 0.79 m^3/h and pump speed of 750-1200 rpm (optimum pump speed 900-1000 rpm). Feed pressure range of 0.69-1.72 bar is required. The power consumption of the Pearson Pump ranges from 0.46-2.29 kW. The pump head is manufactured from engineered composites and high quality stainless steel for extreme corrosion resistance and oil filtration allows for long maintenance intervals.

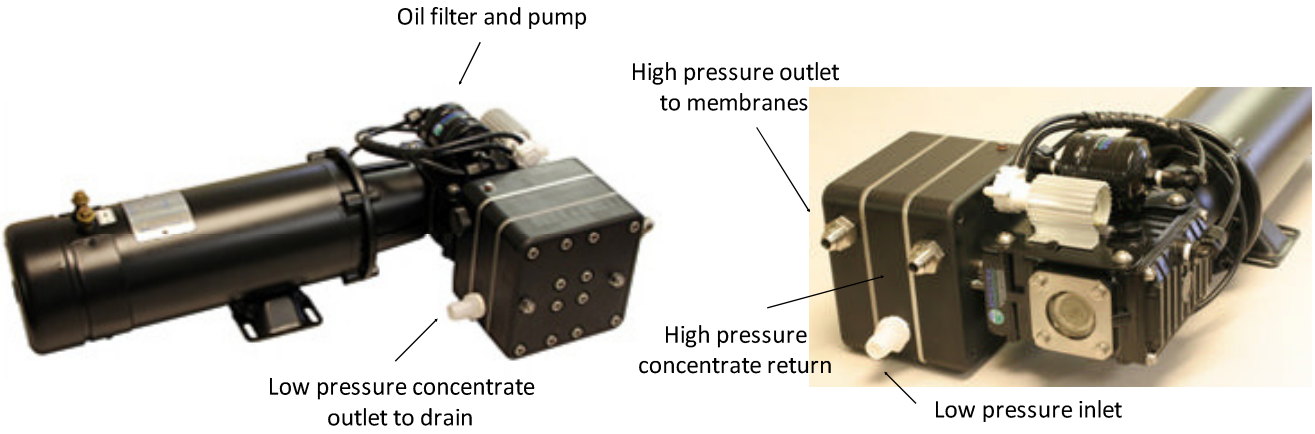

Figure 31: Spectra Pearson Pump (Spectra Watermakers, Inc, 2013)

3.2.1.4. Pressure exchangers with two valve controlled cylinders

These energy recovery devices work on the principle of positive displacement using two separated cylinders in order to transfer the energy of the concentrate stream to the feed water. The operation of these devices is controlled by electronically powered valves. The configuration of the RO desalination system using this type of piston isobaric devices includes an electronic boost pump.

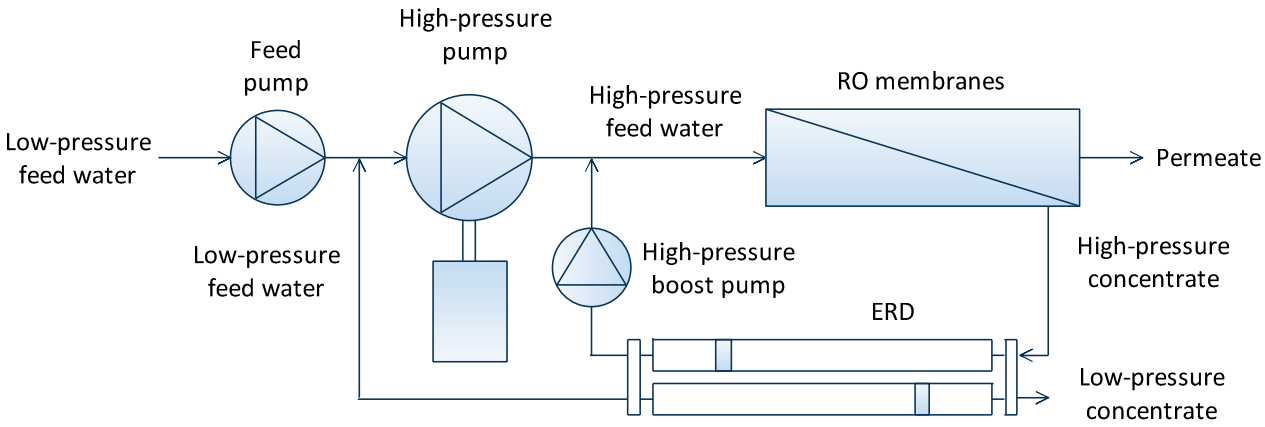

Figure 32: System configuration including the pressure exchangers with two valve controlled cylinders

Current manufacturers of multiple pistons isobaric devices include Calder (Dual Work Exchanger Energy Recovery), KSB AG (SalTec DT), Aqualyng (Pressure Recuperator), RO Kinetic (Tecnovalia), Siemag (PES).

Dual Work Exchanger Energy Recovery (DWEER), developed by Calder, works on the principle of piston isobaric devices. Each unit consists of two pressure vessels, four check valves and one LinX control valve. DWEER conserves energy by using the high pressure brine stream to pressurise the feed water stream. Brine and feed streams are separated by a piston in each vessel in order to ensure minimum mixing. Besides its high capital cost, DWEER also requires a recirculating pump in order to boost the feed pressure equal to the feed pump pressure. DWEER handles brine flows up to 350 m^3/h per unit but not lower than 200 m^3/h due to pulsations and vibrations occurring at lower flow rates. Greater flows can be achieved by using multiple DWEER units in parallel. DWEER is claimed to recover up to 98% of the energy in the concentrate stream (Calder, 2013). Thus, the maximum overall efficiency of DWEER is 98% (Guirguis, 2011).

Figure 33: Dual Work Exchanger Energy Recovery (DWEER) developed by Calder (Calder, 2013)

The Recuperator ERD (Figure 34), developed by Aqualyng, uses the energy of the concentrate flow to pressurise pre-treated seawater in a sequential process regulated by the concentrate flow from the RO membranes. The device consists of vertically standing pairs of duplex stainless steel chambers that work alternatively in a compression-transfer and decompression-discharge sequence. Pre-treated seawater comes from a pressurized feeding

tank that keeps a constant flow and pressure into the system (Aqualyng, 2009). A booster pump is needed in order to compensate for the pressure drop across the membranes (up to 2 bar) and the Recuperator (0.2-0.6 bar). Recuperator makes use of three valves in order to control the flow and maintain it to the level required by the booster pump which circulates the feed water to the membranes (LyngAgua, et al., 2001). The high-pressure pump required is 60% smaller than the traditional technology, while the feed water and brine stream achieve the same flow and pressure without mixing. However, high capital cost is required (Guirguis, 2011). The maximum overall efficiency of the Recuperator is 92%-97% (Guirguis, 2011).

Figure 34: Aqualyng Recuperator (Aqualyng, 2009)

SalTec DT, developed by KSB, works on the principle work exchange. Two sizes of the device are manufactured, DT160 and DT250, corresponding to nominal flow rates of 160 m^3/h and 250 m^3/h respectively. Both types can handle salinity up to 70,000 ppm pressure up to 80 bar and flow rate up to 280 m^3/h.

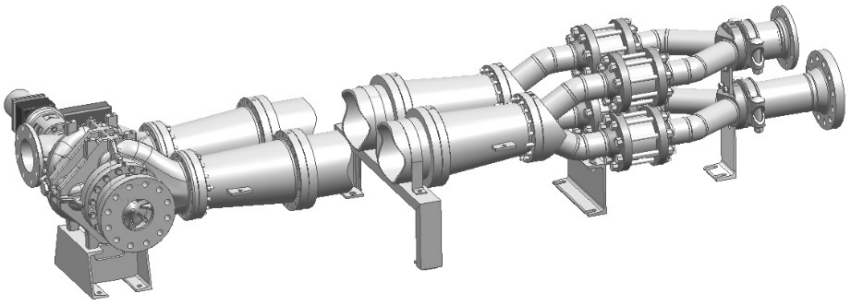

Figure 35: KSB Pressure Exchanger SalTec DT (KSB, 2013)

3.2.2. Rotary Isobaric Energy Recovery Device

The high efficiency of a piston isobaric device and the operational simplicity of centrifugal energy recovery devices are combined in the rotary isobaric device, first applied to the RO systems in 1997. In a RO system equipped with a rotary isobaric device, the membrane reject is directed to the membrane feed.

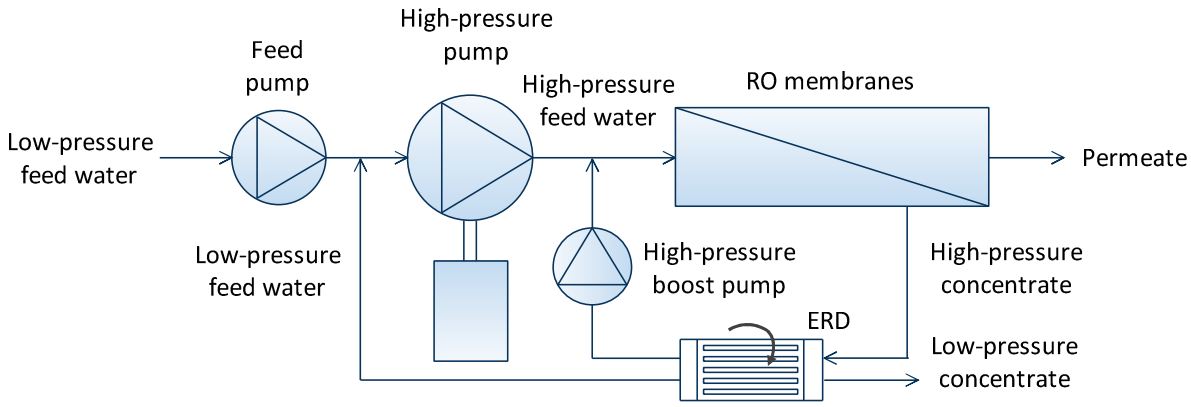

Figure 36: System configuration including the rotary isobaric energy recovery device

The first commercial example is PX Pressure Exchanger developed by Energy Recovery Inc. A rotor, moving between the high-pressure reject stream and a low-pressure feed water stream, removes the brine and replaces it with the feed water. Pressure transfers directly from the high-pressure brine stream to the feed water stream with no intervening piston in the flow path (ERI, 2013). The feed water stream, nearly equal in volume to the brine stream, then passes through a small booster pump, which makes up for the hydraulic losses through the RO system. The absence of piston eliminates the friction and wear that occurs on the pistons but also results in a slightly higher degree of mixing between the streams than in a piston isobaric device (1 to 2.5%). Mixing is minimised with long, small diameter chambers and short brine-feed water contact time (0.05 seconds) (Stover, 2006). The device consists of few parts made of highly durable ceramic materials (alumina), including the moving rotor enclosed with a pair of sealing end-covers. Ceramic is a corrosion resistant and dimensionally stable material that withstands harsh saline environments. In addition, PX achieves stable efficiency over wide range of recoveries. Finally, PX has a high capital cost.

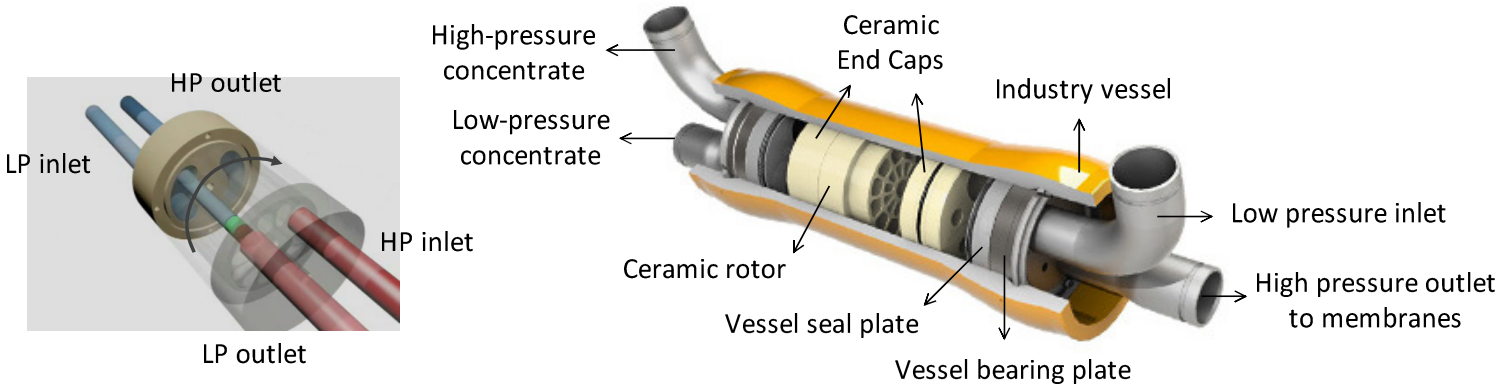

Figure 37: PX S Series Pressure Exchanger developed by Energy Recovery Inc. (ERI, 2013)

PX Pressure Exchanger is manufactured for various flow ranges. S Series includes nine models designed for permeate flow rate from 4.5 m^3/h (PX-30S) up to 45.4 m^3/h (PX-300). Q Series includes two models designed for permeate flow rate of 39.4 m^3/h (PX-Q260) and 45.4 m^3/h (PX-Q300). The minimum guaranteed efficiency, proposed by ERI, starts from 93.4% for PX-30 and reaches 97.2% for PX-Q300 (ERI, 2013). The maximum efficiency of the PX Pressure Exchanger is estimated at 98% (Guirguis, 2011).

PX Pressure Exchanger Devices	Inlet brine flow rate (m^3/h)	Permeate flow rate (m^3/h) (at RR=40%)	Min. Guaranteed Efficiency (%)
PX-30	4.5 – 6.8	4.5	93.4
PX-45	6.8 – 10.2	6.8	94
PX-70	9.1 – 15.9	10.6	95.3
PX-90	13.6 – 20.4	13.6	96
PX-140	20.4 – 31.9	21.2	94.8
PX-180	22.7 – 40.9	27.3	96.7
PX-220	31.9 – 49.9	33.3	96.8
PX-260	40.9 – 59	39.4	96.8
PX-300	45.4 – 68.1	45.4	96.8
PX-Q260	40.9 – 59	39.4	96.8
PX-Q300	45.4 – 68.1	45.4	97.2

Table 2: PX Pressure Exchanger Devices operating parameters (ERI, 2013)

Another commercial example of rotary isobaric energy recovery device is the X-Changer developed by Grundfos. The X-changer works on the working principle as the ERI pressure exchanger and hence the system requirements and configuration are the same. The outlet feed pressure before the boost pump is 4-5 bar.

Figure 38: Grundfos X-Changer with two energy recovery units (Grundfos A/S, 2013)

Finally, the iSave pressure exchanger (Figure 39a), developed by Danfoss, is also a rotary isobaric energy recovery device and works on the same principle as the PX Pressure Exchanger. However, it is provided directly coupled with built-in booster pump and electric motor (Figure 39c). The boost pump consists of a rotor with vanes and works on the principle of positive displacement (Figure 39b). Hence, its rotational speed is proportional to the flow rate. The iSave 21 handles flow rate in the range of 7-21 m^3/h and iSave 40 handles flow rate in the range of 22-41 m^3/h. Pressure ranges from 10-82 bar and efficiency reaches 93% for both models.

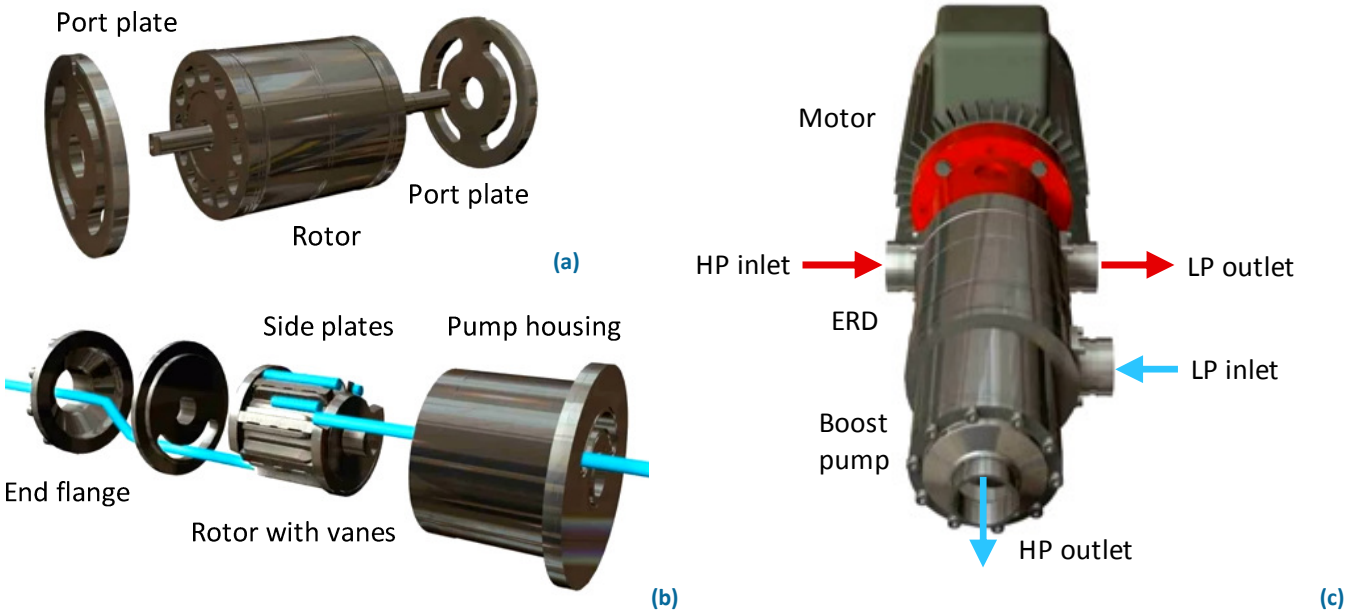

Figure 39: Danfoss iSave [Danfoss, 2013]

3.3. Inverse positive displacement pump

Seawater pump with energy recovery device (SWPE), developed by Danfoss, uses an Axial Piston Pump (APP) as a high pressure boost pump and an inverse APP, namely an Axial Piston Motor (APM), as an energy recovery device. The APP is a rotating positive displacement pump that pressurises the feed water using the rotary mechanical energy provided by the shaft (Figure 40). Inversely, the APM rotates using the energy of the inlet high pressure brine stream.

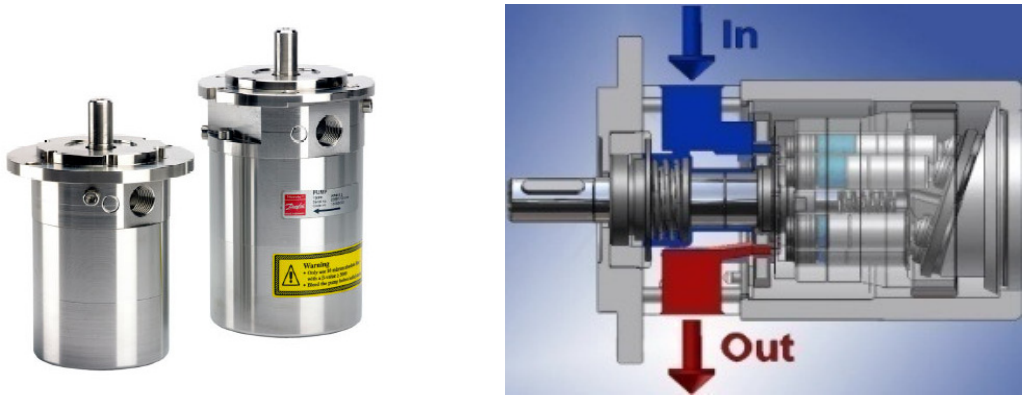

Figure 40: Axial Piston Pump developed by Danfoss [Danfoss, 2013]

In SWPE, the APP and the APM are both connected to a double shafted electric motor (Figure 41). SWPE cannot be classified in pressure exchangers since the energy extracted from the concentrate in the APM is converted to rotary mechanical energy which is used to drive the APP. As both the APM and the APP have fixed volumetric displacement, the recovery ratio is fixed between 28-32%. The SWPE requires inlet feed flow rate in the range of 0.5-1.25 m^3/h (at 1450 rpm of the APP/APM) and 1.05-2.55 m^3/h (at 2900 rpm), inlet feed pressure between 0.5-5 bar, inlet brine pressure between 10-80 bar, outlet feed pressure in the range 20-80 bar and outlet brine pressure in the range 0.5-5 bar. It delivers permeate

flow rate of 0.14-0.4 m^3/h (at 1450 rpm of the APP/APM) and 0.3-0.82 m^3/h (at 2900 rpm). The feed and the permeate flow rate increases with higher rotational speed of the shaft. The power delivered by the electric motor ranges from 1.1 to 2 kW (at 1450 rpm) and from 2.2 to 3 kW (at 2900 rpm).

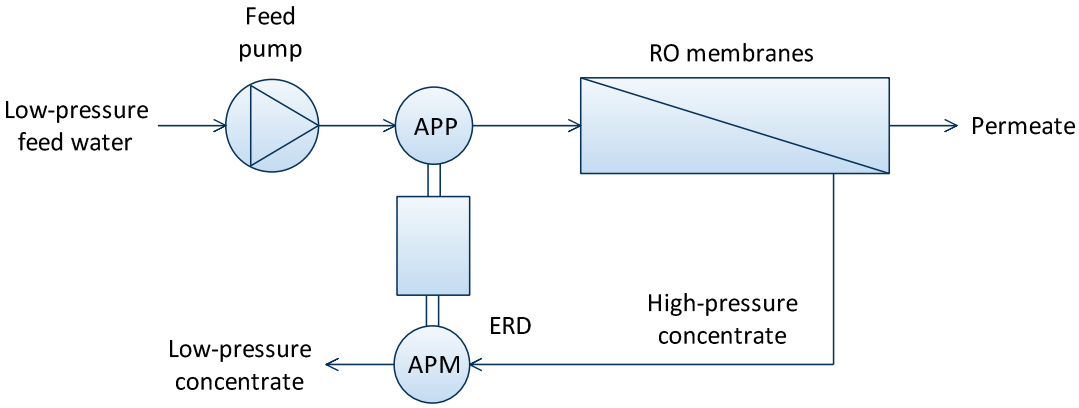

Figure 41: System configuration including Seawater pump with energy recovery device (Danfoss, 2013)

Figure 42: SWPE developed by Danfoss (Danfoss, 2013)

3.4. Comparative overview

The operating parameters and other characteristics and limitations of the ERDs, discussed in this chapter, are summarized at the following table.

ERD type		Feed flow rate (m^3/h)	Brine flow rate (m^3/h)	Inlet brine pressure (bar)	Recovery ratio (%)	Feed water salinity	Max. overall efficiency (%)	Electronic control	Motorised boost pump	Main pressure pump required	Price (€)
Centrifugal ERD	Hydraulic to mechanical-assisted pumping										
	Francis turbine	Electricity generation	High/ Medium	Low/ Medium	Not specific	Brackish/ Seawater	53 [gen.]	No	No	HP	-
	Pelton turbine	Electricity generation	Low/ Medium	High/ Medium	Not specific	Brackish/ Seawater	57 [gen.]	No	No	HP	-
	ERT, Calder	Electricity generation	15 – 1,200	< 80	20 – 50	Brackish/ Seawater	60 [gen.]	No	No	HP	25.000 – 30.000
	Hydraulically driven pumping in series										
	LPT, ERI	6.8 – 908	-	< 45	-	Brackish	-	No	No	MP	-
	HTC AT, ERI	11 – 2,272	-	45 - 80	-	Brackish/ Seawater	-	No	No	MP	-
	HPB, FEDCO	3.5 – 3,500	0.9 – 2,800	< 80	25	Brackish/ Seawater	64 - 85	No	No	MP	6,340 – 12,133
	BMET, Grundfos	4 – 130	2.64 – 85.8	< 80	< 34	-	-	No	No	HP	-

ERD type			Feed flow rate (m^3/h)	Permeate flow rate (m^3/h)	Inlet feed pressure (bar)	Recovery ratio (%)	Feed water salinity	Max. overall efficiency (%)	Electronic control	Motorised boost pump	Main pressure pump required	Price (€)
Pressure Exchangers	Piston Isobaric ERD											
	Double-acting cylinder	Power Survivor	0.06 – 0.13	0.006 – 0.013	-	10 *	Seawater	98.4	No	Included	No	2,965 – 3,346
		2 cylinders: Clark Pump	0.4 – 0.9	0.02 – 0.15	4.2 – 12.6	7 – 20 *	Seawater	97	No	No	MP	1,777.78
		2 cylinders: Schenker ERD	0.35 – 1.43	0.035 – 0.21	8 – 12	10 – 14.67 *	Seawater	-	No	No	MP	3,300
		2 cylinders: ST-08-PRO	0.3 – 0.89	0.03 – 0.09	10 – 19	10 – 20 *	Seawater	-	No	No	MP	-
		2 cylinders: EfficientSea	0.3 – 0.78	0.03 – 0.09	6 – 15		Seawater	-	No	No	MP	-
		3 cylind.: Pearson pump	0.79 – 1.58	0.16 – 0.79	0.69 – 1.72	20, 30, 50 *	Brackish/ Seawater	-	Piston	No	LP	-
		3 cylind.: ERS, Enercon	-	-	-	25 *	Brackish/ Seawater	-	Yes	No	MP	-
		3 cylind.: VARI-RO IPER	-	-	-	-	-	-	Valve		-	-
	2 cylind.	DWEER, Calder	200 – 350 (brine)	(164 – 286)	< 75	(45)	Seawater	98	Valve	Required	HP	-
		Recuperator	20 - 417	-	-	-	Brackish/ Seawater	92 – 97	Valve	Required	HP	-
		SalTec DT, KSB	160 – 280	-	< 4	-	Seawater	-	Valve	Required	HP	-
	Rotary Isobaric ERD											
	PX, ERI		11.2 – 113.5	4.5 – 45.4	-	(40)	Seawater	98	No	Required	HP	-
	X-changer, Grundfos		39, 77, 116, 155	21, 42, 63, 84	3 – 5 (< 70)	35	Brackish/ Seawater	-	No	Required	HP	-
	iSave, Danfoss		7 – 41	> 7	10 – 82	-	Seawater	93	No	Included	HP	-
Seawater Pump, Danfoss			0.5 – 2.55	0.14 – 0.82	0.5 – 5	29 – 32 *	Seawater	-	-	Included	LP	3,050

*: fixed recovery ratio

Table 3: Overview of the characteristics of the ERDs examined

[gen] : including turbine, generator, motor and pump efficiency

4. Compatibility with desalination system constraints

In Chapter 4 the constraints set by the examined renewable-driven RO desalination system are presented and energy recovery technologies that apply to these requirements are suggested.

4.1. System requirements

The energy recovery device should be able to deliver production flow rate in the range of 1-100 m^3/day (0.04-4.17 m^3/h). In addition the energy recovery device should provide the RO membranes with feed water pressurised at least at 8 bar and up to 60 bar (pressures of 8, 12, 16, 40, 50, 60 bar will be examined). The recovery ratio should take values between 15-50%.

Moreover, the reference RO system is powered by renewable energy sources which fluctuate over time. A buffer system is able to provide medium pressure feed water. When power supply is not available the buffer system is able to provide water for the RO system. Thus, a constant water pressure is delivered, resulting in the continuous operation of the energy recovery device. Furthermore, the energy generated by renewable energy sources won't be available continuously. As a result the energy recovery device should not require auxiliary power supply, unless the power consumption (e.g. control of the device) is so limited that the use of a small battery pack can be considered. Besides that, since the energy recovery device is an important cost driver of the complete system, it has to be a cost effective solution.

Thus, the main constraints deriving from the reference system are:

- Permeate flow rate in the range of 0.04-4.17 m^3/h
- Feed pressure between 8-60 bar
- Recovery ratio between 15-50%
- No additional power supply required

4.2. ERDs selection

According to Table 3, centrifugal ERDs require neither motorised boost pump nor electronic control. At hydraulic to mechanical assisted pumping, the turbine-driven pump requires additional shaft power that is provided by a motor. However, as mentioned above, additional power supply is not applicable for the reference system, so attention is paid only to turbine-driven generators that power a motorised pump. In addition, turbochargers require a medium-pressure main pump. Moreover, the efficiency of turbochargers is higher than that of Francis-driven generators and similar to that of Pelton-driven generators. It should be noted that turbine-driven generator efficiency includes the generator and motor efficiency too, while the turbocharger efficiency only includes the turbine and the pump efficiency.

Pressure exchangers with two double-acting cylinders deliver the required permeate flow, do not need additional power supply and use a medium pressure pump in order pressurise the feed water.

Although, the Pearson Pump and the Seawater pump with energy recovery device provide very low permeate flow rate and require low feed pressure, they both require additional power supply to operate their boost pump.

Pressure exchangers with two valve controlled cylinders and rotary isobaric ERDs are excluded due to the system configuration required (Figure 32, Figure 36). The high pressure pump, that delivers high pressure feed water to the RO membranes, needs to operate continuously. However, as already mentioned, the power supply is not constantly provided by the renewable energy source. It must be outlined that, despite the additional power supply needed, iSave does provide low permeate flow rate.

Moreover, the system configuration of the BMET, developed by Grundfos, also requires the high pressure pump to operate continuously and thus this ERD is excluded too.

Thus, turbine-driven generators, turbochargers and pressure exchangers with two double-acting cylinders respond more adequately to the reference system characteristics. Since the Pelton turbine efficiency is higher than the efficiency of the Francis turbine, the Pelton-driven generator and the Pelton-driven pump are further evaluated. In addition, the Pearson Pump and the Seawater pump with energy recovery device also meet the system requirements and they may have such working characteristics that in principle zero power consumption can be accomplished by increasing the inlet pressure. Further investigation is therefore required for both the pressure exchanger with three double-acting cylinders and the use of inverse positive displacement pump as a motor.

Consequently, the possibilities provided by the following energy recovery technologies should be further investigated:

- Pelton-driven generator
- Pelton-driven pump
- Pressure exchanger with two double-acting cylinders
- Pressure exchanger with three double-acting cylinders
- Inverse positive displacement pump

5. Evaluation of energy recovery concepts

In this chapter the five energy recovery designs suggested in Chapter 4 are presented and evaluated according the six criteria set.

The selected ERDs are evaluated according to their energy efficiency, power and pressure requirements, energy autonomy, operational stability, cost effectiveness and manufacturing complexity. In order to examine the operating range specified in the previous chapter, permeate flow rate of 5, 50 and 100 m^3/day and recovery ratio of 20% and 40% are used in the calculations made for the selected ERDs. At the following table the selected values of permeate flow rate, Q_p, are given in m^3/hr and the correspondent feed flow rate, Q_f, and the brine flow rate, Q_b, are provided for recovery ratio, RR, of 20% and 40%.

RR (%)	20			40		
Qp (m^3/h)	4.17	2.08	0.21	4.17	2.08	0.21
Qf (m^3/h)	20.83	10.42	1.04	10.42	5.21	0.52
Qb (m^3/h)	16.67	8.33	0.83	6.25	3.13	0.31

Table 4: Flow rate and recovery ratio examined values

As mentioned in the first chapter, the operating pressure for brackish water RO desalination ranges from 10-30 bar, while for seawater from 40-80 bar (Charcosset, 2009). Therefore, feed pressure (p_f) of 8 bar, 12 bar and 16 bar is examined for the case of brackish water RO desalination and pressure of 40 bar, 50 bar and 60 bar is examined for seawater RO desalination.

In order to derive a realistic estimation of the pressure drop in the RO membranes the Reverse Osmosis System Analysis (ROSA), developed by the Dow Chemical Company, is used. Assuming salinity of 8,000 ppm for brackish water and 40,000 ppm for seawater, the membrane pressure drop is calculated for the selected flow rates and recovery ratios. The type and the configuration of the membrane elements are selected with the aim to deliver permeate TDS lower than 400 ppm and permeate flux around 20 lmh. As it is shown in the following tables a mean pressure drop of 0.3 bar can be assumed for brackish water and 0.4 bar for seawater.

Qp (m^3/h)	RR (%)	Qf (m^3/h)	Qb (m^3/h)	Element	Configuration Vessels-elements	Permeate flux (lmh)	pf (bar)	pb (bar)	Permeate TDS (mg/l)	Membrane Δp (bar)
0.21	20	1.04	0.83	LC LE-4040	1-2	12.03	9.7	9.53	255.54	0.17
2.08	20	10.42	8.33	LE-440	2-2	12.72	10.18	9.97	246.12	0.21
4.17	20	20.83	16.67	LE-440i	2-2	25.5	13.51	12.94	130.22	0.57
0.21	40	0.52	0.31	BW30-2540	1-3	26.91	18.76	18.33	104.05	0.43
2.08	40	5.21	3.13	LE-440i	1-3	16.96	12.95	12.69	227.56	0.26
4.17	40	10.42	6.25	LE-440i	2-3	17	12.96	12.69	227.07	0.27
						Mean membrane pressure drop for BW				0.32

Table 5: Membrane pressure drop for brackish water desalination (8,000 ppm)

Qp (m^3/h)	RR (%)	Qf (m^3/h)	Qb (m^3/h)	Element	Configuration Vessels-elements	Permeate flux (lmh)	pf (bar)	pb (bar)	Permeate TDS (mg/l)	Membrane Δp (bar)
0.21	20	1.04	0.83	SW30-4040	1-2	14.17	50.28	50.18	354.01	0.10
2.08	20	10.42	8.33	SW30ULE-400i	2-2	13.99	48.13	47.89	402.11	0.24
4.17	20	20.83	16.67	SW30ULE-440i	2-2	25.5	57.72	57.13	229.88	0.59
0.21	40	0.52	0.31	SW30-2540	1-4	20.18	64.98	64.4	611.57	0.58
2.08	40	5.21	3.13	SW30HRLE-370/34i	1-6	10.08	59.07	58.74	295.44	0.33
4.17	40	10.42	6.25	SW30XLE-400i	2-4	12.76	59.72	59.37	297.10	0.35
						Mean membrane pressure drop for SW				0.36

Table 6: Membrane pressure drop for seawater desalination (40,000 ppm)

Taking into account the pressure drop across the membranes, the brine pressure (p_b) is also calculated, $p_b = p_{fout} - \Delta p$.

pfout (bar)	Δp (bar)	pb (bar)
8	0.3	7.7
12		11.7
16		15.7
40	0.4	39.6
50		49.6
60		59.6

Table 7: RO membranes feed pressure and brine pressure examined values

5.1. Pelton-driven generators

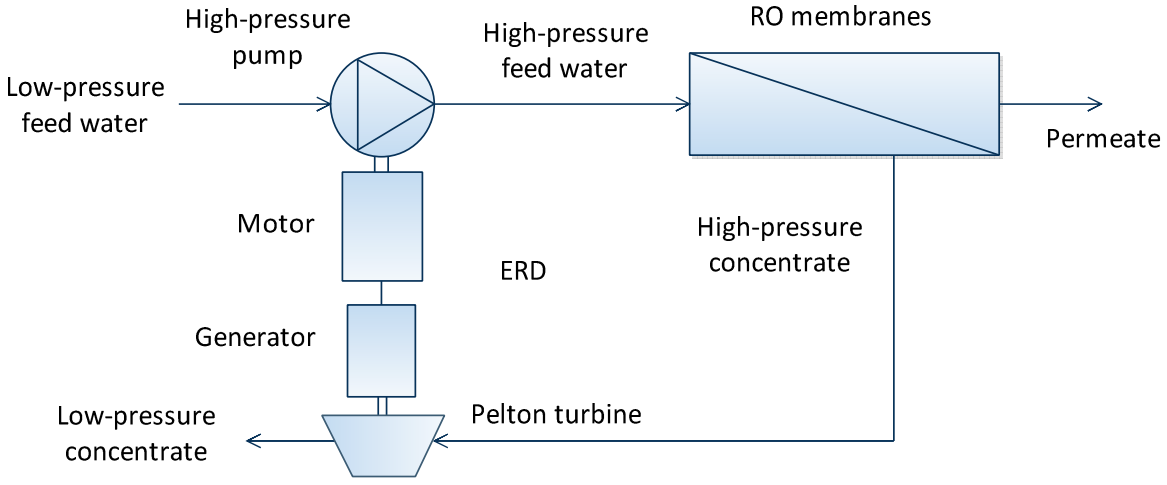

Figure 43: Pelton-driven generator connected to motorised pump

5.1.1. Energy efficiency

The advantage of the configuration with a Pelton-driven generator that powers the motorized pump is that the Pelton wheel and the pump impeller may rotate with different rotational speeds. In addition, the frequency of the motor of the pump is not restricted by the generator. Since the characteristics of each component may be differentiated, they may

selected appropriately in order maximise its efficiency. In order examine the maximum possible overall efficiency of the energy recovery device, high values of the efficiency of each component are taken into account.

5.1.1.1. Pelton turbine

In order to estimate the overall efficiency of a Pelton turbine-driven energy recovery device, focus should first be led on the flow characteristics of the jet stream directed onto each blade of the Pelton wheel. The velocity of the jet stream ejected by the nozzle is c_1 and the blade speed is U, so that the relative velocity at the entry is $w_1 = c_1 - U$. At the exit from the bucket, one half of the jet stream flows away with a relative velocity w_2 and at an angle β_2 to the original direction of the flow (typical value of β_2 is $165°$), as shown in the velocity diagram (Figure 44). From the velocity diagram the much smaller absolute exit velocity c_2 is determined (Dixon, 2005).

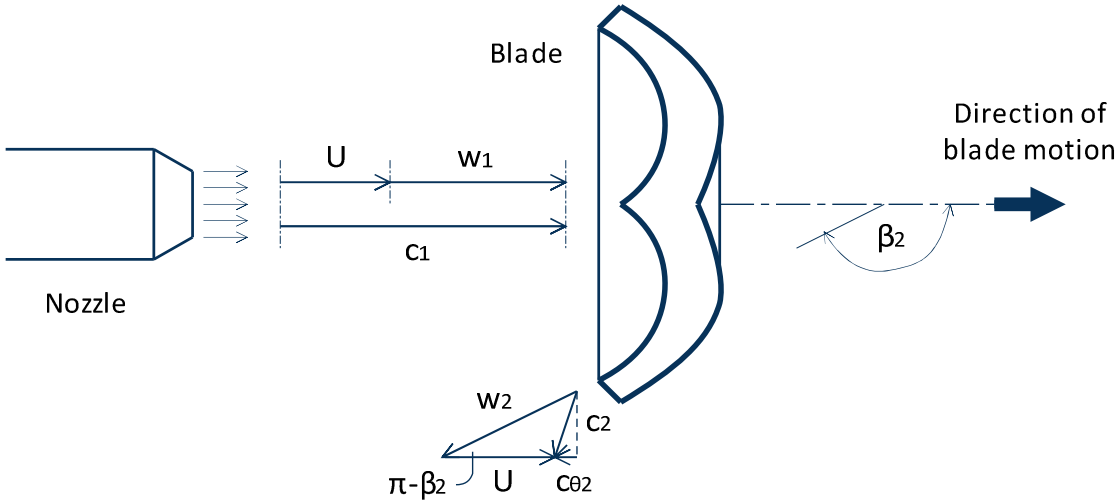

Figure 44: Relative and absolute velocities of the flow ejected onto each blade of the Pelton wheel (only one half of the emergent velocity diagram is shown) (Dixon, 2005)

5.1.1.1.1. Nozzle efficiency

For a perfect nozzle, with no losses, the Bernoulli's equation between the nozzle inlet and the jet is:

$$h_0 + \frac{c_0^2}{2 \cdot g} + z_0 = h_1 + \frac{c_1^2}{2 \cdot g} + z_1$$

Where h_0 is the pressure head before the nozzle, c_0 is the water velocity at the nozzle inlet, z_0 is the height of nozzle centreline, h_1 is the pressure head in the jet and z_1 is the height of jet centreline (Thake, 2000). Since $z_0 = z_1$ and $h_1 = 0$ (atmospheric pressure), the equation becomes:

$$h_0 + \frac{c_0^2}{2 \cdot g} = H_E = \frac{c_1^2}{2 \cdot g}$$

$$\Rightarrow c_1 = \sqrt{2 \cdot g \cdot H_E} \qquad \textbf{[13]}$$

H_E is the effective head (or delivered head) at the nozzle inlet. In practice, the nozzle is not perfect and the losses are accounted by the velocity coefficient, C_v, so using equation 13 and 15 the actual velocity in the jet is:

$$c_1 = C_v \cdot \sqrt{2 \cdot g \cdot H_E} \qquad [14]$$

Assuming an inlet nozzle diameter $d_0 = 0.04\text{m}$, the inlet velocity to the nozzle, c_0, is calculated using the brine flow rate Q_b:

$$c_0 = \frac{Q_b}{\left(\pi \cdot \frac{d_0^2}{4}\right)}$$

Assuming a velocity coefficient $C_v = 0.98$ and calculating the pressure head of the brine stream $h_0 = p_b/\gamma$ ($\gamma = 9.8\,\text{kN/m}^3$), the outlet velocity of the nozzle, c_1, is calculated according to equation 14:

c1 (m/s)		Qf (m^3/h)					
		20.83	10.42	1.04	10.42	5.21	0.52
pfout (bar)	8	38.65	38.52	38.48	38.50	38.48	38.48
	12	47.57	47.46	47.43	47.45	47.44	47.43
	16	55.07	54.97	54.94	54.96	54.95	54.94
	40	87.33	87.28	87.26	87.27	87.26	87.26
	50	97.72	97.67	97.66	97.67	97.66	97.66
	60	107.11	107.06	107.05	107.06	107.05	107.05

Table 8: Nozzle outlet velocity, c1 (m/s)

The volumetric flow rate is the same at the nozzle inlet and outlet:

$$Q = A_0 \cdot c_0 = A_1 \cdot c_1 \Rightarrow \left(\pi \cdot \frac{d_0^2}{4}\right) \cdot c_0 = \left(\pi \cdot \frac{d_1^2}{4}\right) \cdot c_1 \Rightarrow d_1 = \sqrt{\frac{c_0}{c_1}} \cdot d_0 \qquad [15]$$

Hence, using equation 14 the outlet nozzle diameter, d_1, is calculated:

d1 (cm)		Qf (m^3/h)					
		20.83	10.42	1.04	10.42	5.21	0.52
pfout (bar)	8	1.24	0.87	0.28	0.76	0.54	0.17
	12	1.11	0.79	0.25	0.68	0.48	0.15
	16	1.03	0.73	0.23	0.63	0.45	0.14
	40	0.82	0.58	0.18	0.50	0.36	0.11
	50	0.78	0.55	0.17	0.48	0.34	0.11
	60	0.74	0.52	0.17	0.45	0.32	0.10

Table 9: Nozzle outlet diameter, d1 (cm)

A lower limit is set at $d_1 = 0.1\text{ cm}$ related to the nozzle manufacturing feasibility and the size of the Pelton wheel (moment of inertia). Therefore, the use of nozzle is applicable in all cases, as it can be seen in the above table.

Furthermore, the ratio of the outlet nozzle diameter to the inlet nozzle diameter $\lambda = d_1/d_0$ is calculated:

λ		c_0 (m/s)					
		3.68	1.84	0.18	1.38	0.69	0.07
h_0 (m)	79	0.31	0.22	0.07	0.19	0.13	0.04
	119	0.28	0.20	0.06	0.17	0.12	0.04
	160	0.26	0.18	0.06	0.16	0.11	0.04
	404	0.21	0.15	0.05	0.13	0.09	0.03
	506	0.19	0.14	0.04	0.12	0.08	0.03
	608	0.19	0.13	0.04	0.11	0.08	0.03

Table 10: Nozzle diameter ratio, λ

As it can be observed in the following figure, diameter ratio λ increases with higher inlet velocity and lower pressure head. Higher values of λ are preferred since they lead to higher outlet velocity.

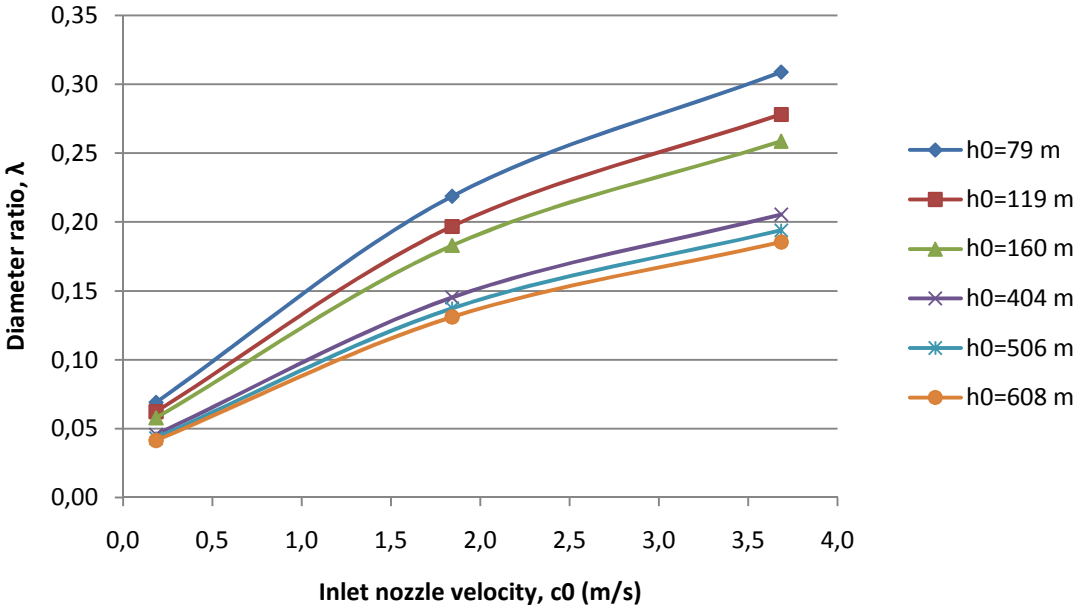

Figure 45: Diameter ratio λ as a function of inlet velocity c_0 for different values of brine pressure head h_0

As it can be observed in the following table, the outlet diameter of the nozzle in the case of permeate flow rate of $0.21\,\mathrm{m^3/h}$ for both $\mathrm{RR} = 20\%$ ($\mathrm{Q_f} = 1.04\,\mathrm{m^3/h}$) and 40% ($\mathrm{Q_f} = 0.52\,\mathrm{m^3/h}$) needs to be from 14 up to 39 times smaller than the inlet diameter of the nozzle.

1/λ		Qf (m^3/h)					
		20.83	10.42	1.04	10.42	5.21	0.52
pf (bar)	8	3.24	4.57	14.45	5.28	7.46	23.60
	12	3.59	5.08	16.05	5.86	8.29	26.20
	16	3.87	5.46	17.27	6.31	8.92	28.20
	40	4.87	6.88	21.76	7.95	11.24	35.54
	50	5.15	7.28	23.02	8.41	11.89	37.60
	60	5.39	7.62	24.11	8.80	12.45	39.37

Table 11: Inverse nozzle diameter ratio, 1/λ

The nozzle efficiency represents energy losses that occur in the nozzles.

$$\text{Nozzle efficiency, } \eta_N = \text{energy at nozzle exit (jet)}/\text{energy at nozzle inlet}$$

$$\Rightarrow \eta_N = \frac{(c_1^2/2 \cdot g)}{(h_0 + c_0^2/2 \cdot g)}$$

$$\Rightarrow \eta_N = \frac{(c_1^2/2 \cdot g)}{H_E}$$

$$\Rightarrow \eta_N = c_1^2/2 \cdot g \cdot H_E \qquad [16]$$

$$\Rightarrow \eta_N = C_v^2$$

Therefore in order to achieve high nozzle efficiency a nozzle with high velocity coefficient needs to be chosen. The velocity coefficient $C_v = 0.97$ for a 60° rounded nozzle and for a rounded orifice and $C_v = 0.98$ for 14° tapered nozzle and a sharp-edged orifice (Thake, 2000). The diameter ratio of a 14° tapered nozzle $\lambda = 0.4$ and the nozzle length $L_{nozzle} = 6 \cdot d_1$. According to equation 14 $c_0 = \lambda^2 \cdot c_1 \Rightarrow c_1 = 6.25 \cdot c_0$. In addition, a nozzle with low diameter ratio λ is preferred, since it results to high outlet velocity. Furthermore, a highly efficient nozzle needs to be as short as possible, in order to minimize friction losses, while its shape has to provide a smooth transition from the inlet diameter to the outlet diameter, as shown in the following figure.

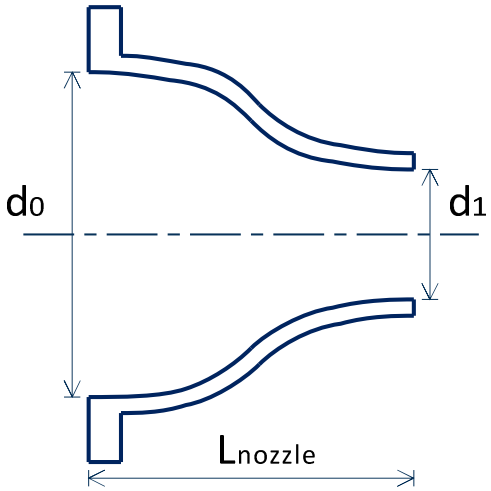

Figure 46: Required nozzle

The number jets, and hence nozzles, does not influence the power output or the efficiency of the Pelton wheel since the same inlet hydraulic energy is subdivided in many streams which exert lower forces on each blade of the wheel and subtracted result to the same overall torque and rotational speed as the one that would be generated by the total inlet stream. However, multiple nozzles are needed since they provide an even distribution of the forces on the wheel that ensures the non-pulsate operation of the wheel and facilitates its angular acceleration at the beginning of its operation (moment of inertia). Therefore, at least four nozzles should be used.

5.1.1.1.2. Runner efficiency

Using Euler's turbine equation, the specific work done by the water is:

$$\Delta W = \frac{\dot{W}}{\dot{m}} = U_1 \cdot c_{\theta 1} - U_2 \cdot c_{\theta 2} > 0$$

For the Pelton turbine, $U_1 = U_2 = U$, $c_{\theta 1} = c_1$ and $c_{\theta 2} = U + w_2 \cdot \cos\beta_2$. So:

$$\Delta W = U \cdot (c_1 - U) \cdot (1 - f \cdot \cos\beta_2)$$

where $f = w_2/w_1 < 1$ is the friction factor and represents the effect of friction on the fluid inside the bucket. In practice, the value of f is usually found to be between 0.8 and 0.9. The friction factor f is defined by the Reynolds number Re and the absolute roughness coefficient k through Moody diagram.

The density of water is $\rho = 998\ kg/m^3$ and the dynamic viscosity $\mu = 1.002 \cdot 10^{-3}\ Pa \cdot s$. The Reynolds number is calculated:

$$Re = \frac{\rho \cdot c_1 \cdot d_1}{\mu}$$

Re		Qf (m^3/h)					
		20.83	10.42	1.04	10.42	5.21	0.52
pfout (bar)	8	4.77E+05	3.37E+05	1.06E+05	2.92E+05	2.06E+05	6.52E+04
	12	5.30E+05	3.74E+05	1.18E+05	3.24E+05	2.29E+05	7.24E+04
	16	5.70E+05	4.03E+05	1.27E+05	3.49E+05	2.46E+05	7.79E+04
	40	7.17E+05	5.07E+05	1.60E+05	4.39E+05	3.11E+05	9.82E+04
	50	7.59E+05	5.37E+05	1.70E+05	4.65E+05	3.29E+05	1.04E+05
	60	7.95E+05	5.62E+05	1.78E+05	4.86E+05	3.44E+05	1.09E+05

Table 12: Reynolds number, Re

Since the Reynolds number is considerably high in all cases, the friction losses are insignificant so the friction factor can be assumed to take the value $f = 0.9$.

Furthermore, due to the shape of the buckets, during the operation of the Pelton wheel, the inlet jet is directed to the following bucket as soon as it stops exerting force to the precedent one. Therefore, no losses occur at this transition and the number of buckets of the Pelton wheel is assumed to be the maximum attainable one (12-16 buckets).

The runner efficiency η_R represents the effectiveness of converting the kinetic energy of the jet into the mechanical energy of the runner.

$$\text{Runner efficiency,}\quad \eta_R = \Delta W / \left(\frac{1}{2} \cdot c_1^2\right) \quad \textbf{[17]}$$

Using the blade speed to jet speed ratio, $\nu = U/c_1$, the runner efficiency is written:

$$\eta_R = U \cdot (c_1 - U) \cdot (1 - f \cdot \cos\beta_2) / \left(\frac{1}{2} \cdot c_1^2\right)$$
$$\Rightarrow \eta_R = 2 \cdot \nu \cdot (1 - \nu) \cdot (1 - f \cdot \cos\beta_2)$$

The variation of the runner efficiency with blade speed-jet speed ratio ν for assumed values of $f = 0.8, 0.9$ and 1.0 and $\beta_2 = 165°$ is shown in the following figure.

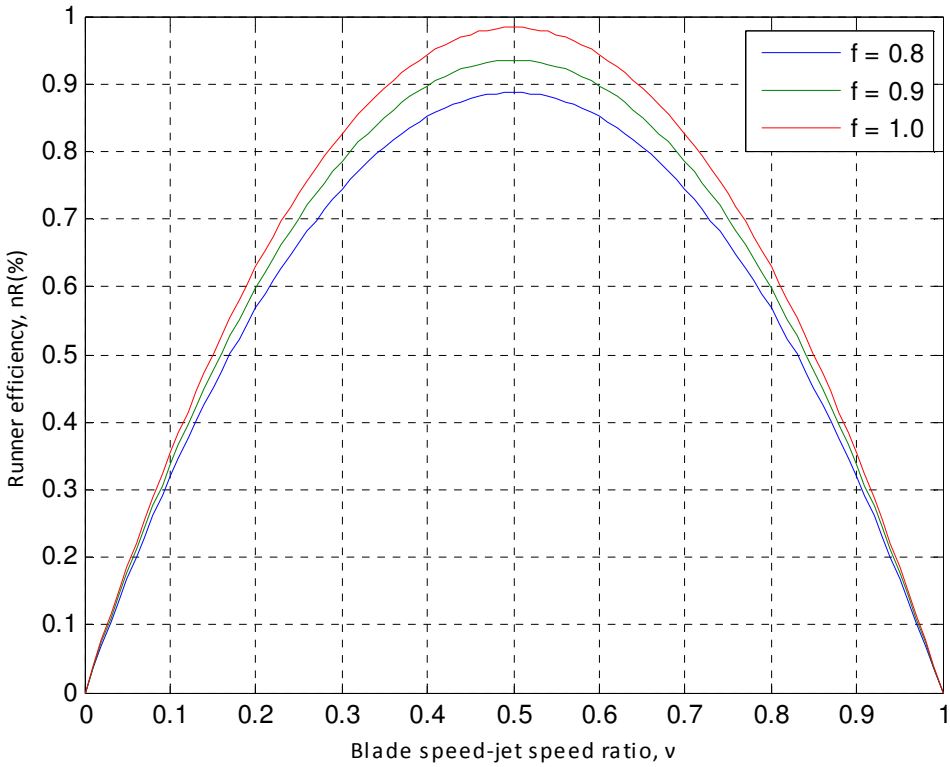

Figure 47: Runner efficiency nR as a function of blade speed-jet speed ratio ν

Thus, it can be derived that maximum efficiency of the runner occurs when $\nu = 0.5$:

$$\eta_{Rmax} = (1 - f \cdot \cos\beta_2)/2$$

By substituting $\beta_2 = 165°$ and $f = 0.9$, the maximum efficiency of the Pelton runner is calculated:

$$\eta_{Rmax} = 93\%$$

5.1.1.1.3. Mechanical efficiency

The mechanical efficiency is related to the energy deficit between the runner and the shaft caused by external losses, such as bearing friction and "windage" losses inside the casing of the runner.

$$\text{Mechanical efficiency, } \eta_m = 1 - (2 \cdot K \cdot \nu^2/\eta_R) = 1 - (K \cdot U^2/\Delta W) \quad \textbf{[18]}$$

Where K is a dimensionless constant of proportionality used to express $\text{loss/unit mass flow} = K \cdot U^2$.

By using the blade speed to jet speed ratio, ν, the mechanical efficiency is written:

$$\eta_m = 1 - \left(K \cdot U^2/\left(U \cdot (c_1 - U) \cdot (1 - f \cdot \cos\beta_2)\right)\right)$$

$$\Rightarrow \eta_m = 1 - \frac{K}{\left(\frac{1}{\nu} - 1\right) \cdot (1 - f \cdot \cos\beta_2)}$$

5.1.1.1.4. Overall efficiency

The overall efficiency of the Pelton turbine is defined as:

$$\eta_0 = \frac{\text{mechanical energy available at output shaft in unit time}}{\text{maximum energy difference possible for the fluid in unit time}}$$

It can be calculated as the product of the hydraulic efficiency η_h and the mechanical efficiency η_m. And since for Pelton turbines the hydraulic efficiency η_h equals to the product of the efficiency of the runner η_R and the nozzle efficiency η_N:

$$\eta_0 = \eta_h \cdot \eta_m = \eta_R \cdot \eta_N \cdot \eta_m \qquad \textbf{[19]}$$

Thus, the overall efficiency of the Pelton turbine can be written as:

$$\eta_0 = \eta_N \cdot (\eta_R - 2 \cdot K \cdot \nu^2) = (\Delta W - K \cdot U^2)/g \cdot H_E \qquad \textbf{[20]}$$

The peak overall efficiency is progressively reduced as the value of K is increased and occurs at lower values of ν than the optimum determined for the runner (ν < 0.5) (Dixon, 2005). Using equation 15 $H_E = c_1^2/(C_v^2 \cdot 2 \cdot g)$ the overall efficiency is written:

$$\eta_0 = (\Delta W - K \cdot U^2)/g \cdot H_E$$

$$\Rightarrow \eta_0 = 2 \cdot C_v^2 \cdot (\nu \cdot (1 - \nu) \cdot (1 - f \cdot \cos\beta_2) - K \cdot \nu^2) \qquad \textbf{[21]}$$

Assuming values of $K = 0, 0.2$ and 0.4 and $\beta_2 = 165°$, $f = 0.9$ and $C_v = 0.98$ the variation of the overall efficiency with blade speed-jet speed ratio is derived.

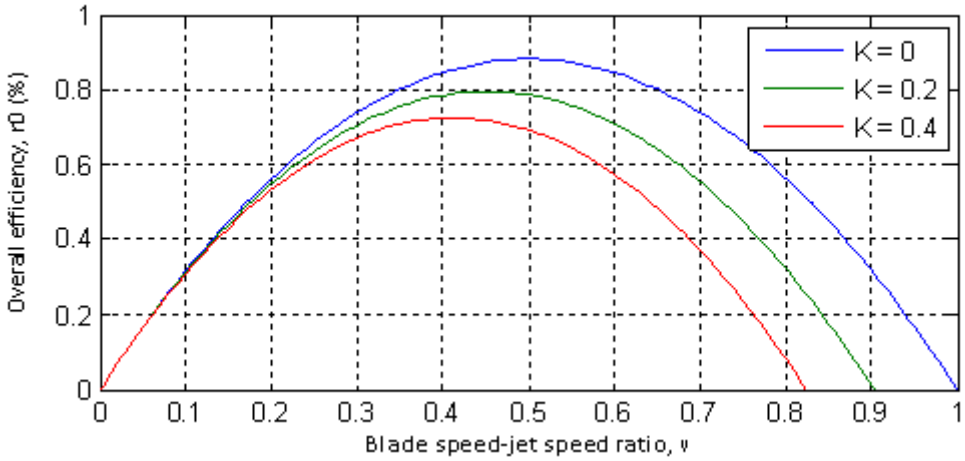

Figure 48: Overall efficiency n_0 as a function of blade speed-jet speed ratio ν

The peak overall efficiency is achieved at lower blade speed-jet speed ratio for higher mechanical losses. In order to determine an average value of the overall efficiency of the Pelton turbine, it is assumed that the blade speed to jet speed ratio takes a typical value $\nu = 0.45$ and $K = 0.2$.

$$\Rightarrow \eta_0 = 0.81$$

According to equation 23 the overall efficiency of the Pelton turbine is dependent on the blade speed-jet speed ratio ν, the velocity coefficient C_v, the bucket angle β_2, the friction factor k and the windage coefficient K. $C_v = 0.98$ is provided by the 14° tapered nozzle. A typical bucket angle is $\beta_2 = 165°$. The friction factor f is assumed to be $f = 0.9$ and the windage coefficient $K = 0.2$. The external losses described by the windage coefficient can reach the value of 10%. The blade speed-jet speed ratio is assumed to take the value $\nu = 0.45$.

5.1.1.2. Motor

Depending on size and type motors are usually 80-95% efficient. The efficiency of a particular motor is provided by the manufacturer (Spellman, et al., 2001). According to DP Pumps (Duijvelaar Pompen, 2013), the efficiency of the motor of the pump can be even higher than 95%. Therefore, the motor efficiency is assumed to be 95%. Using this efficiency the motor power output is calculated. Then, taking into account the motor power output and the rotational speed of the pump (Table 18), the matching motor efficiency is selected (Brook Crompton, 2013). Using this efficiency the motor power output is redefined and the efficiency calculation continues until the power output remains the same. Subsequently, the motor efficiency is presented.

nm (%)		Qf (m^3/h)					
		20.83	10.42	1.04	10.42	5.21	0.52
pfout (bar)	8	84	82	54	78	62	45
	12	87	84	55	82	70	46
	16	90	85	57	83	76	47
	40	92	89	72	88	85	58
	50	93	90	73	90	85	59
	60	93	91	79	90	86	60

Table 13: Motor efficiency, nm (%)

5.1.1.3. Generator

Peak efficiencies of generators at full output vary from 55% to almost 80% (Bradfield, 2008). The efficiency of the generator may exceed 80% but since no gearbox is used between the Pelton turbine and the generator the generator may run at lower speed resulting to lower peak efficiency and therefore the efficiency of 80% is taken account. Using this efficiency the generator power output is calculated. Taking into account the generator power output and the rotational speed of the Pelton turbine (Table 23), the correspondent motor efficiency is selected (Brook Crompton, 2013). A 5% reduction is assumed since induction machines have lower efficiency when used as generators (Smith, 2008). Using the derived generator efficiency the generator power output is redefined and the efficiency calculation continues until the power output remains the same. Subsequently, the generator efficiency is presented.

ne (%)		Qf (m^3/h)					
		20.83	10.42	1.04	10.42	5.21	0.52
pfout (bar)	8	79	74	49	73	60	40
	12	82	78	48	75	66	41
	16	85	81	56	78	71	42
	40	88	85	69	84	80	53
	50	88	86	70	85	81	55
	60	88	87	74	85	82	56

Table 14: Generator efficiency, ne (%)

5.1.1.4. Pump

In the case Pelton-driven generator connected to a motorised pump various types of pumps are applicable according to the flow rate and the pressure head required. Different types of centrifugal pumps may be applied such as single stage pumps and multistage pumps. In addition, positive displacement pumps are also applicable, such as axial piston pumps.

The efficiency of the centrifugal pump is calculated:

$$n_1 = n_m \cdot n_v \cdot n_h$$

The mechanical efficiency, n_m, accounts for the bearing, stuffing box, and all disk friction losses including those in the wearing rings and balancing disks or drums present. The volumetric efficiency, n_v, accounts for leakage through the wearing rings, internal labyrinths, balancing devices and glands. The hydraulic efficiency, n_h, accounts for friction losses in all through flow passages, including the suction elbow or nozzle, impeller, diffusion vanes, volute casing, and the crossover passages of multistage pumps (Karassik, et al., 2008).

The efficiency of a centrifugal pump as well as the capacity (flow rate), the total head and the power required by the pump are shown on the pump curve which is provided by the manufacturer. The characteristics of the pump are related to each other. The pump efficiency changes as the head against which the pump is working changes, as the power supplied to the pump changes and as the flow rate changes (Spellman, et al., 2001). In addition, centrifugal pumps that operate at higher range of flow rate have higher efficiency. The peak efficiency of centrifugal pumps proposed by manufacturers varies between 30-80%.

As observed in Figure 49, the efficiency of centrifugal pumps decreases with lower feed flow rate. Therefore, centrifugal pumps are mostly applicable for low recovery ratio and high permeate flow rate that result to high feed flow rate.

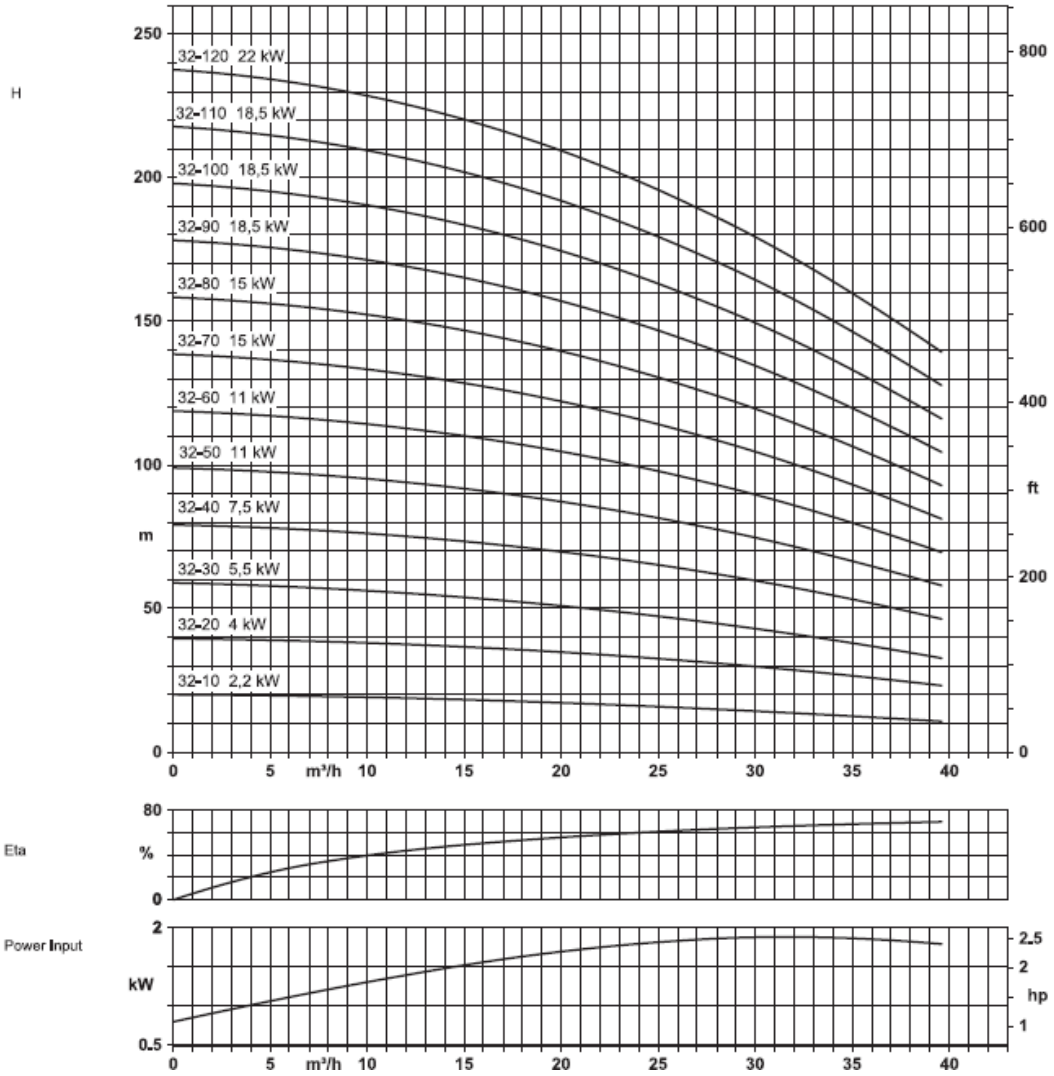

Figure 49: Performance curve, efficiency curve and power curve of multistage centrifugal pump (Duijvelaar Pompen, 2013)

Multistage pumps have higher efficiency than single stage pumps. In addition, multistage pumps deliver higher pressure head and handle lower flow rate than single stage pumps. Hence, multistage pumps, which reach their peak efficiency at the selected values of feed flow rate, are chosen. Their efficiencies are presented below (Duijvelaar Pompen, 2013).

Qf (m^3/h)	20.83	10.42	1.04	10.42	5.21	0.52
n1 (%)	71	67	34	67	60	25

Table 15: Multistage centrifugal pump efficiency (Duijvelaar Pompen, 2013)

Qf (m^3/h)	20.83	10.42	1.04	10.42	5.21	0.52
DP Series	32	16	2	16	4	2
N (rpm)	2900					

Table 16: DP multistage centrifugal pumps (Duijvelaar Pompen, 2013)

On the other hand, piston pumps are proposed to deliver peak efficiency from 61% up to 90% (Grundfos A/S, 2013). In addition, piston pumps deliver much higher pressure build-up (around 100 bar) and have higher efficiency than centrifugal pumps, but handle lower flow

rate. Furthermore, the flow rate is dependent on the rotational speed of the piston pump. Grundfos Booster Module Piston (BMP) Pumps series BMP-R, developed for sea water applications, deliver rated pressure build-up of 80 bar and handle flow rate up to 10.2 m^3/h.

As it is shown in Figure 50, the performance curve of piston pumps is linear, constant pressure head is delivered at any flow rate. Since in the case of the energy recovery device the required pressure head is lower than the rated pressure head provided by the piston pumps, it is assumed that for lower pressure head delivered the efficiency remains the same.

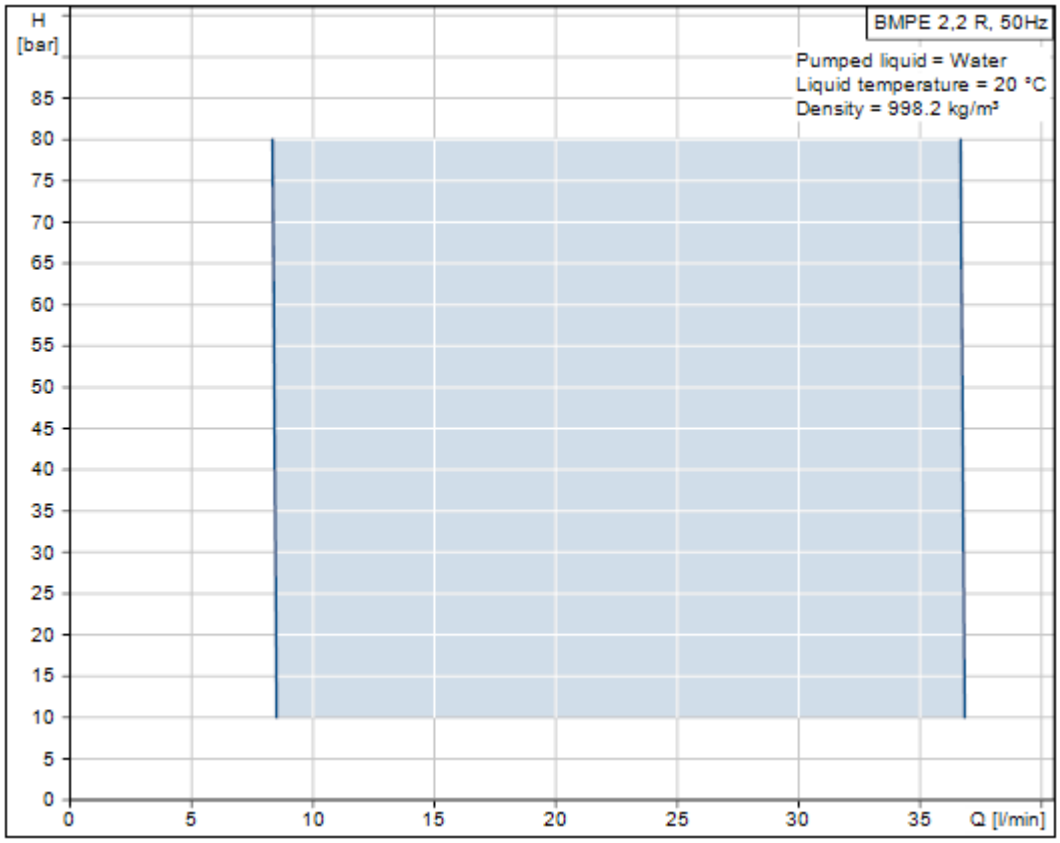

Figure 50: Performance curve of piston pump (Grundfos A/S, 2013)

The efficiency of piston pumps at the selected feed flow rates are presented below.

Qf (m^3/h)	20.83	10.42	1.04	10.42	5.21	0.52
n1 (%)	-	81	89	81	84	76

Table 17: Axial piston pump efficiency (Grundfos A/S, 2013)

Qf (m^3/h)	20.83	10.42	1.04	10.42	5.21	0.52
BMPE (50Hz)	-	10.2 R	1.0 R	10.2 R	5.1 R	0.6 R
N (rpm)	-	700, 1800	700, 3000	700, 1800	700, 1800	700, 3000

Table 18: Grundfos BMPE piston pumps (Grundfos A/S, 2013)

The peak efficiency of 89% is achieved at $1.04\,m^3/h$ while the maximum attainable feed flow rate for piston pumps is $10.2\,m^3/h$ and hence piston pumps cannot handle feed flow rate of $20.83\,m^3/h$. Therefore, piston pumps are suggested for low feed flow rates.

5.1.1.5. Gearbox

The efficiency of gear units is mainly determined by the gearing and bearing friction. Different gear types exist that deliver different gear ratios. The gear ratio is the ratio of the input gear rotational speed to the output gear rotational speed.

Spur gearing, the most common gear type, is a parallel shaft arrangement that handles low gear ratios and provides much higher efficiency than other gear types. Straight bevel gearing is similar to spur gearing with perpendicular shaft arrangement. As in the case of spur gearing, straight bevel gearing delivers only low gear ratios with high efficiency. Because of the different tooth shape, spiral bevel gearing delivers less noise and vibrations compared to straight bevel gears, resulting to higher efficiency. The efficiency of helical, parallel shaft and helical-bevel gear units varies with number of gear stages, between 94% (3-stage) and 98% (1-stage). The efficiency of worm gearing can be significantly low due to the different configuration of the gears. Cycloid gearing can work at high efficiency at relatively high gear ratios, above 30:1. Hypoid gearing is also designed for high gear ratios. The gear ratio and the efficiency of the aforementioned gearing types are presented at the following table.

Type	Gear ratio R	Efficiency ng (%)
Spur	1:1 to 6:1	94-98
Straight bevel	3:2 to 5:1	93-97
Spiral bevel	3:2 to 4:1	95-99
Helical	3:2 to 10:1	94-98
Worm	5:1 to 75:1	50-90
Cycloid	10:1 to 100:1	75-85
Hypoid	10:1 to 200:1	80-95

Table 19: Gearbox efficiency comparison

In the case of Pelton-driven generator, the generator used is available at different rotational speeds between 750 rpm and 3,000 rpm, while the Pelton turbine rotational speed ranges from 827 rpm to 2301 rpm. Hence, the difference between the rotational speed of the Pelton turbine and the generator is minor and no gearbox is used at this configuration.

In the case of Pelton-driven pump (Paragraph 5.2) the use of gearbox is considered since both the Pelton turbine and the pump are critical components that define the operational stability of the energy recovery device and RO process. In the case of Pelton-driven centrifugal pump, the centrifugal pump rotates with 2900 rpm (Duijvelaar Pompen, 2013), while the rotational speed of the Pelton turbine ranges between 827 rpm and 2301 rpm. In the case of Pelton-driven piston pump, the rotational speed of the piston pump is 700 rpm, 1800 rpm and 3000 rpm for the examined feed flow rates (Table 18), while the rotational speed of the Pelton turbine ranges between 827 rpm and 2301 rpm.

Taking into account all cases, the gear ratio required ranges from 1:1.26 to 1:3.63, while the highest power input of the gearbox is 22.37 kW. Therefore, a speed increaser designed for low gear ratios and low power input is required. Spur and helical single stage gearboxes can be applied as speed increasers with maximum gear ratio of 1:4. As long as the input and specifications of the reducer gearbox match with the specifications of the increaser application, the same efficiency is assumed. Hence, it is assumed that a single stage spur gearbox is used as speed increaser with efficiency of 95%.

5.1.1.6. Overall efficiency

Thus, taking into account the efficiency of the Pelton wheel (n_0), the generator (n_e), the pump motor (n_m) and the centrifugal pump or the piston pump (n_1), the overall efficiency is calculated for the different flow rates:

$$n_t = n_1 \cdot n_m \cdot n_e \cdot n_0$$

nt (%)		Qf (m^3/h)					
		20.83	10.42	1.04	10.42	5.21	0.52
pfout (bar)	8	38	33	7	31	18	4
	12	41	36	7	33	22	4
	16	44	37	9	35	26	4
	40	47	41	14	40	33	6
	50	47	42	14	42	33	7
	60	47	43	16	42	34	7

Table 20: Overall efficiency of Pelton-driven generator using multistage centrifugal pump (CP)

nt (%)		Qf (m^3/h)					
		20.83	10.42	1.04	10.42	5.21	0.52
pfout (bar)	8	-	40	19	38	25	11
	12	-	43	19	41	31	12
	16	-	45	23	43	37	12
	40	-	50	36	49	46	19
	50	-	51	37	50	47	20
	60	-	52	42	50	48	21

Table 21: Overall efficiency of Pelton-driven generator using piston pump (PP)

The efficiency of both systems for the examined feed flow rates and recovery ratio $RR = 20\%$ and $RR = 40\%$ is presented at the following figures.

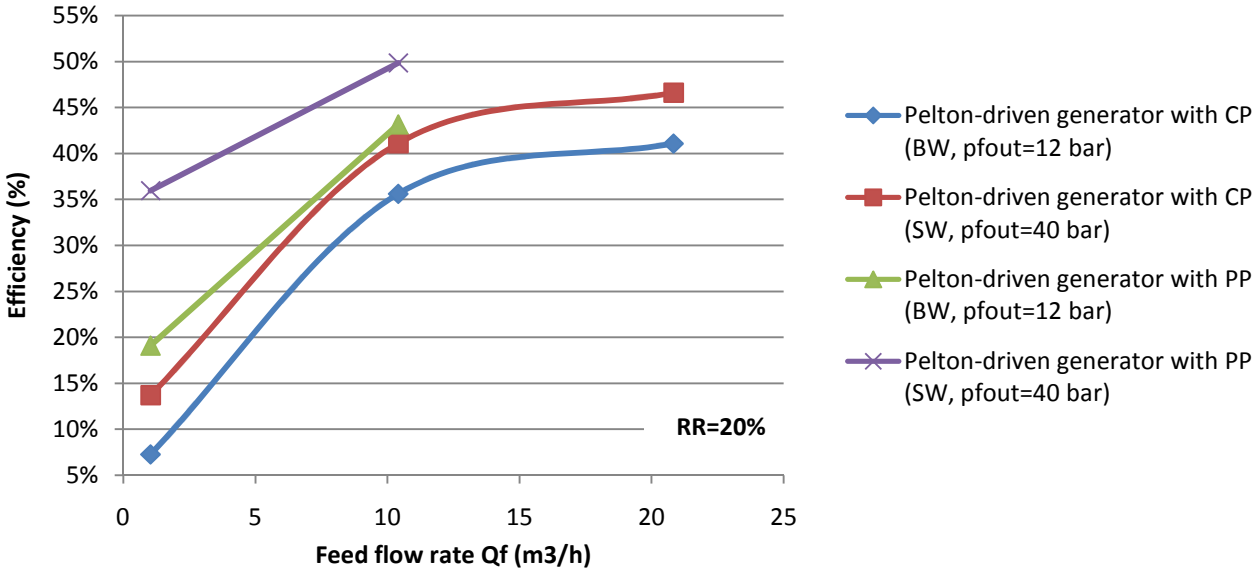

Figure 51: Efficiency of Pelton-driven generator with CP and PP respectively for selected flow rates (RR=20%)

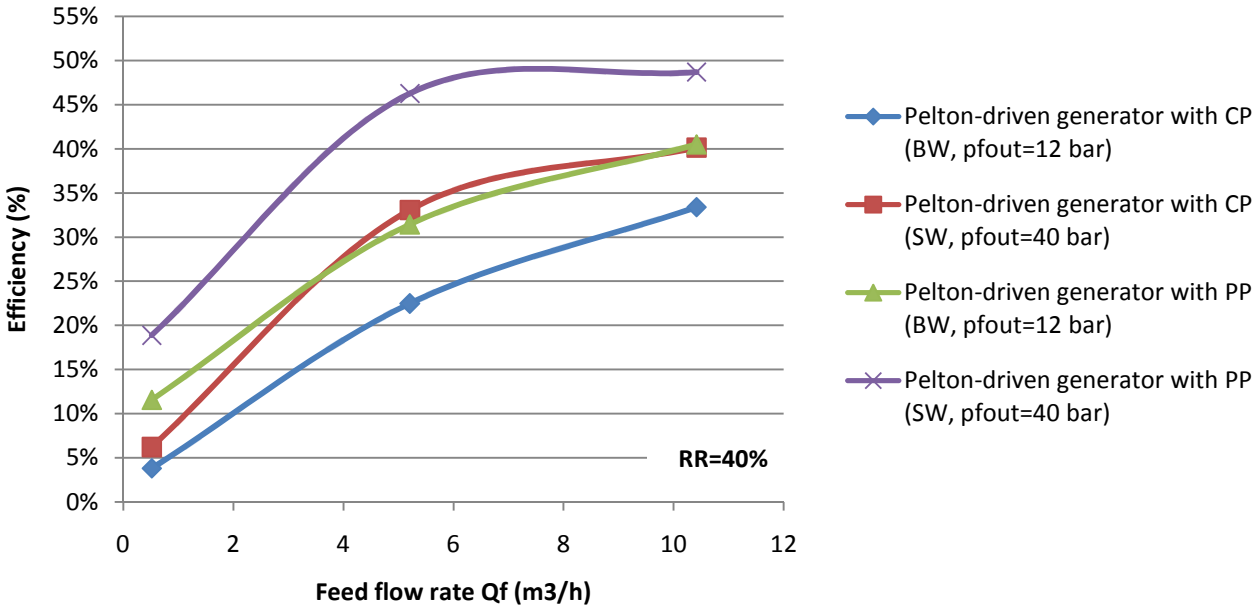

Figure 52: Efficiency of Pelton-driven generator with CP and PP respectively for selected flow rates (RR=40%)

5.1.2. Power and pressure requirements

In order to examine the feasibility of RO desalination using energy recovery with the given configuration, pressure and power requirements of the ERD are estimated.

5.1.2.1. Pelton turbine

The power output of the Pelton turbine delivered to the shaft is given by:

$$P_s = p_0 \cdot Q_0 \cdot \eta_0 \qquad [22]$$

Where $p_0 = \gamma \cdot h_0$ and $Q_0 = A_0 \cdot c_0$ and γ is the specific weight of water.

The mechanical power available at the turbine shaft can also be determined by measuring the torque τ on the shaft at a corresponding angular speed ω (Agar, et al., 2008). The torque

is found by measuring the tangential force F on a brake lever with moment arm length l, while simultaneously measuring the rotational speed r of the shaft. The shaft power is:

$$P_s = \omega \cdot \tau = 2 \cdot \pi \cdot l \cdot F \qquad [23]$$

The angular speed ω is the tangential speed of the turbine U divided by the pitch radius L of the Pelton wheel:

$$\omega = U/L \qquad [24]$$

As already described the blade speed to jet speed ratio is assumed $\nu = 0.45$, so the blade speed is calculated using the equation:

$$U = \nu \cdot c_1$$

U (m/s)		Qf (m^3/h)					
		20.83	10.42	1.04	10.42	5.21	0.52
pfout (bar)	8	17.39	17.33	17.32	17.33	17.32	17.31
	12	21.41	21.36	21.34	21.35	21.35	21.34
	16	24.78	24.74	24.72	24.73	24.73	24.72
	40	39.30	39.27	39.27	39.27	39.27	39.27
	50	43.98	43.95	43.95	43.95	43.95	43.95
	60	48.20	48.18	48.17	48.18	48.17	48.17

Table 22: Blade speed, U (m/s)

Assuming the wheel diameter is $D = 0.4\ m$, the rotational speed of the Pelton wheel is calculated using the equation:

$$\omega_{cyc} = \frac{U \cdot 60}{\pi \cdot D}$$

ωcyc (rpm)		Qf (m^3/h)					
		20.83	10.42	1.04	10.42	5.21	0.52
pfout (bar)	8	830	828	827	827	827	827
	12	1022	1020	1019	1019	1019	1019
	16	1183	1181	1181	1181	1181	1181
	40	1876	1875	1875	1875	1875	1875
	50	2100	2099	2098	2098	2098	2098
	60	2301	2300	2300	2300	2300	2300

Table 23: Rotational speed of the Pelton wheel, ωcyc (rpm)

As it is shown in the following figure the rotational speed of the Pelton wheel is higher for higher pressure provided at the inlet of the membranes, while there is minor difference between the values of the rotational speed for different flow rates. The rotational speed of the Pelton wheel can also be increased by decreasing the diameter of the wheel.

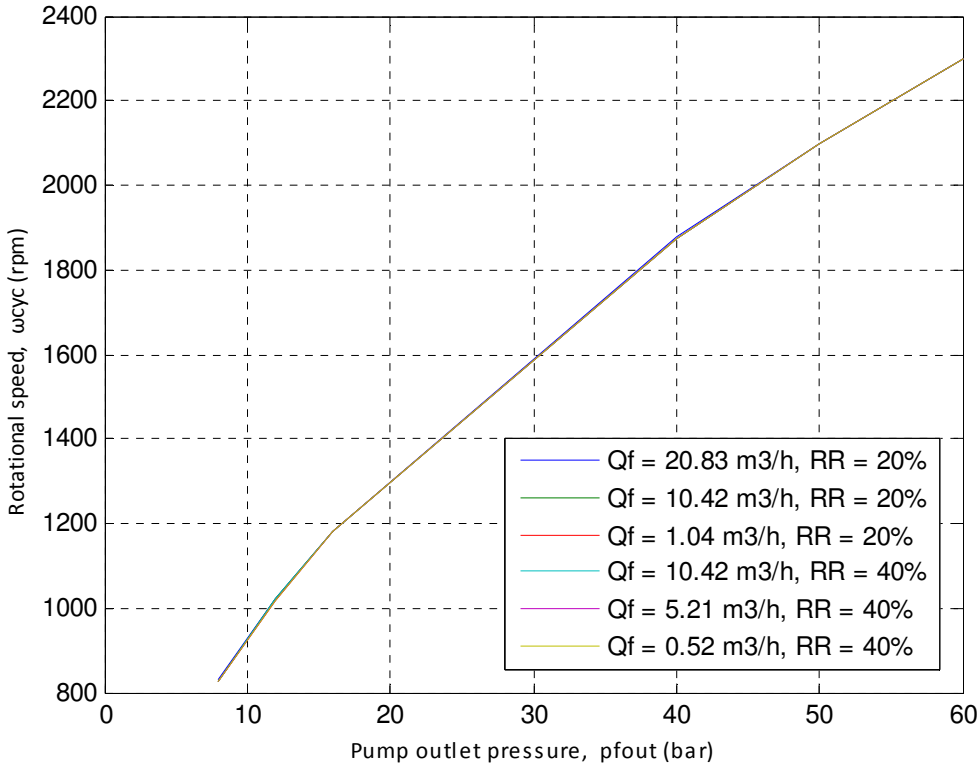

Figure 53: Rotational speed for the selected values of pump outlet pressure

As mentioned in paragraph 5.1.1.1., the Pelton turbine efficiency is assumed to be $n_0 = 81.09\%$, so using the examined values of pressure and flow rate the power output of the Pelton turbine delivered to the shaft is calculated:

$$P_s = p_b \cdot Q_b \cdot n_0$$

Ps (kW)		Qf (m^3/h)					
		20.83	10.42	1.04	10.42	5.21	0.52
pf (bar)	8	2.89	1.45	0.14	1.08	0.54	0.05
	12	4.39	2.20	0.22	1.65	0.82	0.08
	16	5.89	2.95	0.29	2.21	1.11	0.11
	40	14.87	7.43	0.74	5.57	2.79	0.28
	50	18.62	9.31	0.93	6.98	3.49	0.35
	60	22.37	11.19	1.12	8.39	4.20	0.42

Table 24: Pelton turbine power output, Ps (kW)

5.1.2.2. Generator

When the turbine shaft is coupled to an electric generator which supplies electricity to a variable resistive load R, the electrical power Pe of the load is:

$$P_e = I \cdot V \qquad \textbf{[25]}$$

in which I is the load current and V the voltage across the load. The electrical efficiency n_e of the generator is:

$$n_e = P_e/P_s = I \cdot V/2 \cdot \pi \cdot l \cdot F \quad \textbf{[26]}$$

The generator power output is calculated:

$$P_e = n_e \cdot P_s$$

Pe (kW)		Qf (m^3/h)					
		20.83	10.42	1.04	10.42	5.21	0.52
pfout (bar)	8	2.28	1.07	0.07	0.79	0.33	0.02
	12	3.60	1.71	0.11	1.24	0.54	0.03
	16	5.01	2.39	0.17	1.72	0.78	0.05
	40	13.08	6.32	0.51	4.68	2.23	0.15
	50	16.39	8.01	0.65	5.94	2.83	0.19
	60	19.69	9.73	0.83	7.13	3.44	0.23

Table 25: Generator power output, Pe (kW)

5.1.2.3. Motor

Using the motor efficiency, n_m, the motor power output is calculated:

$$P_m = n_m \cdot P_e$$

Pm (kW)		Qf (m^3/h)					
		20.83	10.42	1.04	10.42	5.21	0.52
pfout (bar)	8	1.92	0.88	0.04	0.62	0.20	0.01
	12	3.13	1.44	0.06	1.01	0.38	0.02
	16	4.51	2.03	0.09	1.43	0.60	0.02
	40	12.04	5.62	0.37	4.12	1.90	0.09
	50	15.24	7.21	0.48	5.34	2.40	0.11
	60	18.31	8.86	0.65	6.42	2.96	0.14

Table 26: Motor power output, Pm (kW)

5.1.2.4. Pump

The power output of the pump, P_1^{out}, is calculated by the power input, P_1^{in}, multiplied to the efficiency of the pump n_1.

$$\left(p_f^{out} - p_f^{in}\right) \cdot Q_f = n_1 \cdot P_m \quad \textbf{[27]}$$

$$\Rightarrow \left(p_f^{out} - p_f^{in}\right) \cdot Q_f = n_1 \cdot n_m \cdot n_e \cdot n_0 \cdot p_b \cdot Q_b$$

The pressure drop at the membrane element is Δp, so $p_b = p_f^{out} - \Delta p$:

$$\Rightarrow \left(p_f^{out} - p_f^{in}\right) \cdot Q_f = n_1 \cdot n_m \cdot n_e \cdot n_0 \cdot \left(p_f^{out} - \Delta p\right) \cdot Q_b$$

Using $Q_b = (1 - RR) \cdot Q_f$ and $n_t = n_1 \cdot n_m \cdot n_e \cdot n_0$

$$\Rightarrow \left(p_f^{out} - p_f^{in}\right) = n_t \cdot \left(p_f^{out} - \Delta p\right) \cdot (1 - RR)$$

$$\Rightarrow p_f^{in} = p_f^{out} - n_t \cdot \left(p_f^{out} - \Delta p\right) \cdot (1 - RR) \quad \textbf{[28]}$$

According to equation 31, the pump inlet pressure is not dependent on the flow rate, but on the recovery ratio. However, since the efficiency of the pump is changing for different flow

rates, the pump inlet pressure is indirectly dependent on the flow rate. Using the overall efficiency of Pelton-driven generator with centrifugal pump, n_t, calculated in Table 19, and the examined values of membrane feed pressure p_f^{out} and recovery ratio RR, the required pump inlet feed pressure is calculated.

pfin (bar)		Qf (m^3/h)					
		20.83	10.42	1.04	10.42	5.21	0.52
pfout (bar)	8	5.65	5.97	7.55	6.57	7.16	7.83
	12	8.16	8.67	11.32	9.65	10.42	11.73
	16	10.47	11.30	14.89	12.69	13.53	15.62
	40	25.23	26.98	35.66	30.46	32.14	38.52
	50	31.30	33.31	44.41	37.63	40.03	48.04
	60	37.53	39.49	52.32	45.14	47.73	57.56

Table 27: Pressure required at the inlet of the centrifugal pump

Using the overall efficiency of Pelton-driven generator with piston pump n_t, calculated in Table 20, the correspondent pump inlet feed pressure is calculated:

pfin (bar)		Qf (m^3/h)					
		20.83	10.42	1.04	10.42	5.21	0.52
pfout (bar)	8	-	5.54	6.82	6.27	6.83	7.49
	12	-	7.96	10.21	9.16	9.79	11.19
	16	-	10.30	13.10	11.98	12.54	14.86
	40	-	24.21	28.61	28.43	29.00	35.51
	50	-	29.77	35.33	35.00	36.05	44.07
	60	-	35.13	39.83	41.98	42.83	52.62

Table 28: Pressure required at the inlet of the piston pump

At the following figures the inlet feed pressure, pfin, is shown, for brackish water desalination of RO pressure of 12 bar and seawater desalination of RO pressure of 40 bar, for both Pelton-driven generators with centrifugal pump and piston pump, for $RR = 20\%$ and $RR = 40\%$.

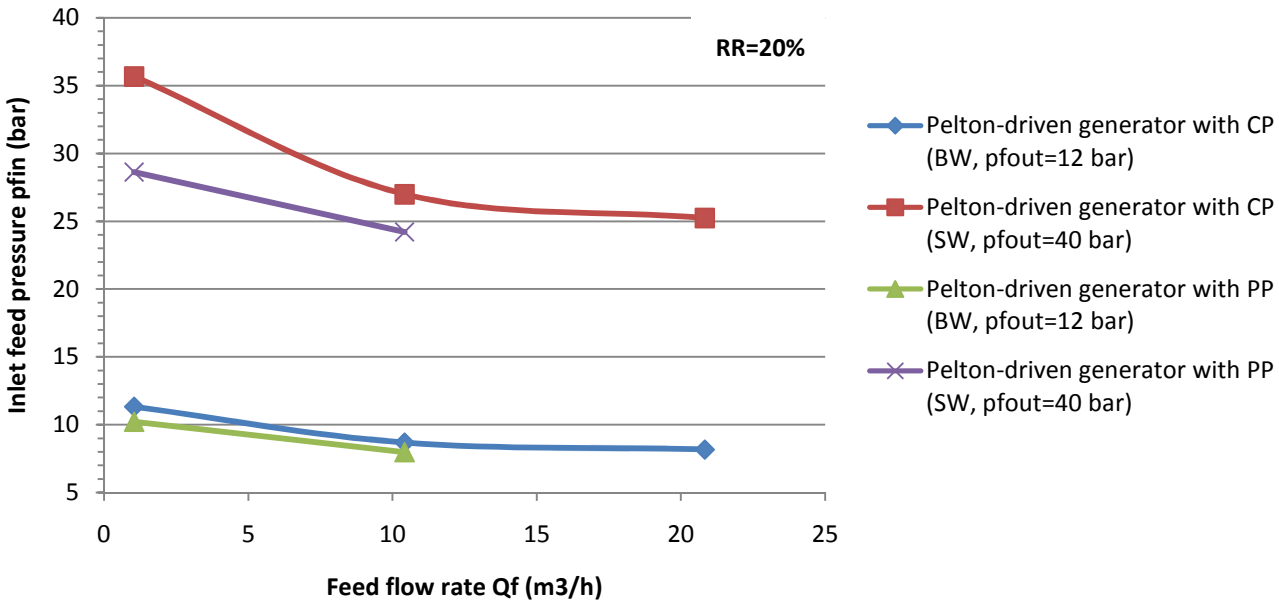

Figure 54: Inlet feed pressure for Pelton-driven generator with CP and PP (RR=20%)

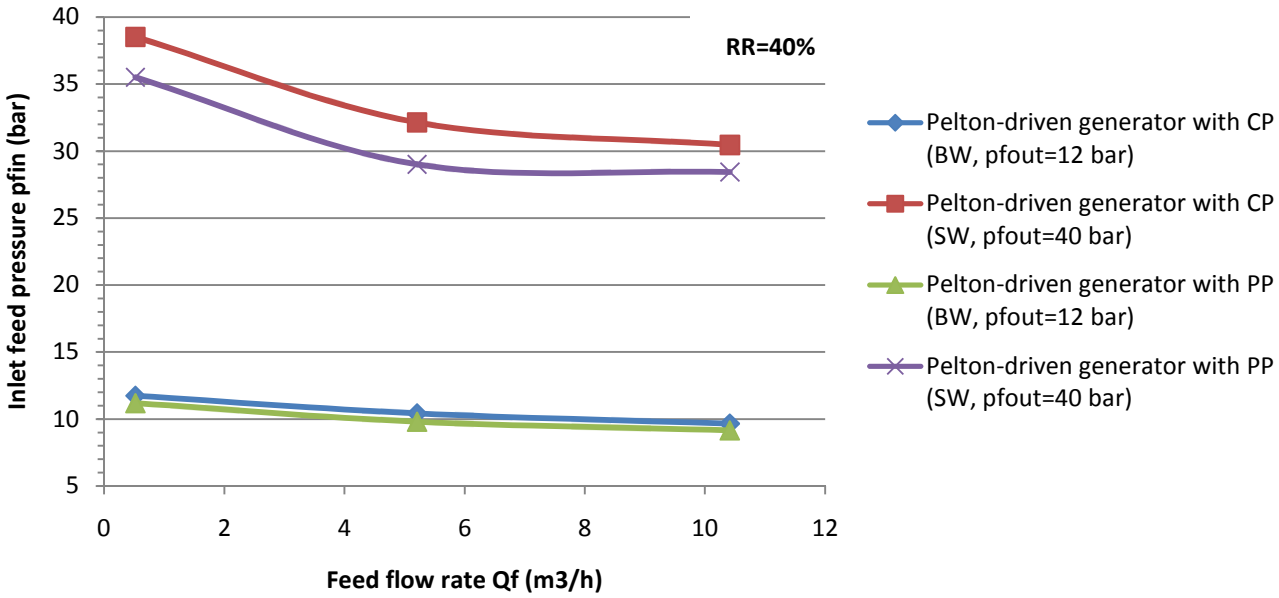

Figure 55: Inlet feed pressure for Pelton-driven generator with CP and PP (RR=20%)

Apart from the pressure required at the inlet of the pump, pfin, another indicator of the performance of the energy recovery device is the percentage of the power required at the inlet of the membranes that is provided by the recovered power:

$$\frac{P_{rec}}{P_{out}} = \frac{p_b \cdot Q_b \cdot n_t}{p_f^{out} \cdot Q_f}$$

But $p_b \cdot Q_b \cdot n_t = \left(p_f^{out} - p_f^{in}\right) \cdot Q_f$, so:

$$\Rightarrow \frac{P_{rec}}{P_{out}} = \frac{\left(p_f^{out} - p_f^{in}\right) \cdot Q_f}{p_f^{out} \cdot Q_f} = \frac{p_f^{out} - p_f^{in}}{p_f^{out}}$$

So in the case of Pelton-driven generator with a centrifugal pump the percentage of the power provided to the membranes that is provided by the recovered power is:

Prec/Pout (%)		Qf (m^3/h)					
		20.83	10.42	1.04	10.42	5.21	0.52
pfout (bar)	8	29	25	6	18	10	2
	12	32	28	6	20	13	2
	16	35	29	7	21	15	2
	40	37	33	11	24	20	4
	50	37	33	11	25	20	4
	60	37	34	13	25	20	4

Table 29: Percentage of power output provided by the recovered power (CP)

In the case of Pelton-driven generator with a piston pump the percentage of the power provided to the membranes that is provided by the recovered power is:

Prec/Pout (%)		Qf (m^3/h)					
		20.83	10.42	1.04	10.42	5.21	0.52
pfout (bar)	8	-	31	15	22	15	6
	12	-	34	15	24	18	7
	16	-	36	18	25	22	7
	40	-	39	28	29	27	11
	50	-	40	29	30	28	12
	60	-	41	34	30	29	12

Table 30: Percentage of power output provided by the recovered power (PP)

At the following figures the power ratio, Prec/Pout (%), is shown, for brackish water desalination of RO pressure of 12 bar and seawater desalination of RO pressure of 40 bar, for both Pelton-driven generators with centrifugal pump and piston pump, for $\mathrm{RR} = 20\%$ and $\mathrm{RR} = 40\%$.

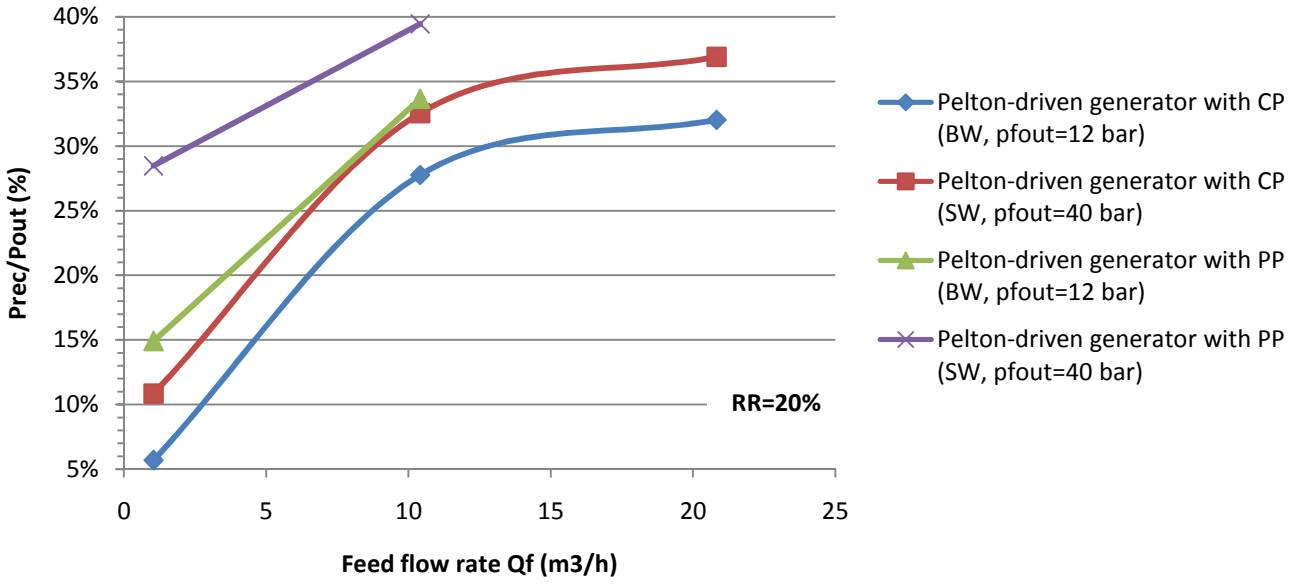

Figure 56: Power ratio Prec/Pout for Pelton-driven generator with CP and PP (RR=20%)

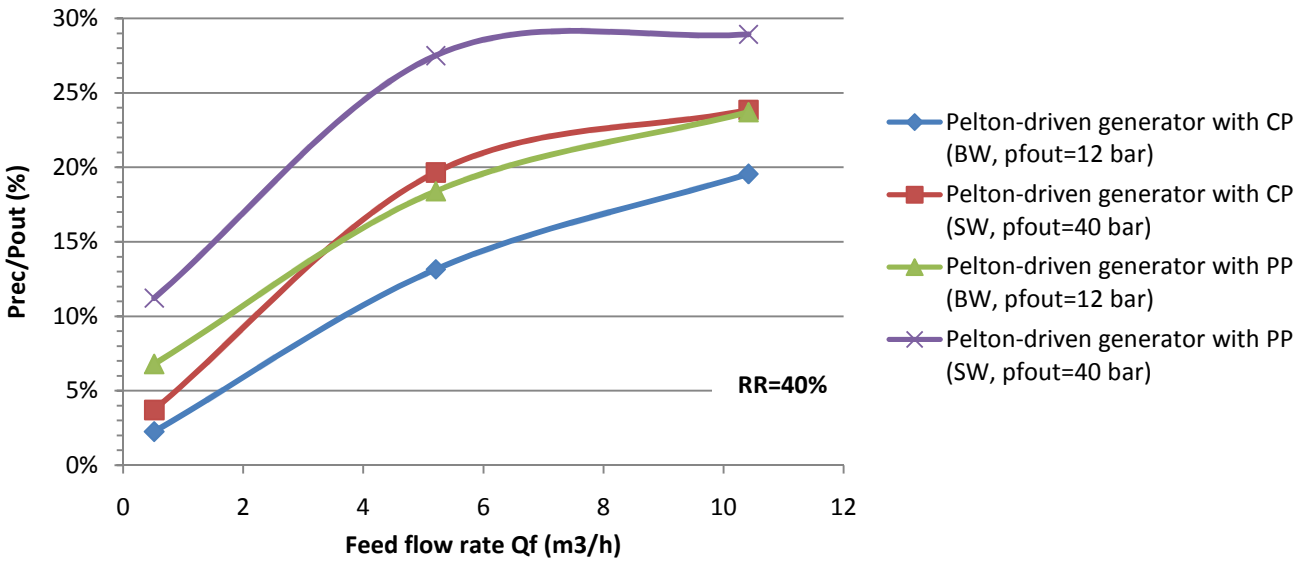

Figure 57: Power ratio Prec/Pout for Pelton-driven generator with CP and PP (RR=40%)

Thus, the power ratio for piston pumps is higher than centrifugal pumps especially for low feed flow rates where the power ratio of centrifugal pumps is significantly low.

5.1.3. Energy autonomy

For the case of Pelton-driven generator the recovery ratio may need to be fixed since the pump and the Pelton turbine are not directly connected. In order to maintain the permeate flow rate at a specific value an electronically controlled valve that will direct the brine stream through an additional nozzle may be used, so additional energy will be required.

5.1.4. Operational stability

The recovery ratio may need to be stabilised using an auxiliary valve at the entrance of the Pelton turbine which will direct the brine stream to an additional nozzle. The nozzles of the Pelton turbine already present in the configuration may also contribute to the regulation of the recovery ratio.

5.1.5. Cost analysis

The cost of the Pelton turbine with a casing with four nozzles is assumed to be 500-1,000 €. The generator cost is estimated around 500-1,500 €.

Regarding the motorised pump the cheapest solution is the single stage centrifugal pump (around 130 €), followed by the multistage centrifugal pump (around 230 €, Grundfos CMV 319-661 €) and the piston pump (Grundfos around 3,783-6,429 €). The multistage pumps taken into account in the previous paragraph are manufactured by DP Pumps and the cost of the series used is presented below.

Qf (m^3/h)	20.83	10.42	1.04	10.42	5.21	0.52
DP pump series	32	16	2	16	4	2
Price (€)	3,000	2,500	2,000	2,500	2,000	2,000

Table 31: DP multistage centrifugal pumps prices (Duijvelaar Pompen, 2013)

The cost of the piston pump is presented at the following table.

Qf (m^3/h)	20.83	10.42	1.04	10.42	5.21	0.52
BMPE pump no.	-	10.2 R	1.0 R	10.2 R	5.1 R	0.6 R
Price (€)	-	7,000	3,500	7,000	5,700	3,500

Table 32: Grundfos BMPE piston pumps (HYDROLOGY, 2013)

Assuming costs of 500 € for the Pelton wheel and its casing, 500 € for the generator and using the cost of the motorised multistage pump estimated above, the total cost of the Pelton-driven generator using a multistage pump is estimated.

Qf (m^3/h)	20.83	10.42	1.04	10.42	5.21	0.52
Total cost (€)	4,000	3,500	3,000	3,500	3,000	3,000

Table 33: Pelton-driven generator with motorised multistage centrifugal pump

In the same way, the overall cost of the Pelton-driven generator using a piston pump is estimated.

Qf (m^3/h)	20.83	10.42	1.04	10.42	5.21	0.52
Total cost (€)	-	8,000	4,500	8,000	6,700	4,500

Table 34: Pelton-driven generator with motorised piston pump

5.1.6. Manufacturing complexity

In order to develop the Pelton-driven generator with pump, the Pelton turbine needs to be connected to the shaft of the generator which has to be wired to the motor of the pump.

5.2. Pelton-driven pump

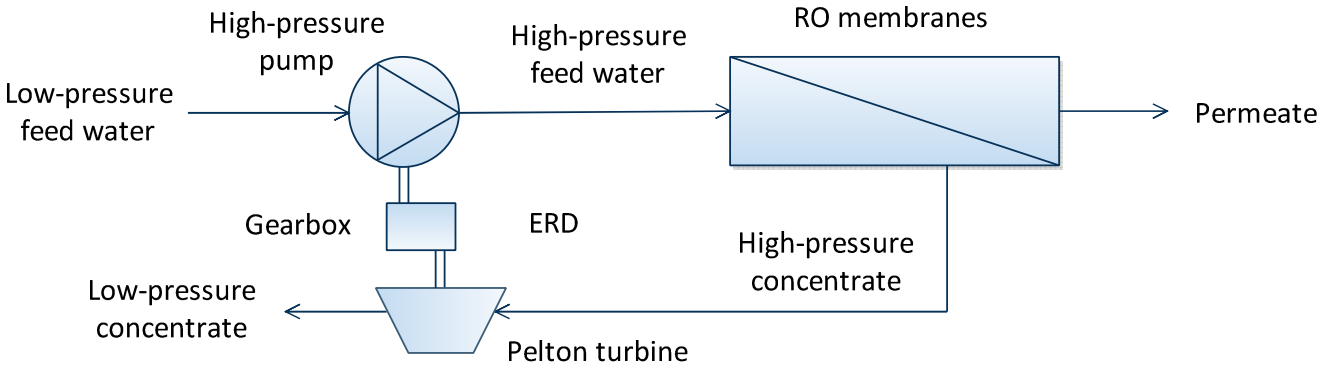

Figure 58: Pelton-driven pump with gearbox

5.2.1. Energy efficiency

In the case of Pelton-driven pump, the Pelton turbine is coupled to the pump but the rotational speed of the two components is different. Both the Pelton turbine and the pump are critical components of the configuration since they define the operational stability of the energy recovery device and RO process and, hence, need to operate at the rated rotational speed. Therefore, the use of gearbox is considered.

As explained in Paragraph 5.1, the efficiency of the Pelton turbine is assumed to be $\eta_0 = 0.81$, the efficiency of the spur gearbox is assumed to be 95% and the efficiency of multistage centrifugal pump and piston pump for the selected flow rates is assumed to be:

Qf (m^3/h)	20.83	10.42	1.04	10.42	5.21	0.52
n1 (%)	71	67	34	67	60	25

Table 35: Multistage centrifugal pump efficiency (Duijvelaar Pompen, 2013)

Qf (m^3/h)	20.83	10.42	1.04	10.42	5.21	0.52
n1 (%)	-	81	89	81	84	76

Table 36: Piston pump efficiency (Grundfos A/S, 2013)

Thus, taking into account the efficiency of the Pelton turbine (n_0), the gearbox (n_g) and the centrifugal pump or the piston pump (n_1), the overall efficiency is calculated for the different flow rates:

$$n_t = n_1 \cdot n_g \cdot n_0$$

Qf (m^3/h)	20.83	10.42	1.04	10.42	5.21	0.52
nt (%)	55	52	26	52	46	19

Table 37: Overall efficiency of Pelton-driven centrifugal pump (CP) with gearbox

Qf (m^3/h)	20.83	10.42	1.04	10.42	5.21	0.52
nt (%)	-	63	69	63	65	58

Table 38: Overall efficiency of Pelton-driven piston pump (PP) with gearbox

The efficiency of both systems for the examined feed flow rates and recovery ratio $RR = 20\%$ and $RR = 40\%$ is shown at the following figures. Thus, the Pelton-driven piston pump with gearbox has the highest overall efficiency (up to 69%) among the Pelton-driven ERDs for both brackish and seawater desalination and all examined flow rates.

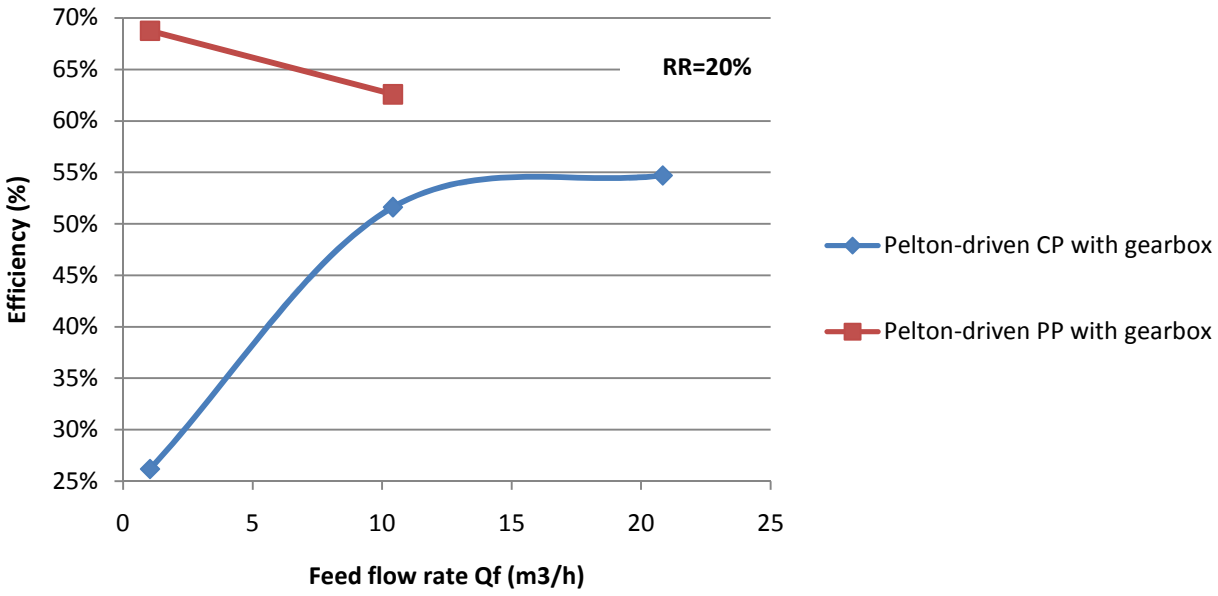

Figure 59: Efficiency of Pelton-driven CP and PP respectively for selected flow rates (RR=20%)

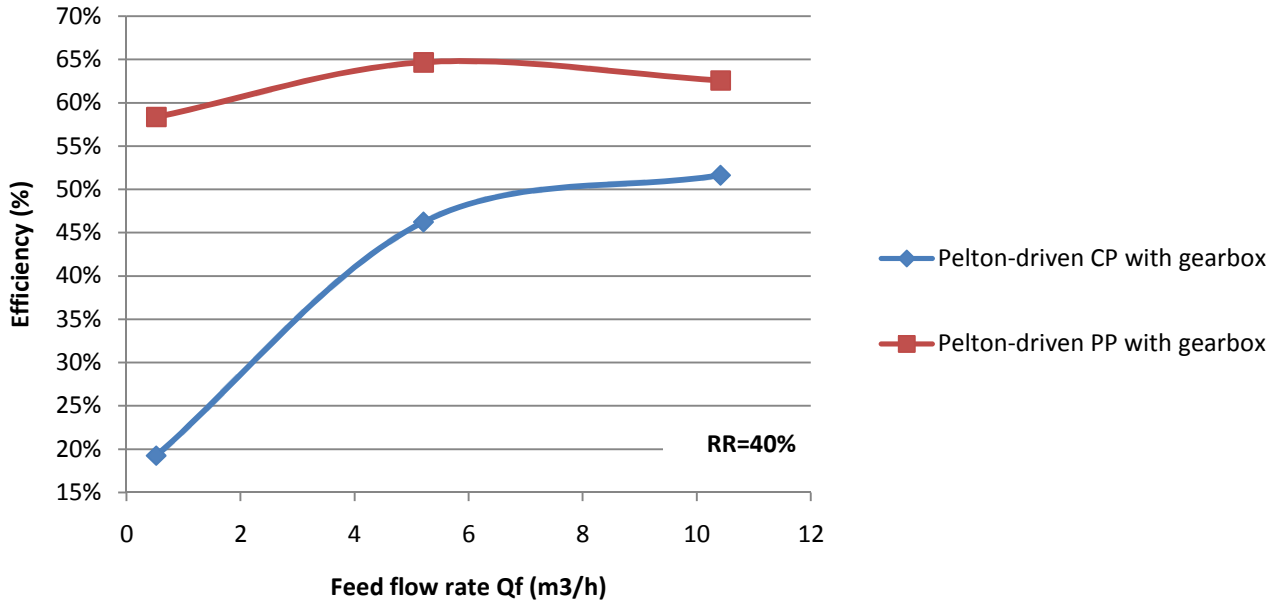

Figure 60: Efficiency of Pelton-driven CP and PP respectively for selected flow rates (RR=40%)

5.2.2. Power and pressure requirements

The power output of the Pelton turbine is the same as in the case of Pelton-driven generator since the same efficiency is assumed for the Pelton turbine (81%).

The pressure required at the inlet of the pump is calculated using the equation 31, as in Pelton-driven generators, but the overall efficiency is defined: $n_t = n_1 \cdot n_g \cdot n_0$

$$\Rightarrow p_f^{in} = p_f^{out} - n_t \cdot \left(p_f^{out} - \Delta p\right) \cdot (1 - RR)$$

Using the overall efficiency of Pelton-driven centrifugal pump with gearbox, n_t, calculated in Table 37, and the examined values of membrane feed pressure p_f^{out} and recovery ratio RR, the required pump inlet feed pressure is calculated.

pfin (bar)		Qf (m^3/h)					
		20.83	10.42	1.04	10.42	5.21	0.52
pfout (bar)	8	4.63	4.82	6.39	5.62	5.86	7.11
	12	6.88	7.17	9.55	8.38	8.76	10.65
	16	9.13	9.52	12.71	11.14	11.65	14.19
	40	22.67	23.65	31.70	27.74	29.02	35.42
	50	28.30	29.52	39.61	34.64	36.24	44.27
	60	33.92	35.39	47.51	41.54	43.47	53.11

Table 39: Pressure required at the inlet of the centrifugal pump

Using the overall efficiency of Pelton-driven generator with piston pump n_t, calculated in Table 34, the correspondent pump inlet feed pressure is calculated:

pfin (bar)		Qf (m^3/h)					
		20.83	10.42	1.04	10.42	5.21	0.52
pfout (bar)	8	-	4.14	3.77	5.11	5.01	5.30
	12	-	6.14	5.57	7.61	7.46	7.90
	16	-	8.14	7.37	10.10	9.91	10.50
	40	-	20.17	18.22	25.13	24.63	26.13
	50	-	25.17	22.72	31.37	30.75	32.63
	60	-	30.16	27.22	37.62	36.87	39.13

Table 40: Pressure required at the inlet of the piston pump

At the following figure the inlet feed pressure, pfin, is shown, for brackish water desalination of RO pressure of 12 bar and seawater desalination of RO pressure of 40 bar, for both Pelton-driven centrifugal pump and piston pump, for the examined feed flow rates and recovery ratio $\mathrm{RR} = 20\%$ and $\mathrm{RR} = 40\%$.

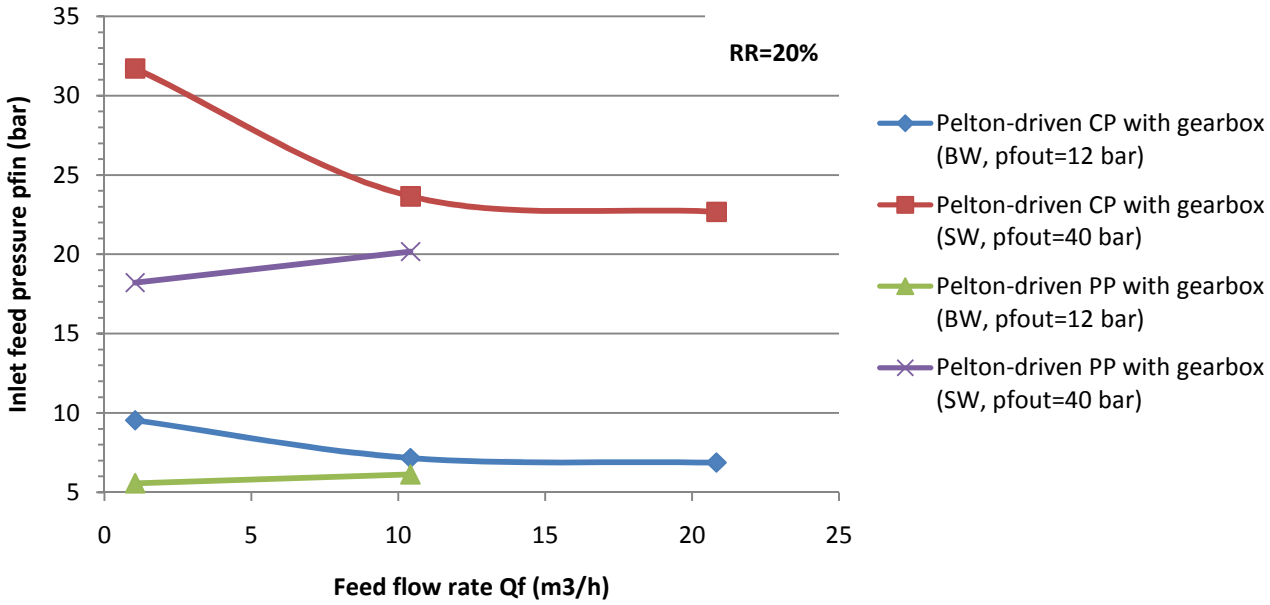

Figure 61: Inlet feed pressure for Pelton-driven CP and PP (RR=20%)

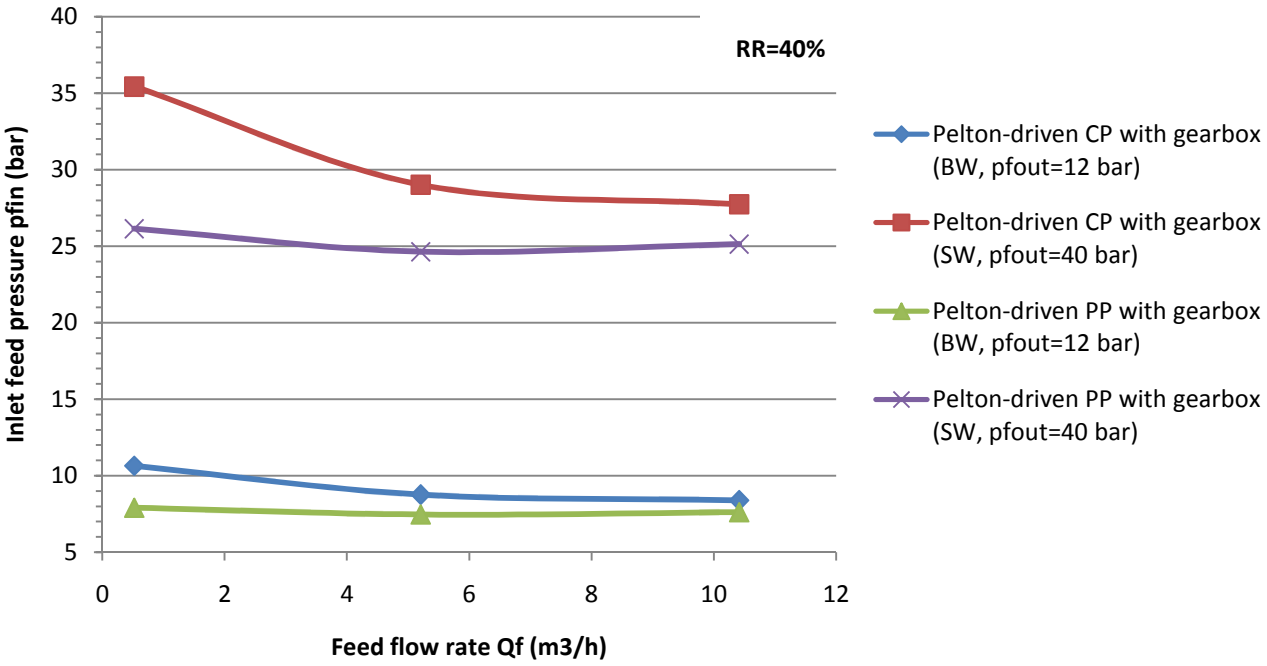

Figure 62: Inlet feed pressure for Pelton-driven CP and PP (RR=40%)

Apart from the pressure required at the inlet of the pump, pfin, another indicator of the performance of the energy recovery device is the percentage of the power required at the inlet of the membranes that is provided by the recovered power:

$$\frac{P_{rec}}{P_{out}} = \frac{p_b \cdot Q_b \cdot n_t}{p_f^{out} \cdot Q_f}$$

But $p_b \cdot Q_b \cdot n_t = (p_f^{out} - p_f^{in}) \cdot Q_f$, so:

$$\Rightarrow \frac{P_{rec}}{P_{out}} = \frac{(p_f^{out} - p_f^{in}) \cdot Q_f}{p_f^{out} \cdot Q_f} = \frac{p_f^{out} - p_f^{in}}{p_f^{out}}$$

So in the case of Pelton-driven centrifugal pump with gearbox the percentage of the power provided to the membranes that is provided by the recovered power is:

Prec/Pout (%)		Qf (m^3/h)					
		20.83	10.42	1.04	10.42	5.21	0.52
pfout (bar)	8	42	40	20	30	27	11
	12	43	40	20	30	27	11
	16	43	41	21	30	27	11
	40	43	41	21	31	27	11
	50	43	41	21	31	28	11
	60	43	41	21	31	28	11

Table 41: Percentage of power output provided by the recovered power (CP)

In the case of Pelton-driven piston pump with gearbox the percentage of the power provided to the membranes that is provided by the recovered power is:

Prec/Pout (%)		Qf (m^3/h)					
		20.83	10.42	1.04	10.42	5.21	0.52
pfout (bar)	8	-	48	53	36	37	34
	12	-	49	54	37	38	34
	16	-	49	54	37	38	34
	40	-	50	54	37	38	35
	50	-	50	55	37	38	35
	60	-	50	55	37	39	35

Table 42: Percentage of power output provided by the recovered power (PP)

At the following figures the power ratio, Prec/Pout (%), is shown, for brackish water desalination of RO pressure of 12 bar and seawater desalination of RO pressure of 40 bar, for both Pelton-driven generators with centrifugal pump and piston pump, for $\mathrm{RR} = 20\%$ and $\mathrm{RR} = 40\%$.

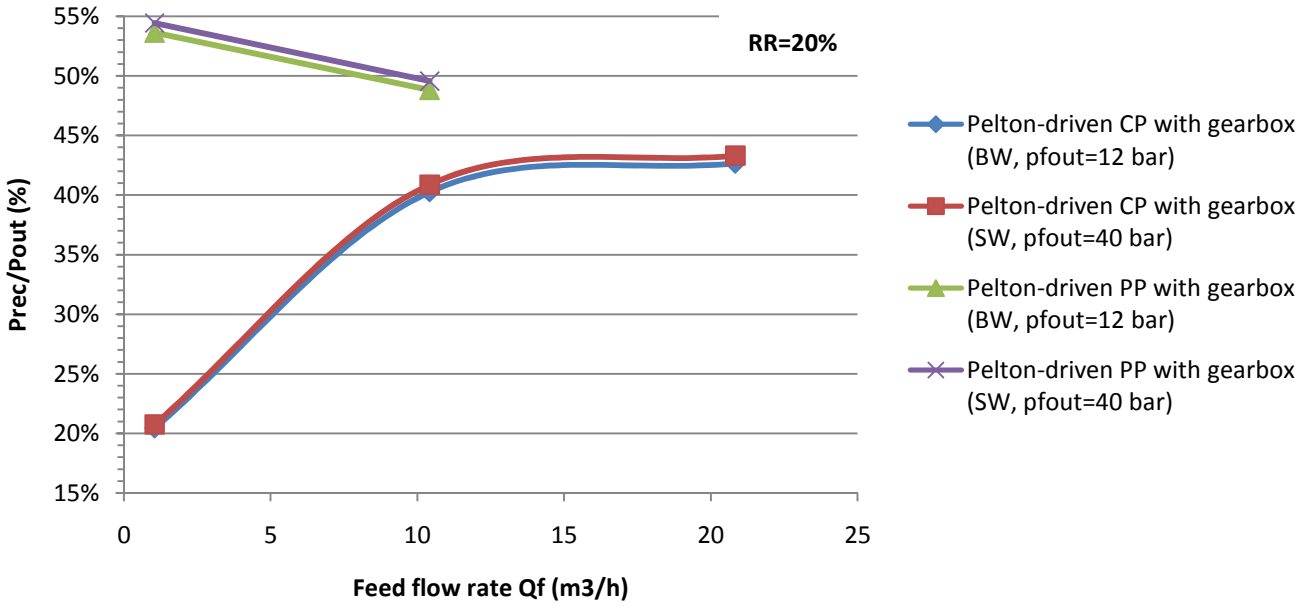

Figure 63: Power ratio Prec/Pout for Pelton-driven generator with CP and PP (20%)

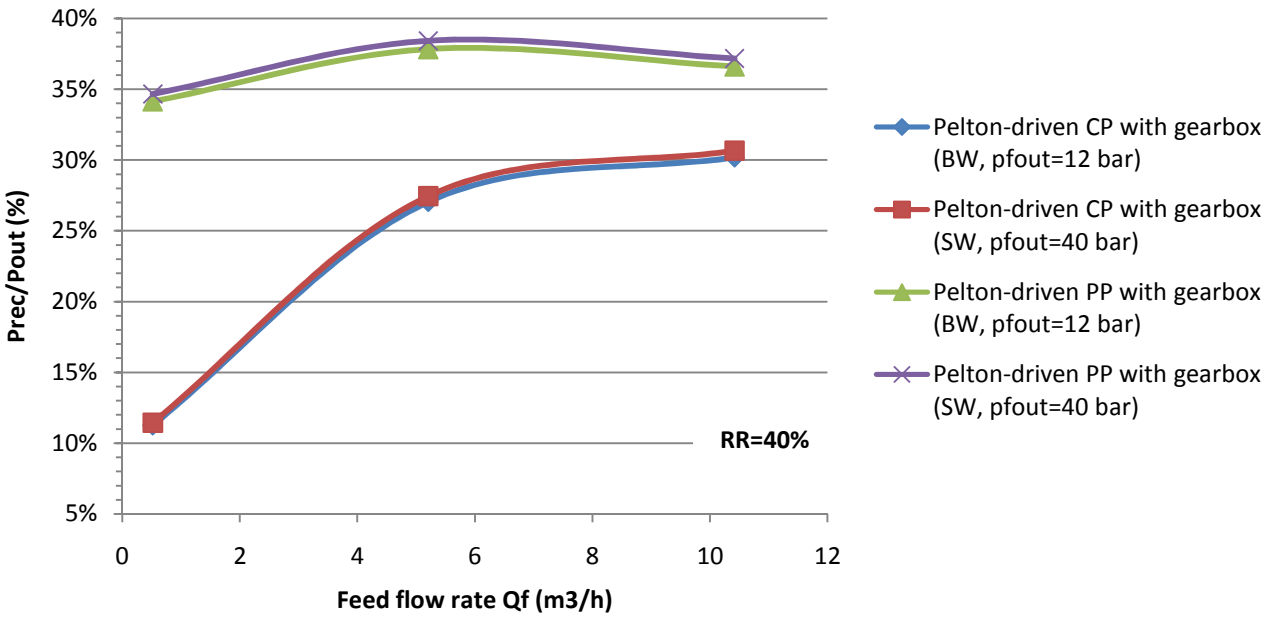

Figure 64: Power ratio Prec/Pout for Pelton-driven generator with CP and PP (40%)

Thus, the power ratio for Pelton-driven piston pumps is higher than Pelton-driven centrifugal pumps, especially for low feed flow rates.

5.2.3. Energy autonomy

For the case of Pelton-driven pump the recovery ratio may need to be fixed. In order to maintain the permeate flow rate at a specific value an electronically controlled valve that will direct the brine stream through an additional nozzle may be used, so additional energy will be required.

In the case of Pelton-driven piston pump the regulation of the operation of the ERD may be less complicated since the feed flow rate is directly related to the rotational speed of the piston pump.

5.2.4. Operation stability

The recovery ratio may need to be fixed using a valve at the brine outlet of the membranes; the nozzles of the Pelton turbine may contribute to this. The fixed relation between the rotational speed of the Pelton turbine and the pump, provided by the gearbox, may also contribute to the stabilisation of the recovery ratio.

5.2.5. Cost analysis

The cost of the Pelton wheel with a casing with four nozzles is assumed to be 500 €. The gearbox cost is estimated at 200 €. The cost of the multistage pump without motor is estimated:

Qf (m^3/h)	20.83	10.42	1.04	10.42	5.21	0.52
Cost (€)	2,500	2,000	1,500	2,000	1,500	1,500

Table 43: Multistage centrifugal pump cost

The cost of the piston pump without motor is estimated:

Qf (m^3/h)	20.83	10.42	1.04	10.42	5.21	0.52
Cost (€)	-	6,500	3,000	6,500	5,200	3,000

Table 44: Piston pump cost

Therefore, the total cost of the Pelton-driven centrifugal pump with gearbox is estimated:

Qf (m^3/h)	20.83	10.42	1.04	10.42	5.21	0.52
Total cost (€)	3,200	2,700	2,200	2,700	2,200	2,200

Table 45: Pelton-driven centrifugal pump with gearbox

In the same way, the overall cost of the Pelton-driven generator using a piston pump is estimated.

Qf (m^3/h)	20.83	10.42	1.04	10.42	5.21	0.52
Total cost (€)	-	7,200	3,700	7,200	5,900	3,700

Table 46: Pelton-driven piston pump with gearbox

5.2.6. Manufacturing complexity

In order to develop the Pelton-driven pump with gearbox, the Pelton turbine needs to be connected to the shaft of the gearbox which has to be coupled to the shaft of the pump.

5.3. Pressure exchangers with two combined double-acting cylinders

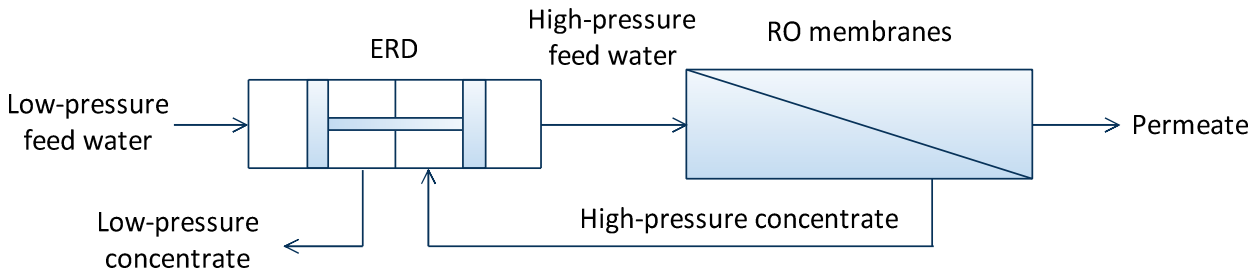

Figure 65: Pressure exchanger with two combined double-acting cylinders

5.3.1. Energy efficiency

Pressure exchangers with two combined double-acting cylinders are designed for seawater applications. As mentioned in paragraph 3.2.1.2, the only efficiency provided by literature is the efficiency of the Clark Pump, designed by Spectra Watermakers, which is claimed to reach 97%. The efficiency of the other pressure exchangers with two combined double-acting cylinders, Schenker ERD, ST-08-PRO and EfficientSea are not estimated. Hence, similar efficiency is assumed for these ERDs.

Taking as a reference case the Schenker ERD, the performance of the Schenker Energy Recovery System has been tested in a singular brackish water installation, resulting to high friction losses (1.87-5.24 bar) that increase with higher feed flow rate (Snieder, et al., 2013). As it can be seen at the following figure friction losses are determined by the feed flow rate, while the salt concentration of water does not influence the friction losses.

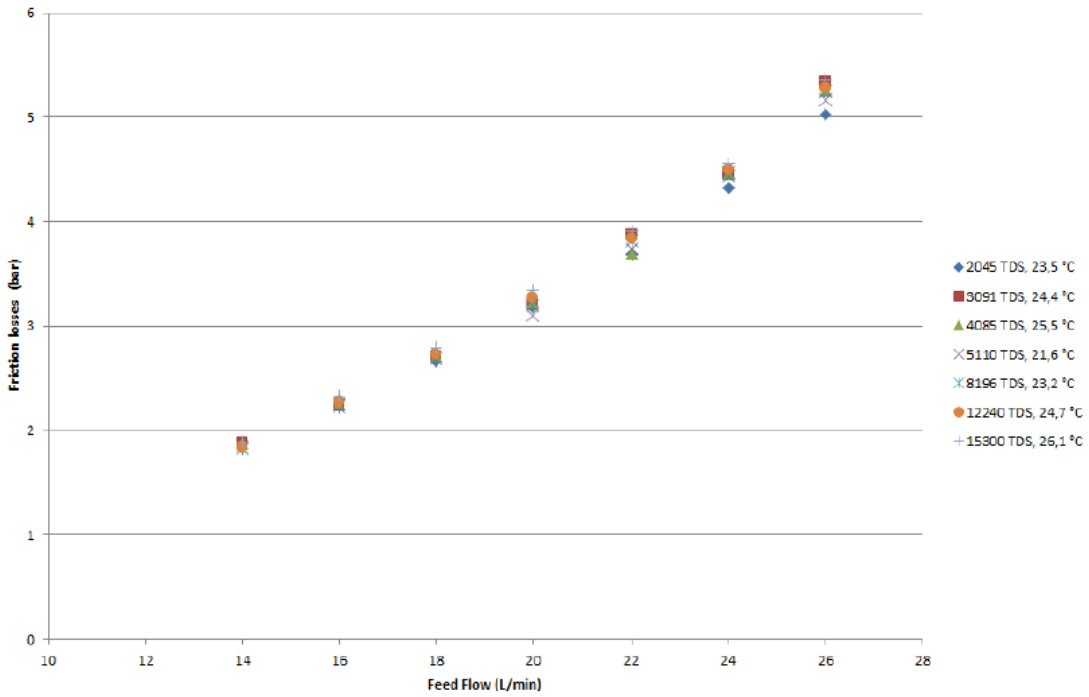

Figure 66: ERD friction losses as a function of feed flow for different salt concentrations (Snieder, et al., 2013)

However, the feed pressure required decreases with lower salinity (Figure 67) and, hence, the ratio of friction losses to feed pressure increases, showing how inefficient the device can get for low salinity (Figure 68). For brackish water of low salinity (2045 TDS), the percentage of the feed pressure wasted in friction losses reaches 80% (for feed flow rate of 26 l/min=1.56 m^3/h) (Snieder, et al., 2013).

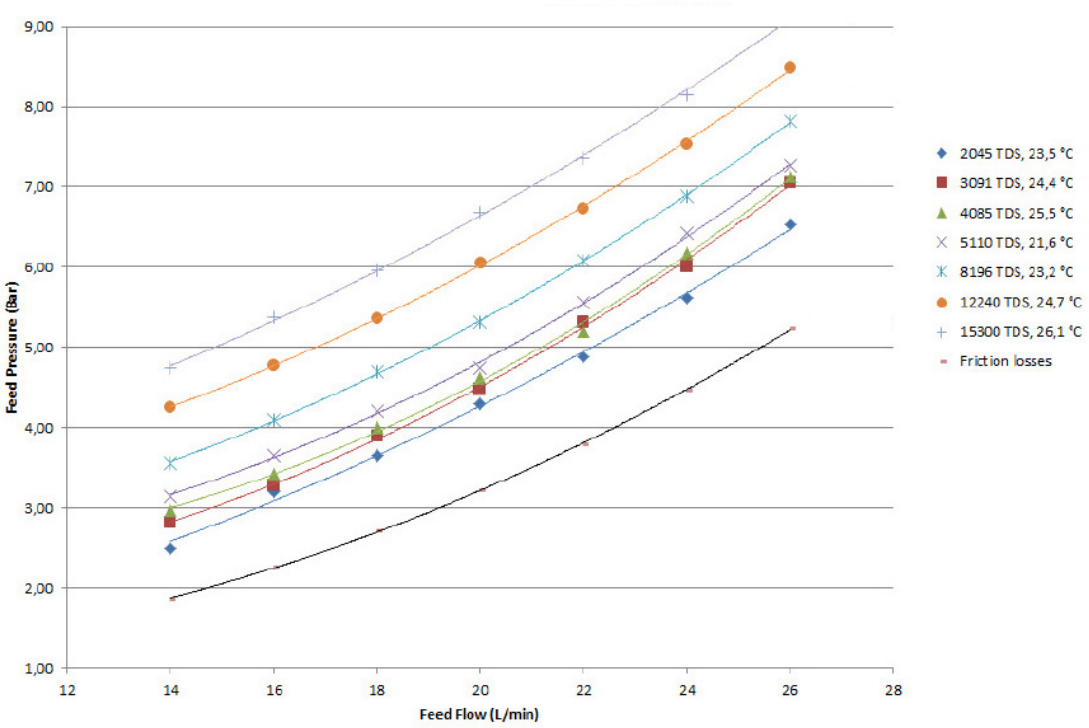

Figure 67: Feed pressure as a function of feed flow (Snieder, et al., 2013)

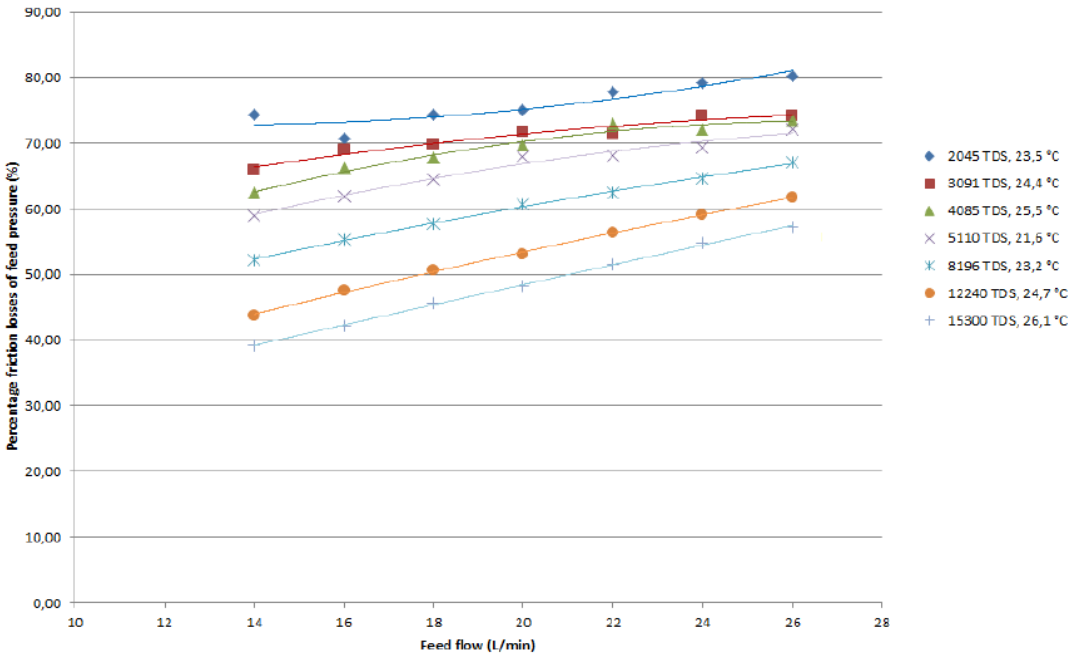

Figure 68: Ratio of friction losses and feed pressure as a function of feed flow (Snieder, et al., 2013)

According to the measurements of the pressure losses due to friction for different feed flows of Figure 66, the following relation is determined: $\Delta p_{fr} = 1.818 \cdot Q_f^2 + 0.218 \cdot Q_f + 0.328$

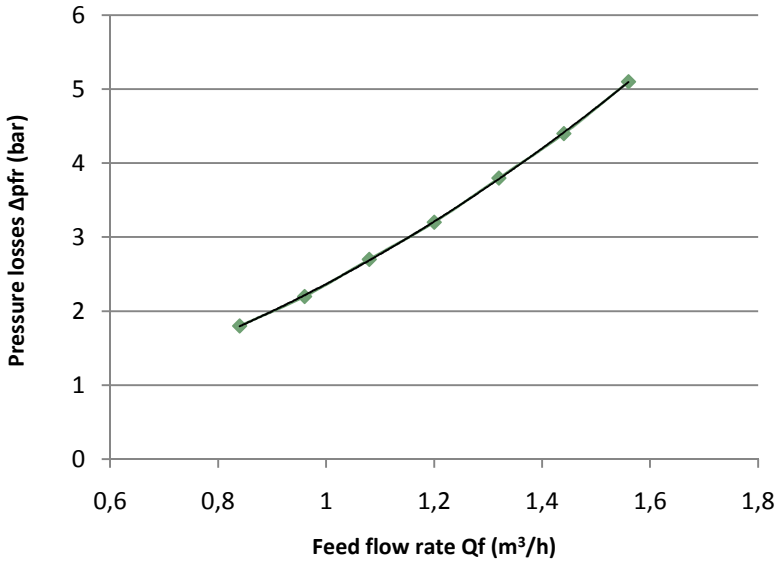

Figure 69: Pressure losses due to friction Δp_{fr} as function of feed flow rate Q_f

The equation above, is applicable for feed flow rate up to $1.42\ m^3/h$, which is the maximum feed flow rate this ERD is designed for. Applying this formula for the examined values of feed flow rate, the pressure losses due to friction are calculated.

							Schenker ERD
Qp (m^3/h)	4.17	2.08	0.21	4.17	2.08	0.21	0.21
RR (%)	20			40			15
Qf (m^3/h)	20.83	10.42	1.04	10.42	5.21	0.52	1.42
Δpfr (bar)	793.93	199.86	2.53	199.86	50.78	0.93	4.30

Table 47: Pressure losses due to friction, Δpfr, for the examined flow rates and for the design characteristics of the Schenker ERD

As expected, feed flow rate higher than $1.42\ \mathrm{m^3/h}$ results to extremely high friction losses. Hence, this equation can only be used for the estimation of pressure losses due to friction for feed flow rates of $0.52\ \mathrm{m^3/h}$ and $1.04\ \mathrm{m^3/h}$ and for the case of the Schenker ERD. For the rest of the cases, with higher values of feed flow rate, the required scaling up of the ERD needs to be estimated first.

Pressure losses due to friction consist of hydraulic losses and mechanical losses. According to the equation describing the flow in tubes (turbulent), the hydraulic pressure losses have a positive quadratic relation with flow rate:

$$\Delta p_{fr}^{H} = K_W \cdot \frac{1}{2} \cdot \rho \cdot v^2$$

In order to estimate the hydraulic pressure losses due to friction, a new design of the Schenker ERD is taken into account. This design is developed for permeate flow rate of $Q_p = 0.42\ \mathrm{m^3/h}\ (= 10\ \mathrm{m^3/day})$, for recovery ratio $RR = 28.70\%$ and hence feed flow rate $Q_f = 1.45\ \mathrm{m^3/h}$ (Walvoort, 2013).

Using the static model developed for the new design of the Schenker ERD (Walvoort, 2013) and assuming hydraulic pressure losses $\Delta p_{fr}^{H} = 1\ \mathrm{bar}$, the required scale factor (with reference to the new design) for the tubing of the system, the switching mechanism and the check valves is calculated:

							Optimised Schenker ERD	New design
Qf (m^3/h)	20.83	10.42	1.04	10.42	5.21	0.52	1.42	1.45
Scale factor f1	3.92	2.41	0.66	2.25	1.45	0.42	0.80	1.00

Table 48: Scale factor of the tubing of the ERD, f1, using the static model developed for the new design and assuming hydraulic pressure losses $\Delta p_{fr}^{H} = 1\ \mathrm{bar}$

Pressure losses due to mechanical friction of the pistons and the rod against the wall of the main tube and the centre block, respectively, are calculated using the highest capacity model of the Schenker ERD as reference. Modelling of the highest capacity Schenker ERD showed it has a constant mechanical friction force of $190\ \mathrm{N}$ resulting to mechanical pressure losses of $0.3\ \mathrm{bar}$. This model is designed to deliver permeate flow rate of $Q_p = 0.21\ \mathrm{m^3/h}\ (= 5\ \mathrm{m^3/day})$, for recovery ratio $RR = 14.67\%$ and, hence, feed flow rate $Q_f = 1.43\ \mathrm{m^3/h}\ (= 3.98 \cdot 10^{-4}\ \mathrm{m^3/s})$. The area of the outer surface of the pistons of the Schenker ERD is $A = 69.40\ \mathrm{cm^2} = 69.40 \cdot 10^{-4}\mathrm{m^2}$ and the diameter is $d = 9.4\ \mathrm{cm}$. Therefore, the velocity of the pistons and the connecting rod is calculated:

$$v_p = \frac{Q_f}{A} = \frac{3.98 \cdot 10^{-4}}{69.398 \cdot 10^{-4}} = 0.057\ \mathrm{m/s} = 5.68\ \mathrm{cm/s}\ (= 204.64\ \mathrm{m/h})$$

In order to calculate the scale factor of the pistons for the selected feed flow rates, it is assumed that the pistons move at the velocity of the Schenker ERD, calculated above, since it is suggested by the manufacturer of the device. Therefore, the required surface area and the inner diameter of the main tube of the device are calculated for the examined flow rates. Furthermore, using the inner diameter of the main tube of the Schenker ERD ($d = 9.4$ cm), the scale factor of the pistons, f_2, is calculated with reference to this value.

							Schenker ERD
Qp (m^3/h)	4.17	2.08	0.21	4.17	2.08	0.21	0.21
RR (%)	20			40			14.67
Qf (m^3/h)	20.83	10.42	1.04	10.42	5.21	0.52	1.42
A (cm^2)	1018.07	509.03	50.90	509.03	254.52	25.45	69.40
d (cm)	36.00	25.46	8.05	25.46	18.00	5.69	9.40
Scale factor f2	3.83	2.71	0.86	2.71	1.92	0.61	1.00

Table 49: Scale factor of the pistons, f2, assuming the piston velocity of the Schenker ERD

Using the recovery ratio the diameter and the surface area of the rod is also calculated:

$$RR = 1 - \frac{B}{A} = \frac{(A - B)}{A} = \frac{A_{rod}}{A} = \frac{(\pi \cdot d_{rod}^2/4)}{(\pi \cdot d^2/4)} = \left(\frac{d_{rod}}{d}\right)^2$$

							Schenker ERD
RR (%)	20			40			14.67
A (cm^2)	1018.07	509.03	50.90	509.03	254.52	25.45	69.40
d (cm)	36.00	25.46	8.05	25.46	18.00	5.69	9.40
Arod (cm^2)	203.61	101.81	10.18	203.61	101.81	10.18	10.18
drod (cm)	16.10	11.39	3.60	16.10	11.39	3.60	3.60

Table 50: Diameter and surface area of the rod

Mechanical pressure losses occur at the interface between the o-rings of the pistons and the rod and the wall of the main tube and the centre block, respectively. Taking as a reference, the o-rings used for the pistons and the rod of the new design (ERIKS, 2013), the relation between the inner diameter d_{in} and the thickness t of the o-rings is estimated.

O-ring piston	New design
din (mm)	132.72
t (mm)	5.33
O-ring rod	
din (mm)	75
t (mm)	4

Table 51: Inner diameter d_{in} and the thickness t for the o-rings of the pistons and the rod of the new design (ERIKS, 2013)

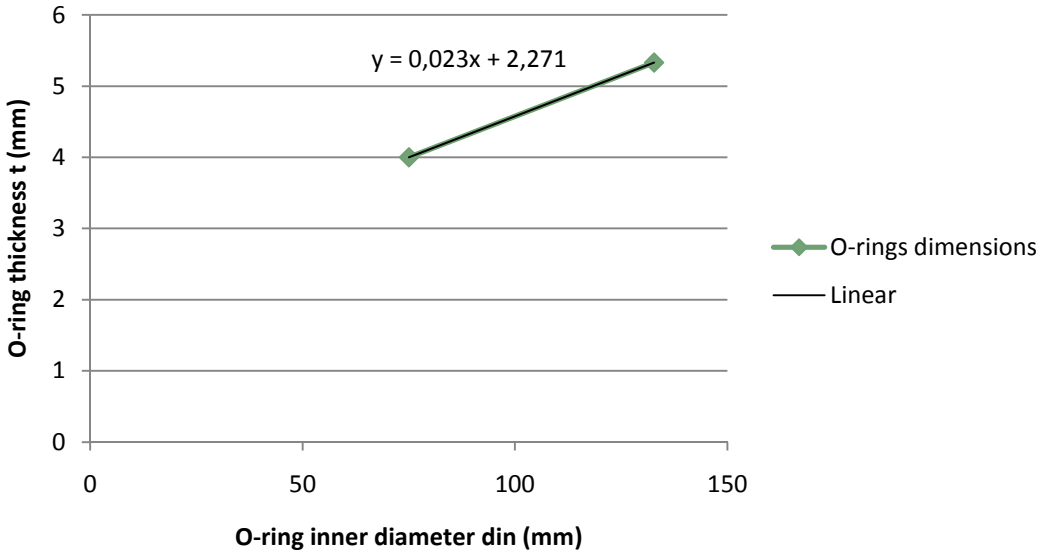

Figure 70: Relation between the inner diameter d_{in} and the thickness t of the o-rings

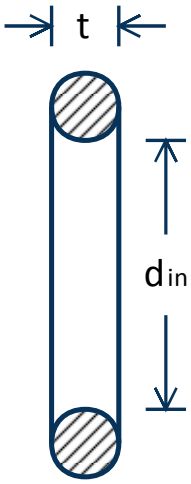

Figure 71: O-ring dimensions

Hence, the inner diameter d_{in} of the o-rings is calculated using the scale factor f_2 derived assuming the piston velocity of the Schenker ERD ($v_p = 5.68\,cm/s$); the thickness t of the o-rings is calculated using the relation derived above. Then, scale factors for both the diameter and the thickness of the o-rings are calculated (with reference to the new design), using the mean value of the piston and the rod cases.

							Schenker ERD
d (cm)	36.00	25.46	8.05	25.46	18.00	5.69	9.40
Scale factor	3.83	2.71	0.86	2.71	1.92	0.61	1.00
O-ring piston							
din (mm)	341.31	241.34	76.32	241.34	170.66	53.97	89.11
t (mm)	10.14	7.83	4.03	7.83	6.20	3.52	4.33
O-ring rod							
din (mm)	161.01	113.85	36.00	161.01	113.85	36.00	36.00
t (mm)	5.98	4.90	3.10	5.98	4.90	3.10	3.10
Scale factor fd	4.15	2.94	0.93	3.59	2.54	0.80	1.00
Scale factor ft	2.14	1.69	0.97	1.87	1.51	0.91	1.00

Table 52: Inner diameter d_{in} and thickness t of the o-rings of the pistons and the rod and respective scale factors

The mechanical pressure losses are calculated using the equation:

$$\Delta p_{fr}^{M} = \frac{F_{fr}}{A}$$

Where A is the surface area of the piston which has a quadratic relation with the scale factor f_2. F_{fr} is the friction force exerted on the surface area of the o-rings ($\approx t \cdot \pi \cdot d_{out}$) that contact the wall of the main tube and the centre block and therefore has a linear relation with the product of the scale factors $f_t \cdot f_d$. Thus, the mechanical pressure losses are calculated using the scale factor $(f_t \cdot f_d)/f_2^2$.

							Schenker ERD
Qp (m^3/h)	4.17	2.08	0.21	4.17	2.08	0.21	0.21
RR (%)	20			40			14.67
Qf (m^3/h)	20.83	10.42	1.04	10.42	5.21	0.52	1.42
ΔpfrM (bar)	0.18	0.20	0.37	0.27	0.31	0.60	0.30

Table 53: Mechanical pressure losses Δp_{fr}^{M} for the selected flow rates and the Schenker ERD

Consequently, the total pressure losses due to friction Δp_{fr} are the sum of the hydraulic Δp_{fr}^{H} and the mechanical losses Δp_{fr}^{M}.

							Optimised Schenker ERD
Qp (m^3/h)	4.17	2.08	0.21	4.17	2.08	0.21	0.21
RR (%)	20			40			14.67
Qf (m^3/h)	20.83	10.42	1.04	10.42	5.21	0.52	1.42
ΔpfrH (bar)	1.00						1.00
ΔpfrM (bar)	0.18	0.20	0.37	0.27	0.31	0.60	0.30
Δpfr (bar)	1.18	1.20	1.37	1.27	1.31	1.60	1.30

Table 54: Total pressure losses due to friction Δp_{fr} for the selected flow rates and the optimised Schenker ERD

At the following figures the total pressure losses due to friction Δpfr and the scaling factors f1 and f2, of the tubing and the pistons of the ERD respectively, are presented for the examined feed flow rates for $RR = 20\%$ and $RR = 40\%$.

							Optimised Schenker ERD
Qf (m^3/h)	20.83	10.42	1.04	10.42	5.21	0.52	1.42
Scale factor f1	3.92	2.41	0.66	2.25	1.45	0.42	0.80
Scale factor f2	3.83	2.71	0.86	2.71	1.92	0.61	1.00
Δpfr (bar)	1.18	1.20	1.37	1.27	1.31	1.60	1.30

Table 55: Scale factor of the tubing (f1) and the pistons (f2) of the ERD and total pressure losses due to friction Δp_{fr} for the selected flow rates and the optimised Schenker ERD

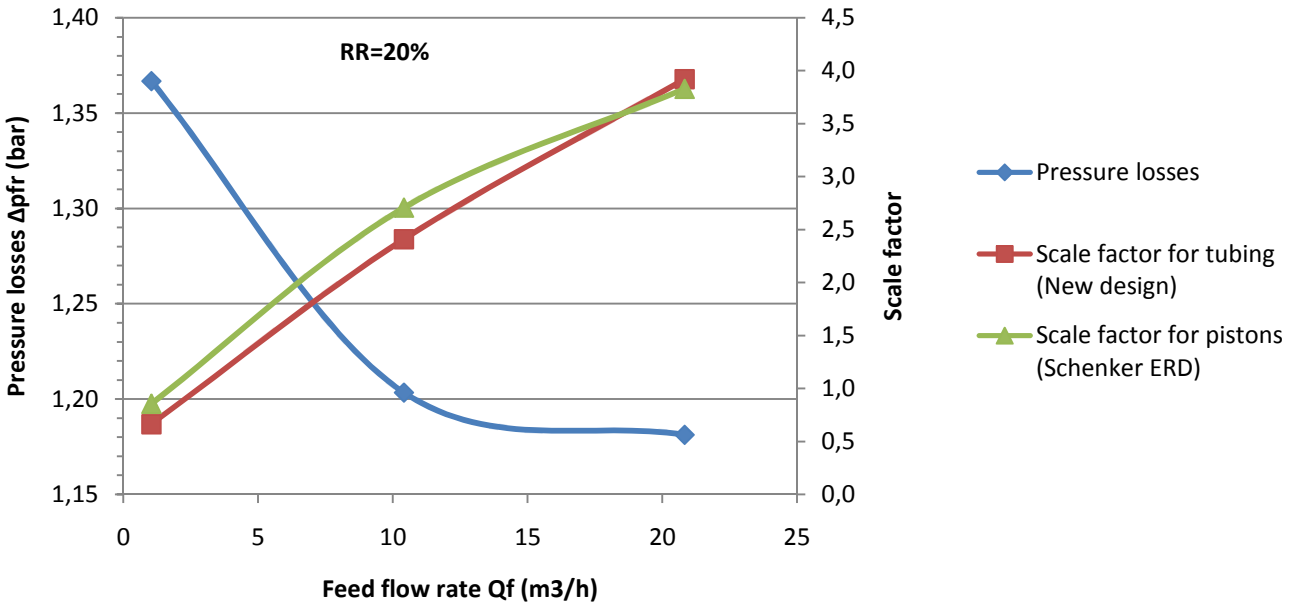

Figure 72: Scale factor of the tubing and the pistons of the ERD and total pressure losses (RR=20%)

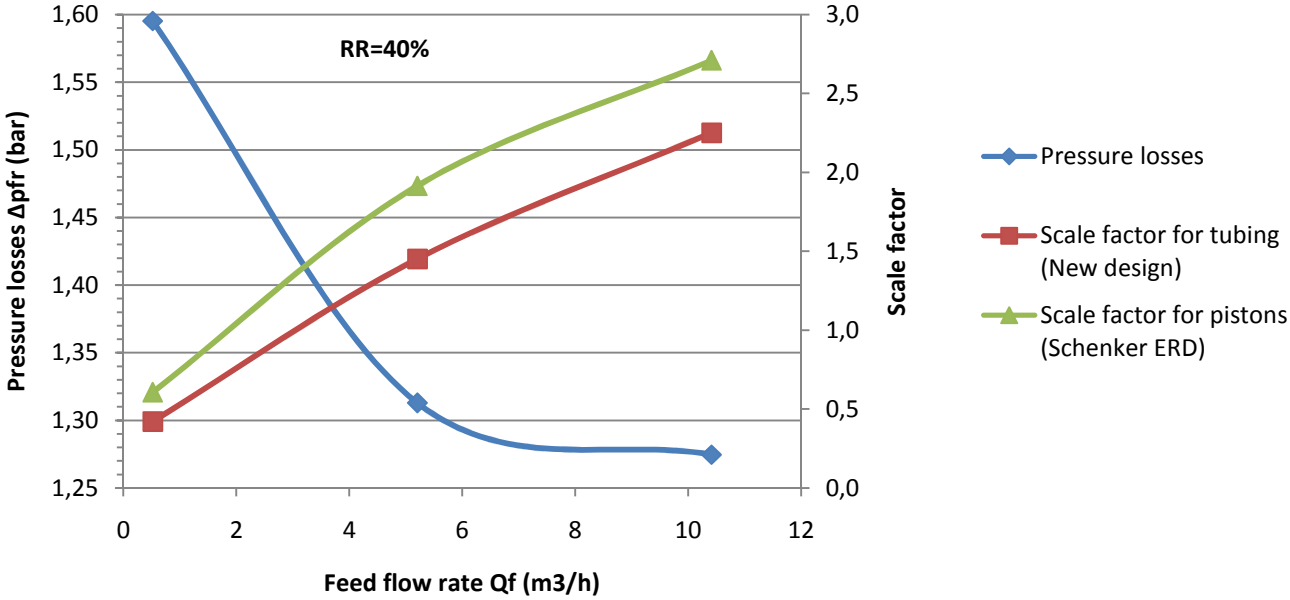

Figure 73: Scale factor of the tubing and the pistons of the ERD and total pressure losses Δp_{fr} (RR=40%)

Using the scheme of the Clark Pump with all the parameters required, the equation for the pressure required at the inlet of the ERD is derived. The brine outlet flow is assumed to have

the same pressure as the environment (Feenstra, et al., 2012). Therefore, the relevant forces developed on the inner and outer surfaces of the pistons are:

$$F_b = p_b \cdot B\,,\ F_f^{in} = p_f^{in} \cdot A\,,\ F_f^{out} = p_f^{out} \cdot A \qquad [29]$$

Assuming no acceleration during operation, no leakage and no friction losses, the following force balance is formed for the pistons and using equations 32 the relation of pressures is also derived:

$$F_b + F_f^{in} = F_f^{out}\,,\quad p_b \cdot B/A + p_f^{in} = p_f^{out} \qquad [30]$$

Where p_f^{in} is the inlet feed pressure, p_f^{out} the outlet feed and p_b the brine pressure.

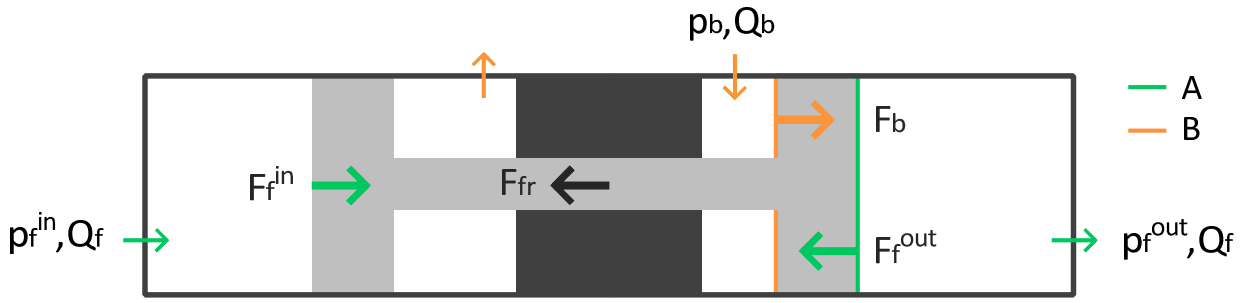

Figure 74: A schematic view of the relevant forces, pressures and surfaces of the Spectra Clark Pump (Spectra Watermakers, Inc, 2013)

Taking into account the friction losses and equation 12, $RR = 1 - B/A$, equations 33 become:

$$F_b + F_f^{in} - F_{fr} = F_f^{out}\,,\quad p_b \cdot (1 - RR) + p_f^{in} - \Delta p_{fr} = p_f^{out} \qquad [31]$$

$$\Rightarrow p_f^{in} = p_f^{out} + \Delta p_{fr} - p_b \cdot (1 - RR) \qquad [32]$$

The efficiency of the device is calculated as the ratio of the power output and the power input:

$$n = \frac{P_{out}}{P_{in}} = \frac{(p_f^{out} - p_f^{in}) \cdot Q_f}{p_b \cdot Q_b}$$

Using equation 35 and $Q_b = Q_f \cdot (1 - RR)$:

$$\Rightarrow n = \frac{\left(p_f^{out} - \left(p_f^{out} + \Delta p_{fr} - p_b \cdot (1 - RR)\right)\right)}{p_b \cdot (1 - RR)}$$

$$\Rightarrow n = \frac{p_b \cdot (1 - RR) - \Delta p_{fr}}{p_b \cdot (1 - RR)}$$

$$\Rightarrow n = 1 - \frac{\Delta p_{fr}}{p_b \cdot (1 - RR)}$$

According to the equation above the efficiency of pressure exchanger with two double-acting cylinders is dependent on the pressure losses due to friction, Δpfr, the brine pressure, pb, and the recovery ratio, RR. Using the pressure loss between the inlet and the outlet of the membrane, Δp, the brine pressure can be written $p_b = p_f^{out} - \Delta p$, so:

$$\Rightarrow n = 1 - \frac{\Delta p_{fr}}{(p_f^{out} - \Delta p) \cdot (1 - RR)}$$

Subsequently, the efficiency of the ERD is calculated for the examined cases and for the design characteristics of the Schenker ERD, using the pressure losses derived from the measurements of the Schenker ERD testing.

							Schenker ERD
Qp (m^3/h)	4.17	2.08	0.21	4.17	2.08	0.21	0.21
RR (%)	20			40			14.67
Qf (m^3/h)	20.83	10.42	1.04	10.42	5.21	0.52	1.42
Δpfr (bar)	793.93	199.86	2.53	199.86	50.78	0.93	4.30

Table 56: Pressure losses due to friction, Δpfr, for the examined flow rates and for the design characteristics of the Schenker ERD derived from the Schenker ERD testing

n (%)		Qf (m^3/h)						Schenker ERD
		20.83	10.42	1.04	10.42	5.21	0.52	1.42
pfout (bar)	8	-	-	59	-	-	80	34
	12	-	-	73	-	-	87	57
	16	-	-	80	-	-	90	68
	40	-	-	92	-	-	96	87
	50	-	-	94	-	-	97	90
	60	-	-	95	-	-	97	92

Table 57: Efficiency of the ERD, n, for the examined flow rates and for the design characteristics of the Schenker ERD

As expected, the efficiency of the ERD decreases with lower feed pressure required and therefore it is considerably lower for brackish water desalination.

Subsequently, the efficiency of the ERD is calculated for the examined cases and for the design characteristics of the Schenker ERD, using the pressure losses derived by scaling the system.

It can be seen that, compared to the efficiency calculated according to the pressure losses derived from the Schenker ERD testing, the efficiency of the ERD, in this case, is much higher especially for brackish water desalination.

							Optimised Schenker ERD
RR (%)	20			40			14.67
Qp (m3/h)	4.17	2.08	0.21	4.17	2.08	0.21	0.21
Qf (m3/h)	20.83	10.42	1.04	10.42	5.21	0.52	1.42
Scale factor f1	4.10	2.43	0.66	2.26	1.45	0.42	0.80
Scale factor f2	3.83	2.71	0.86	2.71	1.92	0.61	1.00
Δpfr (bar)	1.18	1.20	1.37	1.27	1.31	1.60	1.30

Table 58: Pressure losses due to friction, Δpfr, for the examined flow rates and for the design characteristics of the Schenker ERD derived by scaling the system

n (%)		Qf (m^3/h)						Optimised Schenker ERD
		20.83	10.42	1.04	10.42	5.21	0.52	1.42
pfout (bar)	8	81	80	78	72	72	65	80
	12	87	87	85	82	81	77	87
	16	91	90	89	86	86	83	90
	40	96	96	96	95	94	93	96
	50	97	97	97	96	96	95	97
	60	98	97	97	96	96	96	97

Table 59: Efficiency of the ERD, n, for the examined flow rates and for the design characteristics of the Schenker ERD

The following figures show the efficiency of the ERD for the examined feed flow rates for recovery ratio $\mathrm{RR} = 20\%$ and $\mathrm{RR} = 40\%$ for brackish water desalination of RO pressure of 12 bar and seawater desalination of RO pressure of 40 bar. The scale factor calculated for the pistons and the rod is also shown.

It can be seen that the efficiency of the system for brackish water desalination of RO pressure of 12 bar is 10% lower that the efficiency of the system for seawater desalination of RO pressure of 40 bar. In addition, for higher feed flow rate the efficiency is higher but the system also needs to be scaled up by a higher factor.

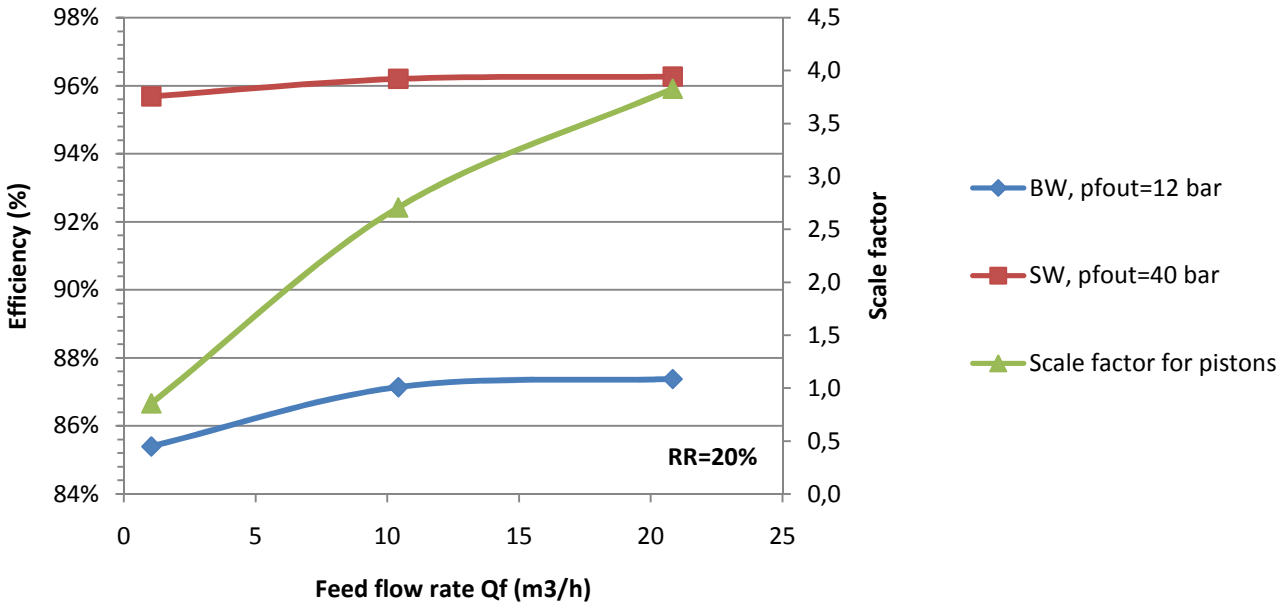

Figure 75: Efficiency of the ERD for BW and SW (RR=20%)

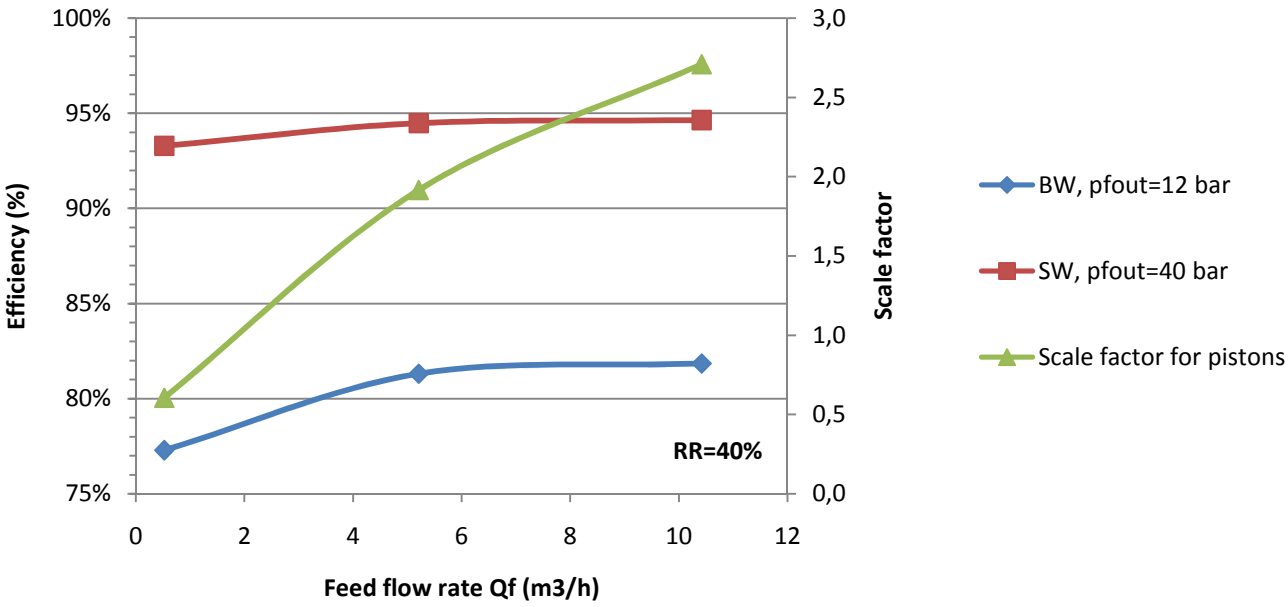

Figure 76: Efficiency of the ERD for BW and SW (RR=40%)

5.3.2. Power and pressure requirements

The feed pressure required at the inlet of the ERD is calculated using equation 35:

$$\Rightarrow p_f^{in} = p_f^{out} + \Delta p_{fr} - p_b \cdot (1 - RR)$$

Using the pressure loss between the inlet and the outlet of the membrane, Δp, the brine pressure can be written $p_b = p_f^{out} - \Delta p$, so:

$$\Rightarrow p_f^{in} = p_f^{out} + \Delta p_{fr} - \left(p_f^{out} - \Delta p\right) \cdot (1 - RR)$$

Subsequently, the inlet feed pressure of the ERD is calculated for the examined cases and for the design characteristics of the Schenker ERD, using the pressure losses derived from the measurements of the Schenker ERD testing.

pfin (bar)		Qf (m^3/h)						Schenker ERD
		20.83	10.42	1.04	10.42	5.21	0.52	1.42
pfout (bar)	8	-	-	4.37	-	-	4.31	5.73
	12	-	-	5.17	-	-	5.91	6.32
	16	-	-	5.97	-	-	7.51	6.91
	40	-	-	10.85	-	-	17.17	10.51
	50	-	-	12.85	-	-	21.17	11.98
	60	-	-	14.85	-	-	25.17	13.45

Table 60: ERD inlet feed pressure, pfin, for the examined flow rates and for the design characteristics of the Schenker ERD

Subsequently, the efficiency of the ERD is calculated for the examined cases and for the design characteristics of the Schenker ERD, using the pressure losses derived by scaling the system. It can be seen that in this case the inlet feed pressure required for the Schenker ERD is much lower.

pfin (bar)		Qf (m^3/h)						Optimised Schenker ERD
		20.83	10.42	1.04	10.42	5.21	0.52	1.42
pfout (bar)	8	3.02	3.04	3.21	4.65	4.69	4.98	2.73
	12	3.82	3.84	4.01	6.25	6.29	6.58	3.32
	16	4.62	4.64	4.81	7.85	7.89	8.18	3.90
	40	9.50	9.52	9.69	17.51	17.55	17.84	7.51
	50	11.50	11.52	11.69	21.51	21.55	21.84	8.98
	60	13.50	13.52	13.69	25.51	25.55	25.84	10.44

Table 61: ERD inlet feed pressure, pfin, for the examined flow rates and for the design characteristics of the Schenker ERD

At the following figure the inlet feed pressure, pfin, is shown, for brackish water desalination of RO pressure of 12 bar and seawater desalination of RO pressure of 40 bar, for the optimised pressure exchanger with two combined double-acting cylinders for the examined feed flow rates for $\mathrm{RR} = 20\%$ and $\mathrm{RR} = 40\%$.

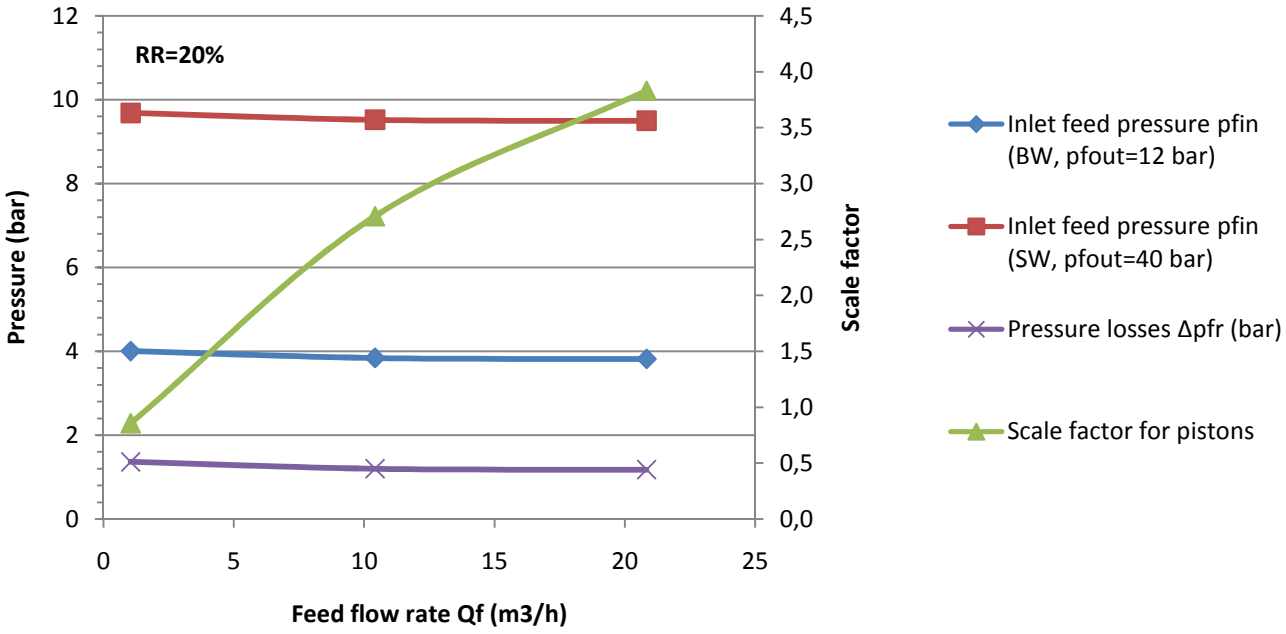

Figure 77: Inlet feed pressure required for BW and SW (RR=20%)

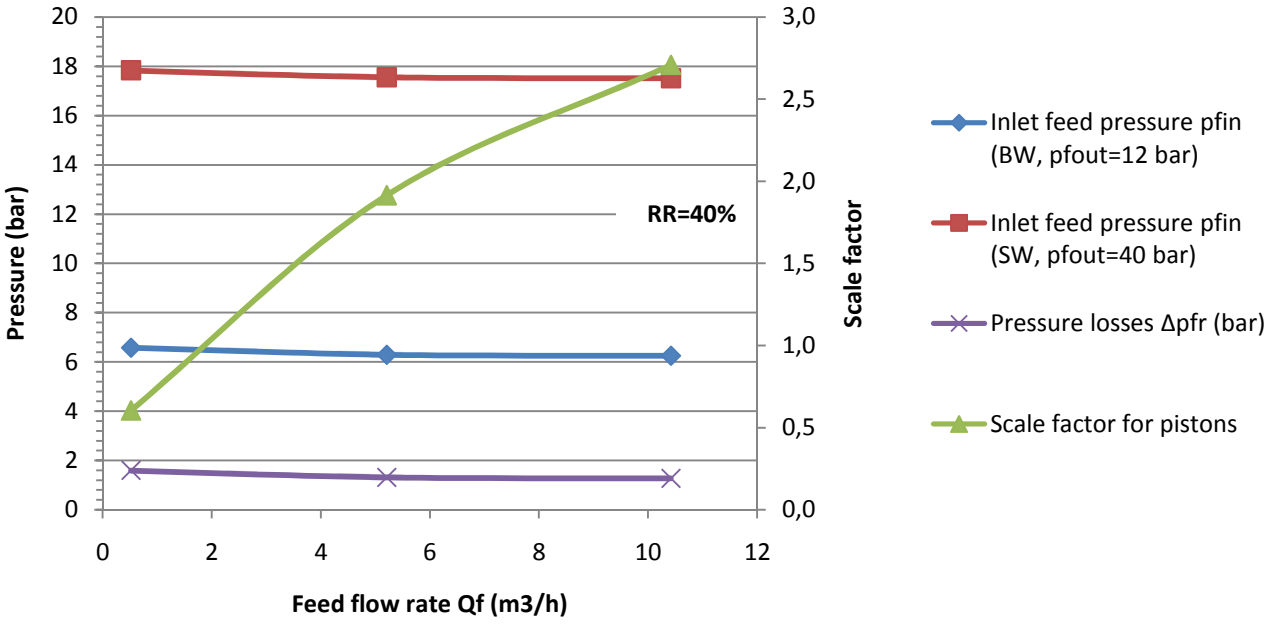

Figure 78: Inlet feed pressure required for BW and SW (RR=40%)

As in the two previous energy recovery concepts, another indicator of the performance of the energy recovery device is the percentage of the power required at the inlet of the membranes that is provided by the recovered power:

$$\frac{P_{rec}}{P_{out}} = \frac{p_f^{out} - p_f^{in}}{p_f^{out}}$$

So in the case of pressure exchangers with two combined double-acting cylinders the percentage of the power provided to the membranes that is provided by the recovered power is:

Prec/Pout (%)		Qf (m^3/h)					
		20.83	10.42	1.04	10.42	5.21	0.52
pb (bar)	8	62	62	60	42	41	38
	12	68	68	67	48	48	45
	16	71	71	70	51	51	49
	40	76	76	76	56	56	55
	50	77	77	77	57	57	56
	60	77	77	77	57	57	57

Table 62: Percentage of power output provided by the recovered power

At the following figures the power ratio, Prec/Pout (%), is shown, for brackish water desalination of RO pressure of 12 bar and seawater desalination of RO pressure of 40 bar, for $RR = 20\%$ and $RR = 40\%$.

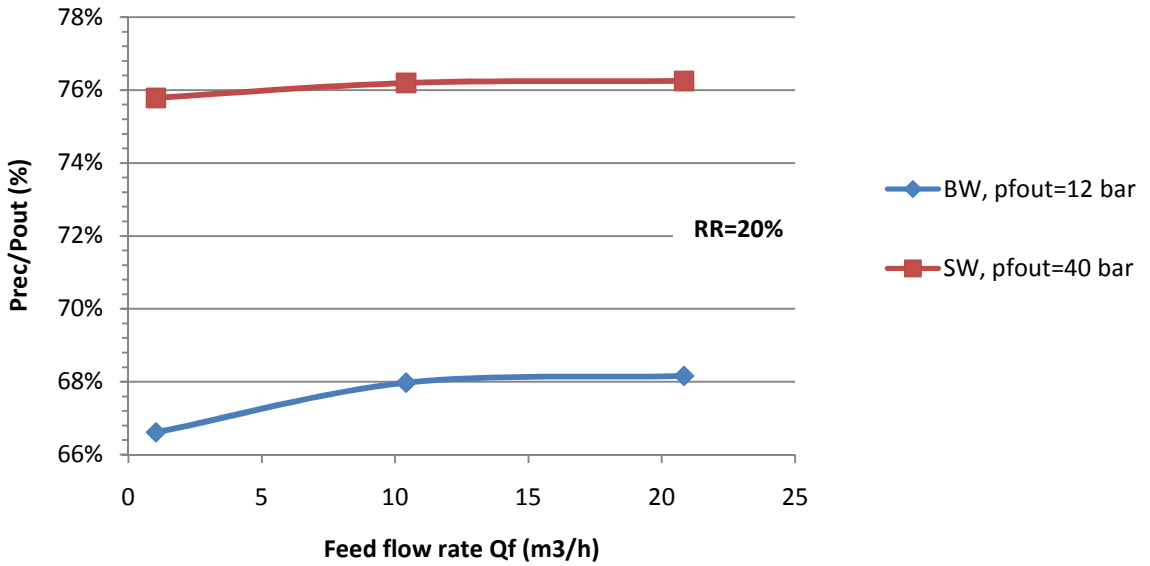

Table 63: Power ratio Prec/Pout for pressure exchangers with two combined cylinders (RR=20%)

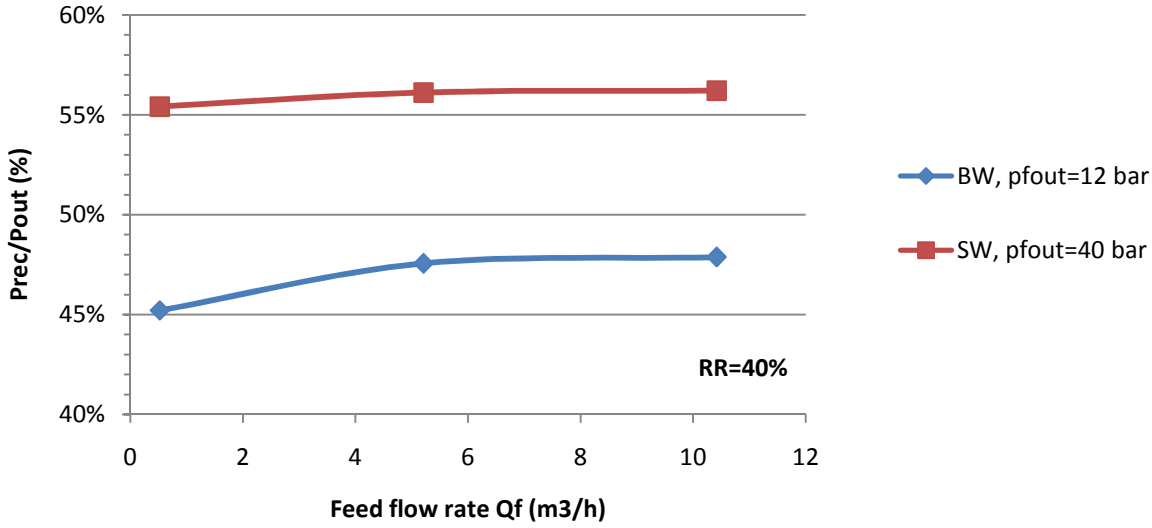

Table 64: Power ratio Prec/Pout for pressure exchangers with two combined cylinders (RR=40%)

5.3.3. Energy autonomy

This solution does not require additional power supply. If needed, it might be possible to steer the switching mechanism electrically.

5.3.4. Operation stability

The recovery ratio of this system is kept constant by the energy recovery device, since it is defined by the area ratio of the inner and the outer surface of the pistons:

$$RR = 1 - \frac{B}{A} = \frac{(A - B)}{A} = \frac{A_{rod}}{A} = \frac{(\pi \cdot d_{rod}^2/4)}{(\pi \cdot d^2/4)} = \left(\frac{d_{rod}}{d}\right)^2$$

5.3.5. Cost analysis

The cost of the energy recovery system is estimated between 1,778 € (Spectra Clark Pump) and 3,300 € (Schenker ERD). Using the cost of the Schenker ERD, it is assumed that 25% of the costs correspond to installation costs, another 25% are related to assembly costs and 50% correspond to material costs.

In addition, taking into account that the Schenker ERD is developed for seawater desalination, it is assumed that the pipe material required for seawater desalination is stainless steel (316 SS), in order to withstand the high pressure, and that for brackish water desalination polymer (PVC) pipes can be used. So assuming that PVC is 4 times cheaper than 316 SS, the material costs for brackish water desalination can also be estimated. Adding with installation and assembly costs and using the scale factors calculated above, the cost of the system is calculated for both brackish and seawater desalination for the selected flow rates.

RR (%)	20			40			Schenker ERD
Qp (m^3/h)	4.17	2.08	0.21	4.17	2.08	0.21	0.21
Qf (m^3/h)	20.83	10.42	1.04	10.42	5.21	0.52	1.42
Cost (€, SW)	13,085	8,478	2,509	8,198	5,554	1,694	3,300
Cost (€, BW)	8,178	5,299	1,568	5,124	3,471	1,059	

Table 65: Cost of the scaled ERD for BW and SW desalination

5.3.6. Manufacturing complexity

In order to develop the pressure exchanger with two combined double-acting cylinders for the selected flow rates, the system the main tube, the pistons and the rod as well as the tubing of the system have to be scaled accordingly. Thus, new resized components have to be manufactured and assembled, making the development of this ERD particularly complex.

5.4. Pressure exchangers with three combined double-acting cylinders

As described in Paragraph 3.2.1.3, pressure exchangers with three combined double-acting cylinders, such as the Spectra Pearson pump, include a motor that enforces the rotation of the connecting shaft of the pistons. Since no additional power supply can be provided at the examined RO desalination system, it is examined whether the pistons, coupled on the same rotational shaft in order to interact with each other, will operate efficiently without the use of a motor. The scheme of the suggested ERD is presented at the following figure.

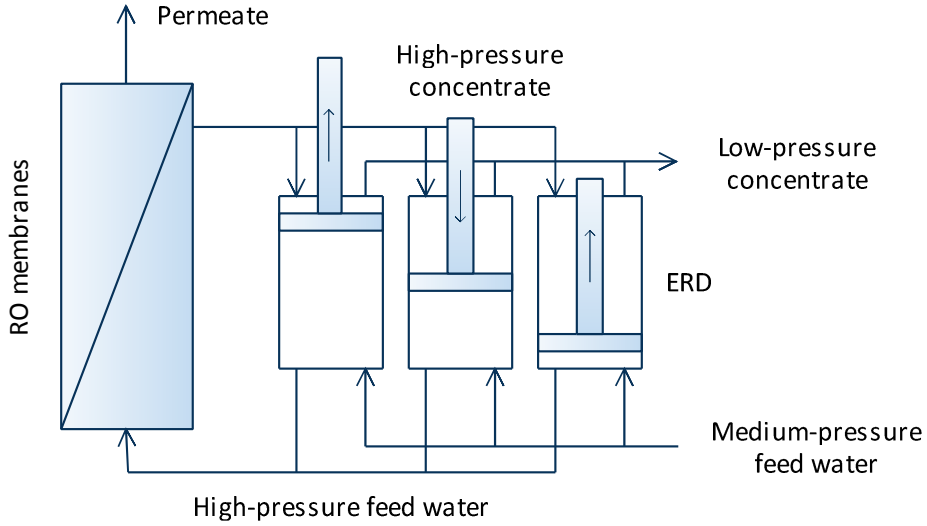

Figure 79: Pressure exchanger with three combined double-acting cylinders

5.4.1. Energy efficiency

Since the efficiency of pressure exchangers with three combined double-acting cylinders is not known, it is estimated for the Spectra Person pump using the specifications provided by the manufacturer for the LB 10000 RO desalination system that includes a Pearson pump as ERD.

System	LB 10000
Qp (m3/h)	1.58
RR (%)	35%
Qf (m3/h)	4.51
Qb (m3/h)	2.93
pfin (bar)	1.4
pfout (bar)	60
Δp (bar)	0.4
pb (bar)	59.6
Pin (W)	176
Preq. (W)	3476
Pm (W)	3300
n (%)	90%

Table 66: Spectra Pearson pump efficiency calculation

The suggested ERD does not include a motor, so the efficiency will not include losses induced by the motor. However, higher inlet feed pressure may be required since the power provided by the brine stream may not be enough to pressurise adequately the feed stream. Therefore, the efficiency calculated above can be taken into account for the pressure exchanger with three combined double-acting pistons without motor.

In order to derive the relation between the inlet feed pressure and the pressure losses, the scheme of the ERD at a random point of operation is used. The forces acting on each piston are drawn and a torque balance at the shaft that connects the three pistons is used.

$$\tau_{net} = 0$$

$$\Rightarrow F_f^{in} \cdot \sin 30 + \left(F_b - F_f^{out}\right) + F_f^{in} \cdot \sin 30 = 0$$

$$\Rightarrow F_f^{in} + F_b = F_f^{out}$$

$$\Rightarrow p_f^{in} \cdot A + p_b \cdot B = p_f^{out} \cdot A \quad \textbf{[33]}$$

Taking into account the friction losses and equation 12, $RR = 1 - B/A$, equation 33 becomes:

$$\Rightarrow p_f^{in} + p_b \cdot (1 - RR) - \Delta p_{fr} = p_f^{out} \quad \textbf{[34]}$$

$$\Rightarrow p_f^{in} = p_f^{out} + \Delta p_{fr} - p_b \cdot (1 - RR) \quad \textbf{[35]}$$

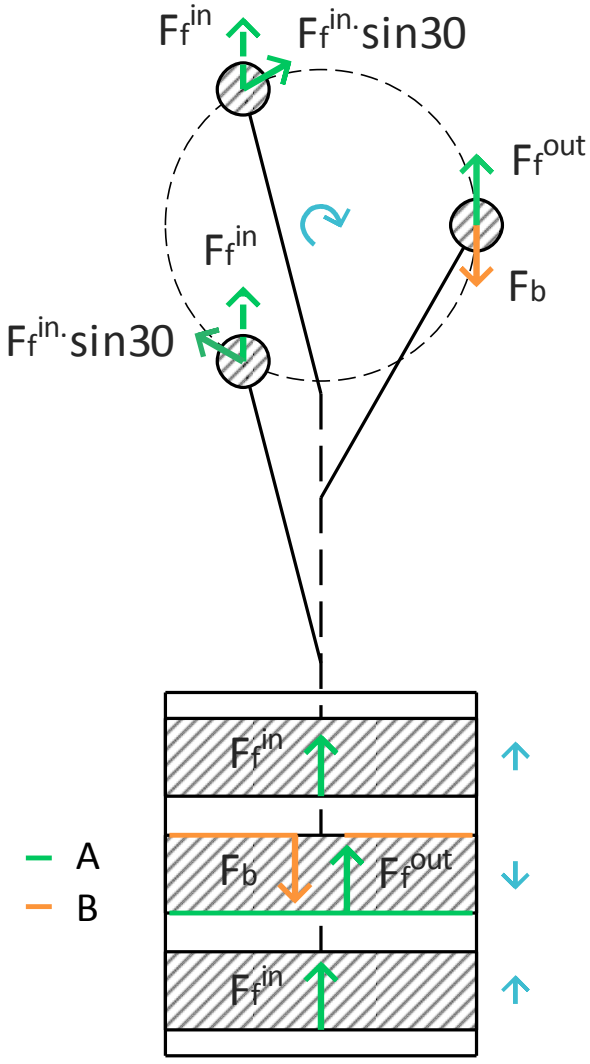

Figure 80: Scheme of the pistons and the connecting rotational shaft with the acting forces

It is observed that the inlet feed pressure is related to the pressure losses occurring in the pressure exchanger with three pistons with the same equation as in the case of the pressure exchanger with two double acting cylinders, described in the previous paragraph (equation 32).

The efficiency of the ERD is calculated as the ratio of the power output to the power input:

$$n = \frac{P_{out}}{P_{in}} = \frac{\left(p_f^{out} - p_f^{in}\right) \cdot Q_f}{p_b \cdot Q_b}$$

Using equation 35 and $Q_b = Q_f \cdot (1 - RR)$:

$$\Rightarrow n = \frac{\left(p_f^{out} - \left(p_f^{out} + \Delta p_{fr} - p_b \cdot (1 - RR)\right)\right)}{p_b \cdot (1 - RR)}$$

$$\Rightarrow n = \frac{p_b \cdot (1 - RR) - \Delta p_{fr}}{p_b \cdot (1 - RR)}$$

$$\Rightarrow n = 1 - \frac{\Delta p_{fr}}{p_b \cdot (1 - RR)}$$

$$\Rightarrow \Delta p_{fr} = p_b \cdot (1 - RR) \cdot (1 - n)$$

So, for feed flow rate $Q_f = 5.21\ m^3/h$ $(RR = 40\%)$ and $p_f^{out} = 60$ bar $(p_b = 59.6$ bar), the efficiency of 90% (Table 66) is taken into account. The pressure losses due to friction are calculated $\Delta p_{fr} = 3.85$ bar. Assuming that mechanical pressure losses account for 7% of total pressure losses as in the case of the Schenker ERD (Table 47), mechanical pressure losses are calculated $\Delta p_{fr}^{M} = 0.27$ bar and hydraulic pressure losses $\Delta p_{fr}^{H} = 3.58$ bar.

Hydraulic pressure losses are assumed to be the same for all examined flow rates and, as in the case of pressure exchangers with two cylinders, a scale factor for the tubing and the switching mechanism of the ERD needs to be estimated. This scale factor is not assessed in this research since a detailed model including all the losses accounting in this device would have to be developed.

As for the mechanical pressure losses occurring in pressure exchanger with three cylinders, these are estimated for the examined flow rates along with the respective scale factor of the pistons. Taking into account the Spectra Pearson pump with capacity $Q_p = 0.5\ m^3/h$ and $RR = 20\%$ the surface area of the piston $A = 9.62$ cm and the feed flow rate $Q_f = 2.5\ m^3/h$ are used in order to calculate the velocity of the piston $v_p = 72$ cm/s. As in pressure exchangers with two cylinders, the velocity provided by the manufacturer is assumed to be the same for all examined flow rates. Hence, the piston surface area and the piston diameter required in all cases is calculated. Then, the scale factor for the pistons, f2, is calculated with reference to the case of $Q_f = 5.21\ m^3/h$ $(RR = 40\%)$ since the pressure losses are known for this case. In addition, the rod diameter and surface area are calculated using the recovery ratio.

							Pearson
Qp (m3/h)	4.17	2.08	0.21	4.17	2.08	0.21	0.5
RR (%)	20			40			20
Qf (m3/h)	20.83	10.42	1.04	10.42	5.21	0.52	2.50
d (cm)	10.10	7.14	2.26	7.14	5.05	1.60	3.5
A (cm2)	80.18	40.09	4.01	40.09	20.04	2.00	9.62
vp (cm/s)	72.18						72.18
Scale factor f2	2.00	1.41	0.45	1.41	1.00	0.32	

Table 67: Scale factor of the pistons, f2, assuming the piston velocity of the Pearson pump

Using the recovery ratio the diameter and the surface area of the rod is also calculated:

$$RR = 1 - \frac{B}{A} = \frac{(A - B)}{A} = \frac{A_{rod}}{A} = \frac{(\pi \cdot d_{rod}^2/4)}{(\pi \cdot d^2/4)} = \left(\frac{d_{rod}}{d}\right)^2$$

RR (%)	20			40			Pearson
A (cm^2)	80.18	40.09	4.01	40.09	20.04	2.00	9.62
d (cm)	10.10	7.14	2.26	7.14	5.05	1.60	3.5
Arod (cm^2)	16.04	8.02	0.80	16.04	8.02	0.80	1.92
drod (cm)	4.52	3.20	1.01	4.52	3.20	1.01	1.57

Table 68: Diameter and surface area of the rod

Mechanical pressure losses occur at the interface between the o-rings of the pistons and the rod and the wall of the cylinders. The diameter of the o-rings is calculated taking into account the relation between the piston and rod diameter and the diameter of the o-rings used for the new design of pressure exchanger with two cylinders. The thickness of the o-rings is calculated using the relation between the o-ring diameter and o-ring thickness derived in . Then, scale factors for both the diameter and the thickness of the o-rings are calculated (with reference to the case of $Q_f = 5.21\ m^3/h$), using the mean value of the piston and the rod cases.

O-ring piston						
din (mm)	95.78	67.73	21.42	67.73	47.89	15.14
t (mm)	4.48	3.83	2.77	3.83	3.38	2.62
O-ring rod						
din (mm)	45.18	31.95	10.10	45.18	31.95	10.10
t (mm)	3.31	3.01	2.50	3.31	3.01	2.50

Scale factor fd	1.71	1.21	0.38	1.41	1.00	0.32
Scale factor ft	1.21	1.07	0.83	1.12	1.00	0.80

Table 69: Inner diameter d_{in} and thickness t of the o-rings of the pistons and the rod and respective scale factors

The mechanical pressure losses are calculated using the equation:

$$\Delta p_{fr}^{M} = \frac{F_{fr}}{A}$$

Where A is the surface area of the piston which has a quadratic relation with the scale factor f_2. F_{fr} is the friction force exerted on the surface area of the o-rings ($\approx t \cdot \pi \cdot d_{out}$) that contact the wall of the main tube and the centre block and therefore has a linear relation with the product of the scale factors $f_t \cdot f_d$. Thus, the mechanical pressure losses are calculated using the scale factor $(f_t \cdot f_d)/f_2^2$.

Qp (m^3/h)	4.17	2.08	0.21	4.17	2.08	0.21
RR (%)	20			40		
Qf (m^3/h)	20.83	10.42	1.04	10.42	5.21	0.52
ΔpfrM (bar)	0.14	0.17	0.42	0.21	0.27	0.68

Table 70: Mechanical pressure losses Δp_{fr}^{M} for the examined flow rates

Consequently, the total pressure losses due to friction Δp_{fr} are the sum of the hydraulic Δp_{fr}^{H} and the mechanical losses Δp_{fr}^{M}.

Qp (m^3/h)	4.17	2.08	0.21	4.17	2.08	0.21
RR (%)	20			40		
Qf (m^3/h)	20.83	10.42	1.04	10.42	5.21	0.52
ΔpfrH (bar)	3.58					
ΔpfrM (bar)	0.14	0.17	0.42	0.21	0.27	0.68
Δpfr (bar)	3.72	3.75	4.00	3.79	3.85	4.26

Table 71: Total pressure losses due to friction Δp_{fr} for the examined flow rates

At the following figures the total pressure losses due to friction Δpfr and the scale factor of the pistons, f2, is presented for the examined feed flow rates for $RR = 20\%$ and $RR = 40\%$.

Qf (m^3/h)	20.83	10.42	1.04	10.42	5.21	0.52
Scale factor f2	2.00	1.41	0.45	1.41	1.00	0.32
Δpfr (bar)	3.72	3.75	4.00	3.79	3.85	4.26

Table 72: Scale factor of the pistons (f2) of the ERD and total pressure losses due to friction Δp_{fr}

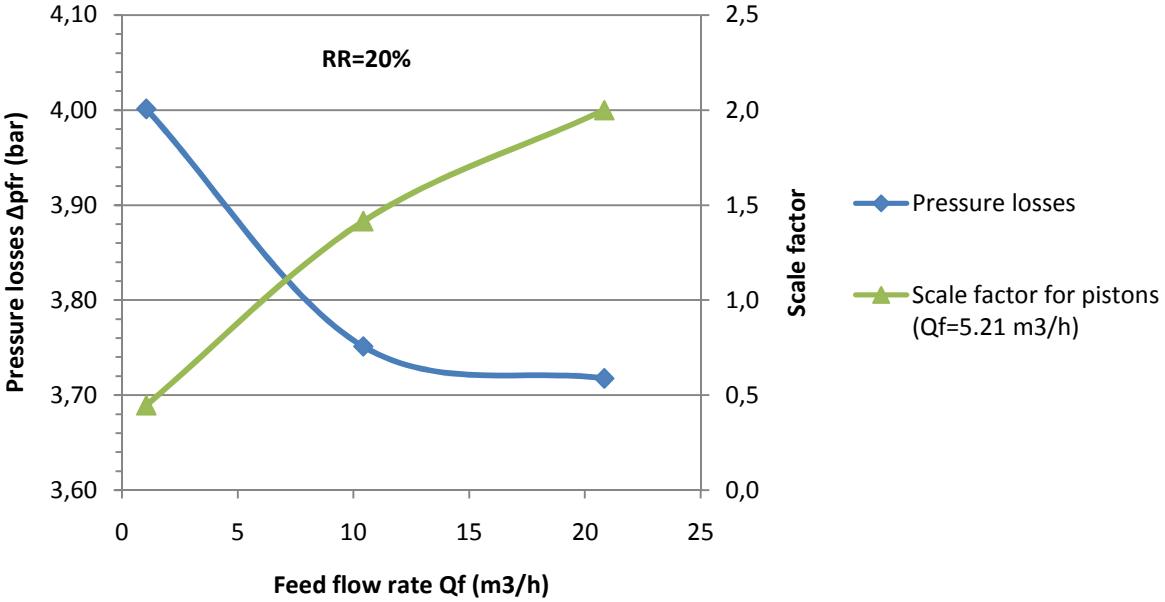

Figure 81: Scale factor of the pistons of the ERD and total pressure losses (RR=20%)

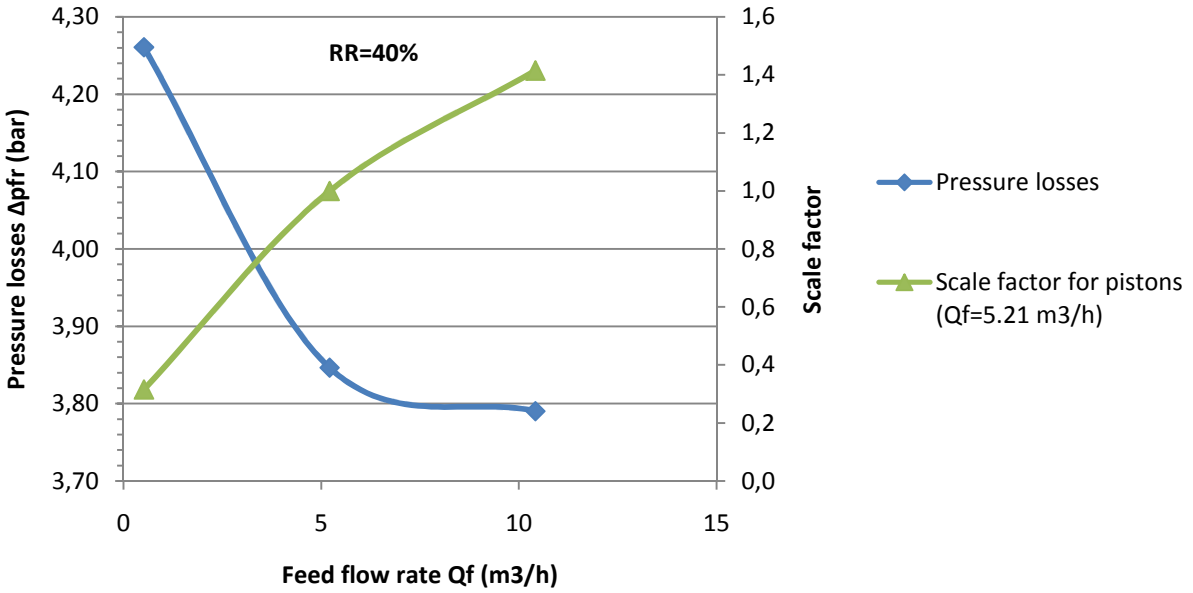

Figure 82: Scale factor of the pistons of the ERD and total pressure losses Δp_{fr} (RR=40%)

Using the pressure losses, the efficiency of pressure exchangers with three pistons is estimated for the examined flow rates and pressures.

$$\Rightarrow n = 1 - \frac{\Delta p_{fr}}{p_b \cdot (1 - RR)}$$

n (%)		Qf (m^3/h)					
		20.83	10.42	1.04	10.42	5.21	0.52
pfout (bar)	8	40	39	35	18	17	8
	12	60	60	57	46	45	39
	16	70	70	68	60	59	55
	40	88	88	87	84	84	82
	50	91	91	90	87	87	86
	60	92	92	92	89	89	88

Table 73: Overall efficiency of pressure exchangers with three combined double-acting cylinders

At the following figures the efficiency of the pressure exchanger with three combined double-acting cylinders is presented for the examined feed flow rates.

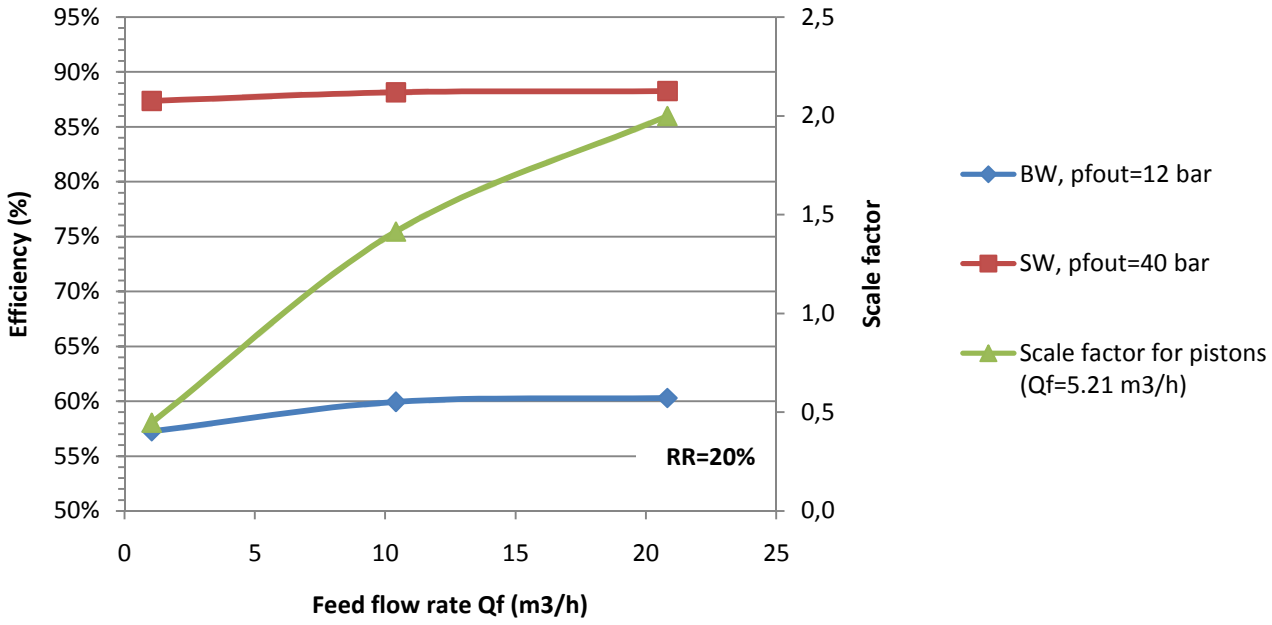

Figure 83: Efficiency and scale factor of pressure exchangers with three combined double-acting cylinders (RR=20%)

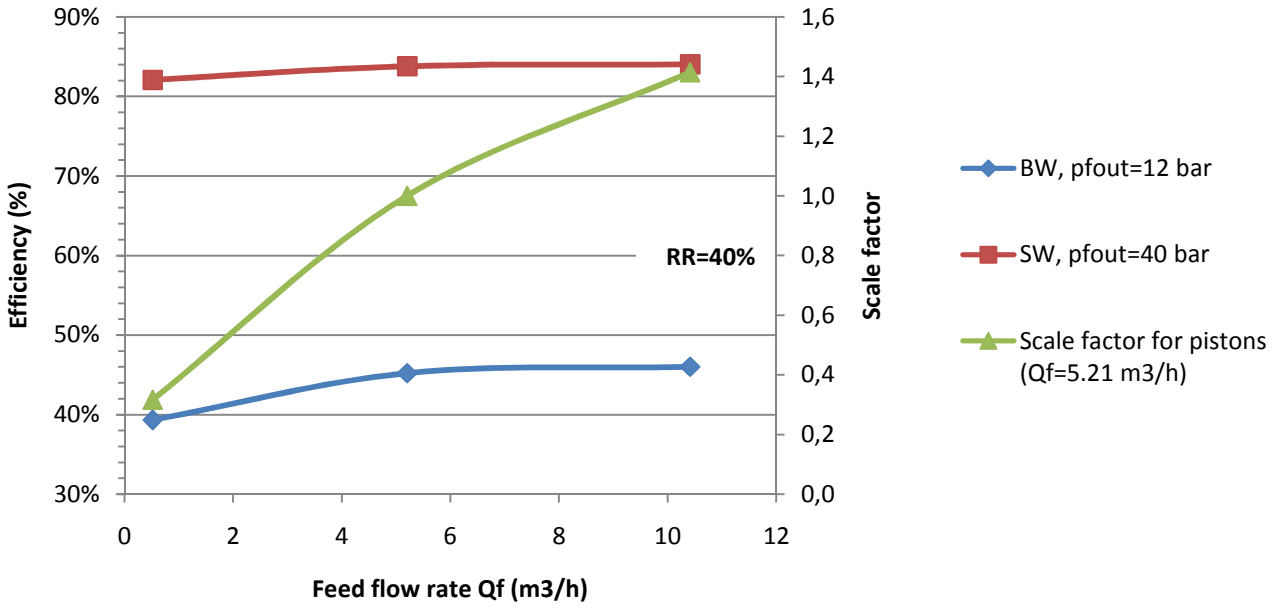

Figure 84: Efficiency and scale factor of pressure exchangers with three combined double-acting cylinders (RR=40%)

5.4.2. Power and pressure requirements

Using the overall efficiency of pressure exchanger with three combined double-acting cylinders, the required inlet feed pressure is calculated:

$$\Rightarrow p_f^{in} = p_f^{out} + \Delta p_{fr} - p_b \cdot (1 - RR)$$

pfin (bar)		Qf (m^3/h)					
		20.83	10.42	1.04	10.42	5.21	0.52
pfout (bar)	8	5.56	5.59	5.84	7.17	7.23	7.64
	12	6.36	6.39	6.64	8.77	8.83	9.24
	16	7.16	7.19	7.44	10.37	10.43	10.84
	40	12.04	12.07	12.32	20.03	20.09	20.50
	50	14.04	14.07	14.32	24.03	24.09	24.50
	60	16.04	16.07	16.32	28.03	28.09	28.50

Table 74: Inlet feed pressure for pressure exchanger with three combined double-acting cylinders

At the following figure the inlet feed pressure, pfin, is shown, for brackish water desalination of RO pressure of 12 bar and seawater desalination of RO pressure of 40 bar, for the APM-driven piston pump for the examined feed flow rates.

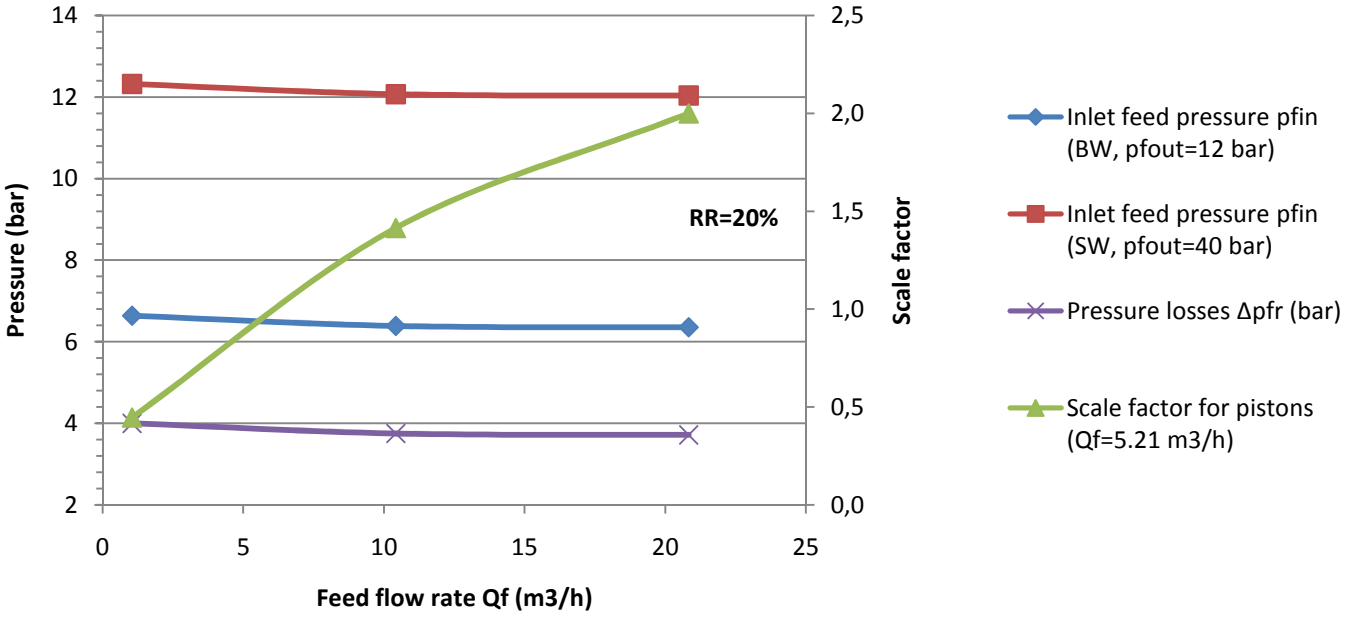

Figure 85: Inlet feed pressure for pressure exchanger with three combined double-acting cylinders (RR=20%)

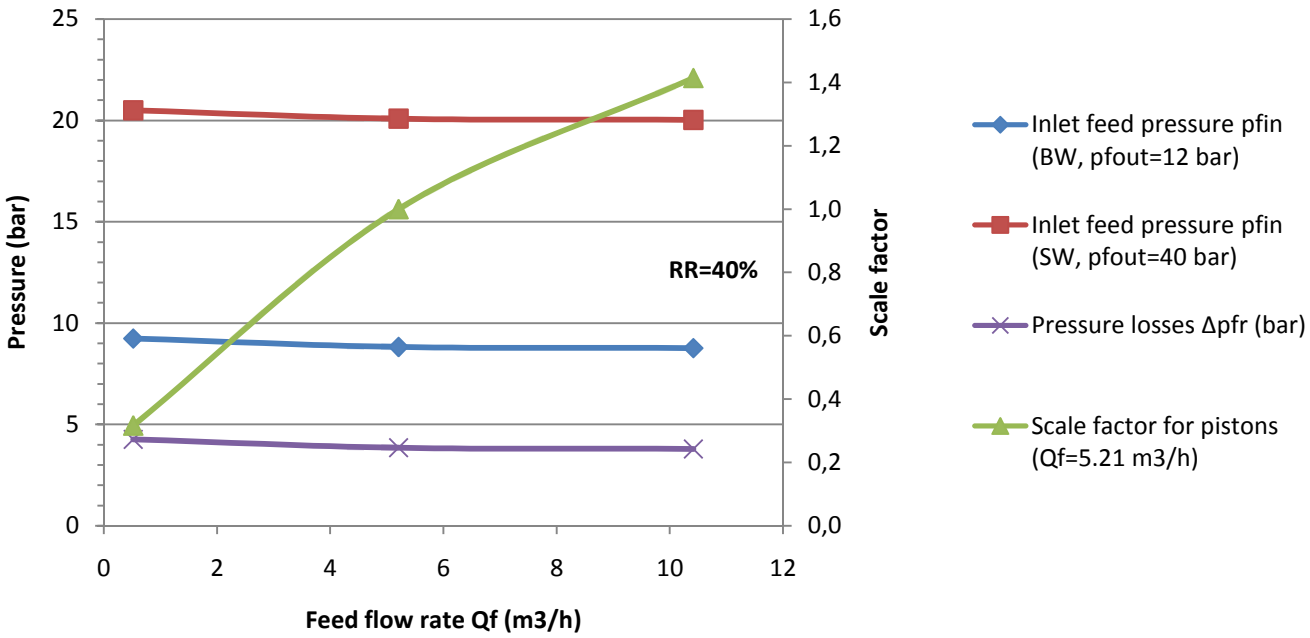

Figure 86: Inlet feed pressure for pressure exchanger with three combined double-acting cylinders (RR=40%)

As in the previous energy recovery concepts, another indicator of the performance of the energy recovery device is the percentage of the power required at the inlet of the membranes that is provided by the recovered power:

$$\frac{P_{rec}}{P_{out}} = \frac{p_f^{out} - p_f^{in}}{p_f^{out}}$$

So in the case of APM-driven piston pump the percentage of the power provided to the membranes that is provided by the recovered power is:

Prec/Pout (%)		Qf (m^3/h)					
		20.83	10.42	1.04	10.42	5.21	0.52
pb (bar)	8	31	30	10	10	10	4
	12	47	47	45	27	26	23
	16	55	55	53	35	35	32
	40	70	70	69	50	50	49
	50	72	72	71	52	52	51
	60	73	73	73	53	53	52

Table 75: Percentage of power output provided by the recovered power

At the following figure the power ratio, Prec/Pout (%), is shown, for brackish water desalination of RO pressure of 12 bar and seawater desalination of RO pressure of 40 bar, for $RR = 20\%$ and $RR = 40\%$.

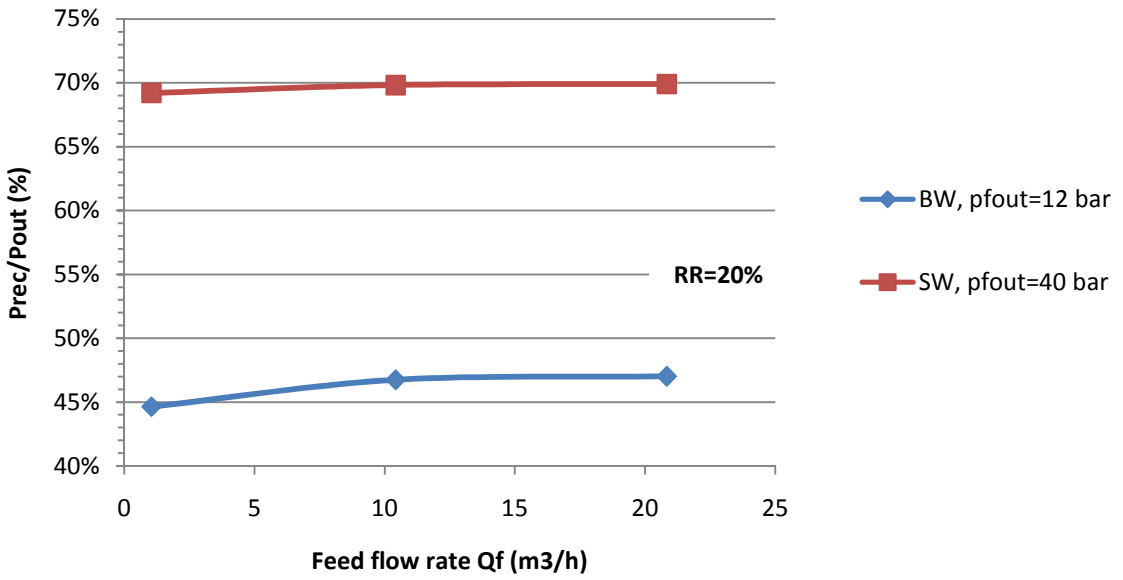

Figure 87: Power ratio Prec/Pout for pressure exchanger with three combined double-acting cylinders (RR=20%)

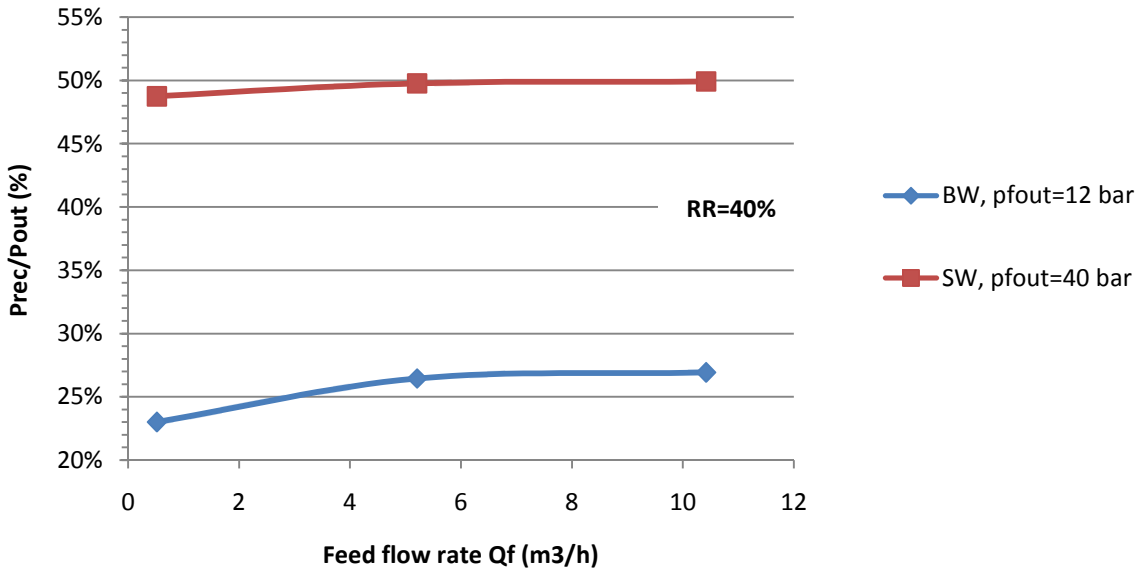

Figure 88: Power ratio Prec/Pout for pressure exchanger with three combined double-acting cylinders (RR=40%)

5.4.3. Energy autonomy

The proposed energy recovery design does not require a motor so additional power supply is not needed.

5.4.4. Operation stability

The recovery ratio of this system is kept constant by the energy recovery device, since it is defined by the area ratio of the inner and the outer surface of the pistons:

$$RR = 1 - \frac{B}{A} = \frac{(A - B)}{A} = \frac{A_{rod}}{A} = \frac{(\pi \cdot d_{rod}^2/4)}{(\pi \cdot d^2/4)} = \left(\frac{d_{rod}}{d}\right)^2$$

5.4.5. Cost analysis

The cost of pressure exchanger with three combined double-acting cylinders is estimated at 4,000 € (Pearson pump). Using this price, it is assumed that 25% of the costs correspond to installation costs, another 25% are related to assembly costs and 50% correspond to material costs.

In addition, taking into account that the Pearson pump is developed for seawater desalination, it is assumed that the pipe material required for seawater desalination is stainless steel (316 SS), in order to withstand the high pressure, and that for brackish water desalination polymer (PVC) pipes can be used. So assuming that PVC is 4 times cheaper than 316 SS, the material costs for brackish water desalination can also be estimated. Adding with installation and assembly costs and using the scale factors calculated above, the cost of the system is calculated for both brackish and seawater desalination for the selected flow rates.

RR (%)	20			40		
Qp (m^3/h)	4.17	2.08	0.21	4.17	2.08	0.21
Qf (m^3/h)	20.83	10.42	1.04	10.42	5.21	0.52
Cost (€, SW)	8,000	5,657	1,789	5,657	4,000	1,265
Cost (€, BW)	5,000	3,536	1,118	3,536	2,500	791

Pearson pump
35
1.58
4.52
4,000

Table 76: Cost of the scaled ERD for BW and SW desalination

5.4.6. Manufacturing complexity

In order to develop the pressure exchanger with three combined double-acting cylinders for the examined flow rates, the main tube, the pistons and the rod as well as the tubing of the system have to be scaled accordingly. Thus, new resized components have to be manufactured and assembled, making the development of this ERD particularly complex.

5.5. Inverse positive displacement pump

As explained in Paragraph 3.3, the Seawater pump with energy recovery device (SWPE), developed by Danfoss, uses an Axial Piston Pump (APP) as a high pressure boost pump and an inverse APP, namely an Axial Piston Motor (APM), as an energy recovery device. In SWPE, the APP and the APM are both connected to a double shafted electric motor (Figure 41). However, for SWPE the inlet feed pressure is required to be positive between 0.5 and 5 bar. At speeds above 3,000 rpm the pressure at the inlet of the pump must be min. 2 bar. The minimum pressure difference required by SWPE is 15 bar, because the motor is water lubricated and if the pressure difference is lower, the motor wears out. By providing higher inlet feed pressure, the pressure difference between the inlet and the outlet becomes lower than 5-10 bar for brackish water. However, the inlet feed flow presses internally the APP housing and the other parts, which are only designed to withstand maximum pressure of 5 bar.

Since, no additional power supply can be provided in the case of the examined RO desalination system, it is investigated whether an ERD with the same configuration as SWPE but without a motor can operate efficiently.

In order to overcome the constraint of maximum 5 bar inlet feed pressure a centrifugal pump or Grundfos BMP piston pump may be used instead of the Danfoss Axial Piston Pump (APP). Thus, the suggested configuration would involve an Axial Piston Motor (APM) directly coupled to a pump impeller.

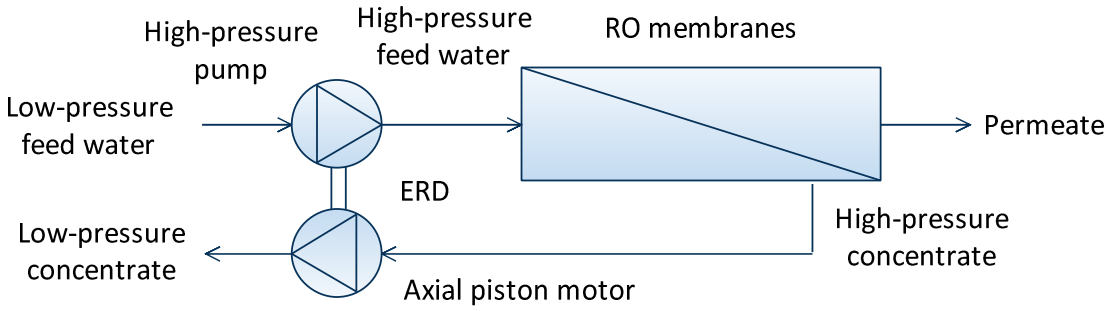

Figure 89: Axial Piston Motor directly coupled to pump

5.5.1. Energy efficiency

Using the characteristics provided by the manufacturer the efficiency of the SWPE is estimated for the lowest and the highest capacity model at 1,450 rpm.

SWPE (1450 rpm)	APP1.0/APM0.8	APP2.5/APM1.8
RR (%)	29	32
Qf (m3/h)	0.50	1.25
Qb (m3/h)	0.36	0.85
pfin (bar)	3	3
pfout (bar)	80	80
Δp (bar)	0.4	0.4
pb (bar)	79.6	79.6
Pm (kW)	1100	2200
n (%)	57	66

Table 77: Efficiency of the SWPE (1450 rpm)

The low efficiency of the SWPE reinforces the need for a new design of the ERD. The overall efficiency of the suggested ERD configuration is estimated as the product of the efficiencies of the components. The efficiency of the APM is shown at the following table.

Danfoss APM	APM 0.8	APM 1.2	APM 1.8	APM 2.9
N (rpm)	3000	3000	3000	3000
Qb (m3/h)	0.8	1.2	1.8	2.9
npm (%)	83	85	89	84

Table 78: Danfoss APM efficiency, npm (%)

It can be seen that the piston motor is developed only for three of the examined brine flow rates. Therefore, the APM-driven pump is applicable for brine flow rate $\mathrm{Q_b} = 0.31, 0.83 \text{ and } 3.13 \ \mathrm{m^3/h}$.

Qb (m3/h)	16.67	8.33	0.83	6.25	3.13	0.31
npm (%)	-	-	83	-	84	83

Table 79: APM efficiency, npm (%)

The efficiency of piston pumps is higher than centrifugal pumps, especially for low brine flow rates. Hence, the use of Grundfos BMP piston pump is considered and the efficiency of the piston pump is taken into account.

Qf (m^3/h)	20.83	10.42	1.04	10.42	5.21	0.52
n1 (%)	-	81	89	81	84	76

Table 80: Piston pump efficiency, n1 (%) (Grundfos A/S, 2013)

The overall efficiency of the APM-driven piston pump for the examined flow rates is estimated:

Qf (m^3/h)	20.83	10.42	1.04	10.42	5.21	0.52
nt (%)	-	-	74	-	67	63

Table 81: APM-driven pump overall efficiency, nt (%)

Since both the piston pump and the piston motor are designed for outlet feed pressure of 80 bar it is assumed the above calculated efficiencies refer to the case of outlet feed pressure of 60 bar and , hence, he efficiency of the ERD for the other examined pressure values needs to be assessed.

As in the case of the pressure exchanger with three combined double-acting cylinders a torque balance at a random point of operation of the ERD is used in order to derive the relation between the inlet feed pressure and the pressure losses.

$$\tau_{net} = 0$$

$$\Rightarrow F_f^{in} + F_b = F_f^{out}$$

$$\Rightarrow p_f^{in} \cdot A + p_b \cdot B = p_f^{out} \cdot A \quad \textbf{[36]}$$

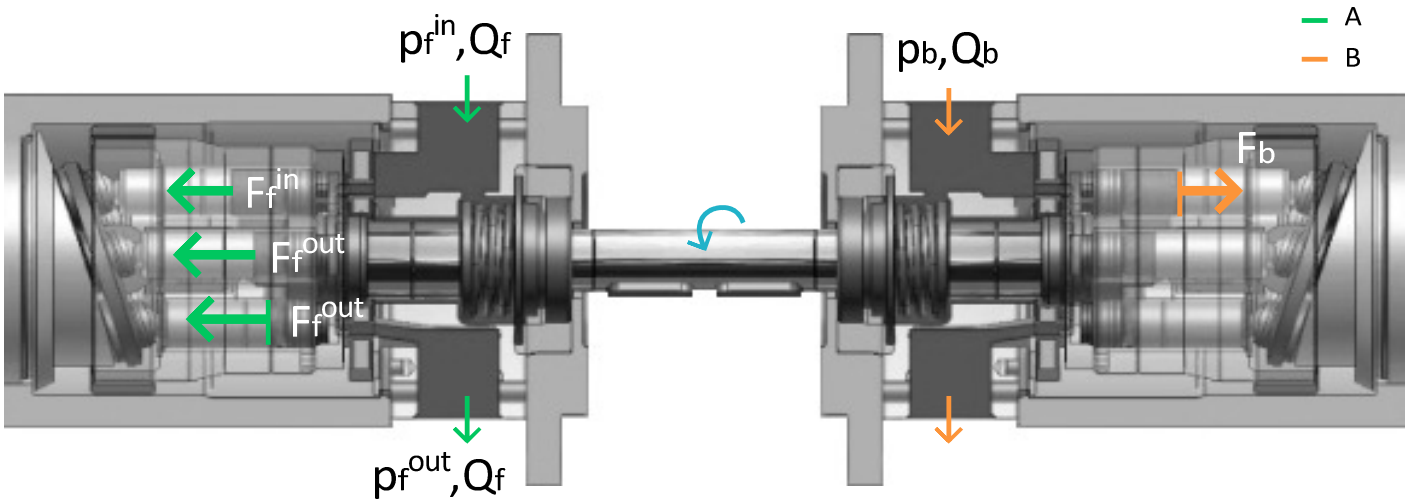

Figure 90: APM-driven piston pump

Taking into account the friction losses and equation 12, $RR = 1 - B/A$, equation 36 becomes:

$$\Rightarrow p_f^{in} + p_b \cdot (1 - RR) - \Delta p_{fr} = p_f^{out} \quad \textbf{[37]}$$

$$\Rightarrow p_f^{in} = p_f^{out} + \Delta p_{fr} - p_b \cdot (1 - RR) \quad \textbf{[38]}$$

The efficiency of the device is calculated as the ratio of the power output and the power input:

$$n = \frac{P_{out}}{P_{in}} = \frac{(p_f^{out} - p_f^{in}) \cdot Q_f}{p_b \cdot Q_b}$$

Using equation 38 and $Q_b = Q_f \cdot (1 - RR)$:

$$\Rightarrow n = \frac{\left(p_f^{out} - \left(p_f^{out} + \Delta p_{fr} - p_b \cdot (1 - RR)\right)\right)}{p_b \cdot (1 - RR)}$$

$$\Rightarrow n = \frac{p_b \cdot (1 - RR) - \Delta p_{fr}}{p_b \cdot (1 - RR)}$$

$$\Rightarrow n = 1 - \frac{\Delta p_{fr}}{p_b \cdot (1 - RR)}$$

$$\Rightarrow \Delta p_{fr} = p_b \cdot (1 - RR) \cdot (1 - n)$$

So, pressure losses due to friction are calculated for the examined flow rates.

Qf (m^3/h)	20.83	10.42	1.04	10.42	5.21	0.52
Δpfr (bar)	-	-	12.40	-	10.56	13.30

Table 82: APM-driven pump pressure losses, Δpfr (bar)

Using pressure losses the efficiency o the ERD is calculated for the examined pressures and flow rates.

$$n_t = 1 - \frac{\Delta p_{fr}}{p_b \cdot (1 - RR)}$$

For the case of feed flow rate of $5.21\ m^3/h$ the rotational speed of the piston pump (1,800 rpm) is different than the rotational speed of the APM (3,000 rpm). Therefore, for $Q_f = 5.21\ m^3/h$, the use of a reducer spur gearbox (gear ratio of 1.67:1) is considered and gearbox efficiency of 95% is taken into account.

nt (%)		Qf (m^3/h)					
		20.83	10.42	1.04	10.42	5.21	0.52
pfout (bar)	8	-	-	-	-	-	-
	12	-	-	-	-	-	-
	16	-	-	-	-	-	-
	40	-	-	61%	-	53%	44%
	50	-	-	69%	-	61%	55%
	60	-	-	74%	-	67%	63%

Table 83: APM-driven pump overall efficiency, nt (%)

Due to high pressure losses the ERD is not applicable in the case of brackish water where the outlet feed pressure required is low compared to the pressure losses. At the following figure the efficiency of the APM-driven pump, for the examined feed flow rates, is presented.

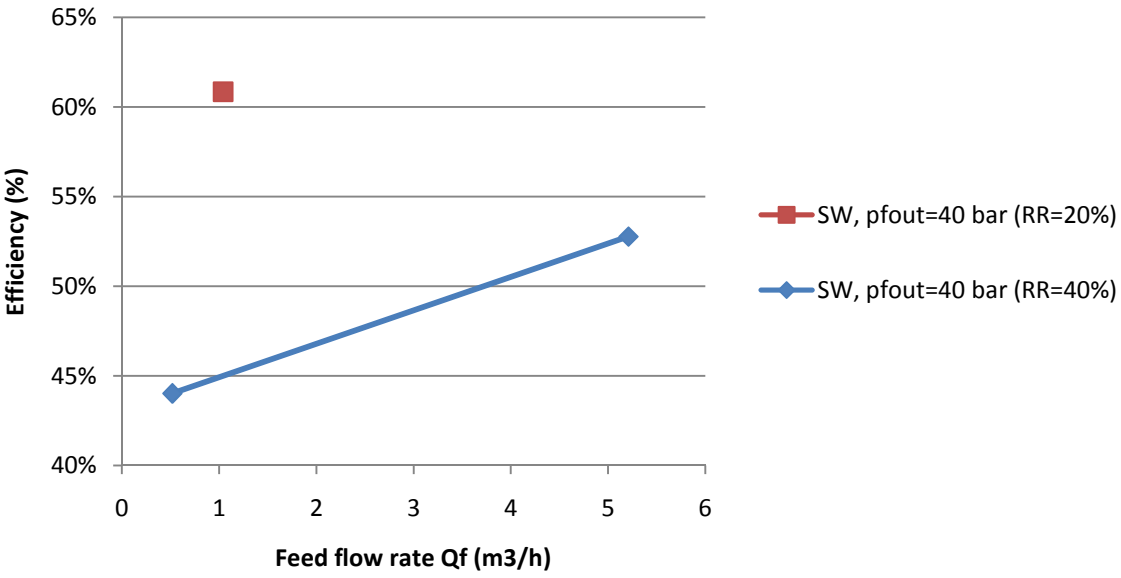

Figure 91: APM-driven piston pump efficiency

5.5.2. Power and pressure requirements

Taking into account the efficiency of the APM the power output of the APM is calculated:

Ppm (kW)		Qf (m^3/h)					
		20.83	10.42	1.04	10.42	5.21	0.52
pb (bar)	8	-	-	0.15	-	0.56	0.06
	12	-	-	0.22	-	0.85	0.08
	16	-	-	0.30	-	1.14	0.11
	40	-	-	0.76	-	2.89	0.28
	50	-	-	0.95	-	3.61	0.36
	60	-	-	1.14	-	4.34	0.43

Table 84: APM power output, Ppm (kW)

The pressure required at the inlet of the piston pump is calculated using the equation 31, as in Pelton-driven generators, but the overall efficiency is defined: $\mathrm{n_t} = \mathrm{n_1} \cdot \mathrm{n_g} \cdot \mathrm{n_{pm}}$

$$\Rightarrow \mathrm{p_f^{in}} = \mathrm{p_f^{out}} - \mathrm{n_t} \cdot \left(\mathrm{p_f^{out}} - \Delta\mathrm{p}\right) \cdot (1 - \mathrm{RR})$$

Using the overall efficiency of APM-driven piston pump (with gearbox in the case of $\mathrm{Q_f} = 5.21\ \mathrm{m^3/h}$), $\mathrm{n_t}$, calculated at Table 81, the required inlet feed pressure is calculated.

pfin (bar)		Qf (m^3/h)					
		20.83	10.42	1.04	10.42	5.21	0.52
pfout (bar)	8	-	-	-	-	-	-
	12	-	-	-	-	-	-
	16	-	-	-	-	-	-
	40	-	-	20.72	-	27.46	29.54
	50	-	-	22.72	-	31.76	33.54
	60	-	-	24.72	-	36.06	37.54

Table 85: Pressure required at the inlet of the piston pump

At the following figure the inlet feed pressure, pfin, is shown, for seawater desalination of RO pressure of 40 bar, for the APM-driven piston pump for the examined feed flow rates.

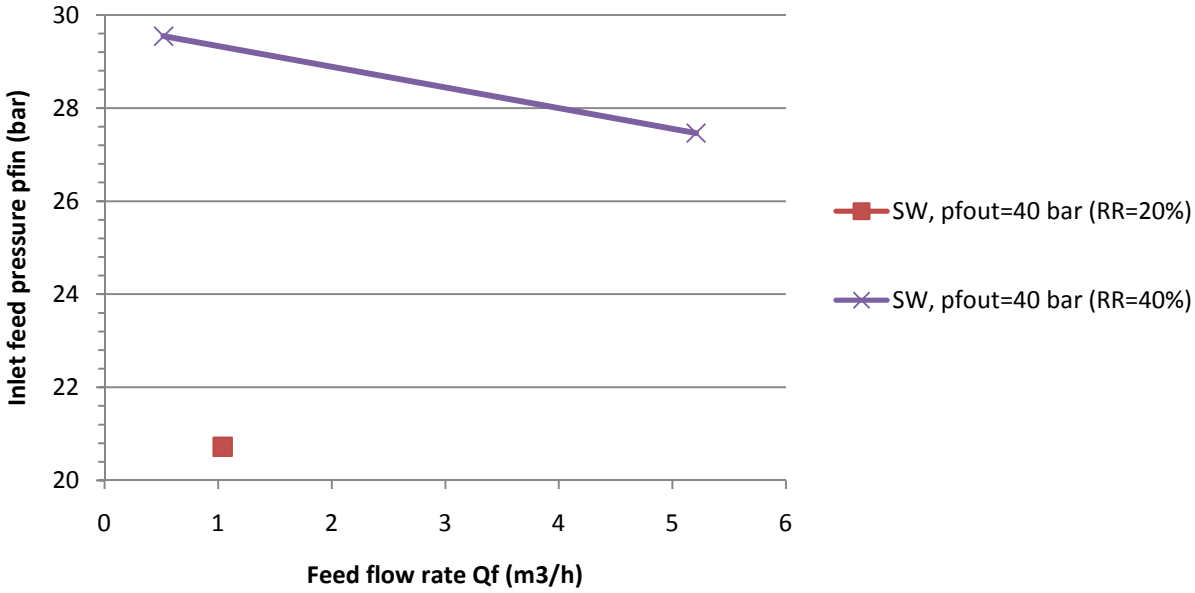

Figure 92: Inlet feed pressure for APM-driven piston pump for BW and SW

As in the previous energy recovery concepts, another indicator of the performance of the energy recovery device is the percentage of the power required at the inlet of the membranes that is provided by the recovered power:

$$\frac{P_{rec}}{P_{out}} = \frac{p_f^{out} - p_f^{in}}{p_f^{out}}$$

So in the case of APM-driven piston pump the percentage of the power provided to the membranes that is provided by the recovered power is:

Prec/Pout (%)		Qf (m^3/h)					
		20.83	10.42	1.04	10.42	5.21	0.52
pb (bar)	8	-	-	-	-	-	-
	12	-	-	-	-	-	-
	16	-	-	-	-	-	-
	40	-	-	48%	-	31%	26%
	50	-	-	55%	-	36%	33%
	60	-	-	59%	-	40%	37%

Table 86: Percentage of power output provided by the recovered power

At the following figure the power ratio, Prec/Pout (%), is shown, for seawater desalination of RO pressure of 40 bar, for $\mathrm{RR} = 20\%$ and $\mathrm{RR} = 40\%$.

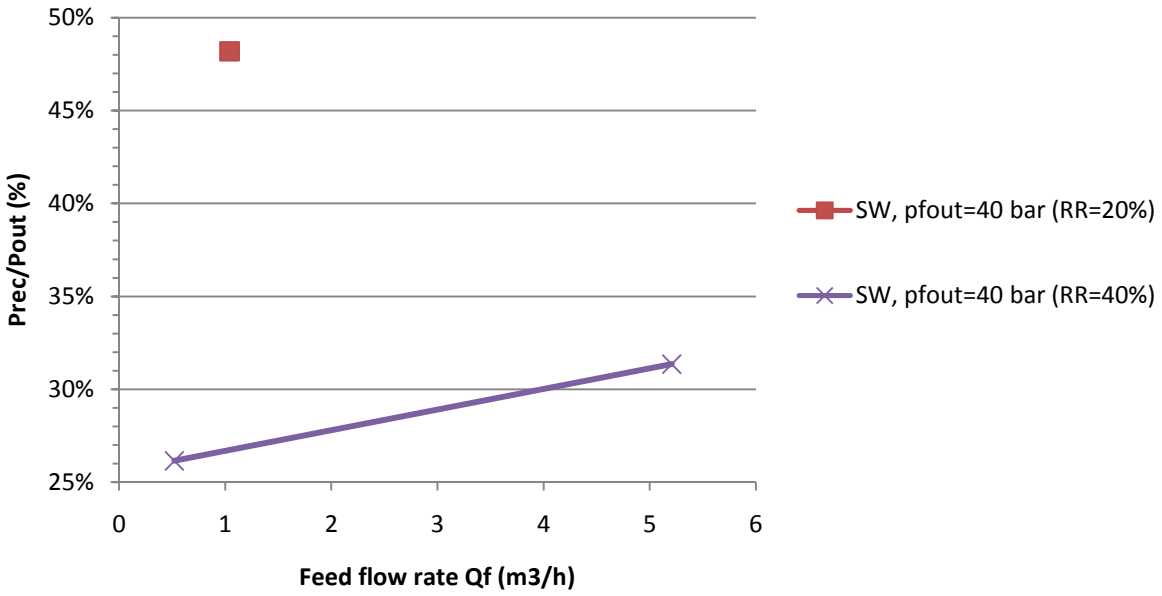

Figure 93: Power ratio Prec/Pout for APM-driven piston pump for BW and SW

5.5.3. Energy autonomy

Since it is assumed that the APM is directly coupled to the piston pump without the use of motor, no additional power supply is required.

5.5.4. Operation stability

As mentioned in the previous chapter, in the case where an APM is coupled to a piston pump, the recovery ratio is constant (assuming no leakage), due to the fixed capacity difference of the two components since they have the same rotational speed. However, at low rotational speed of the pump (<1500 rpm), the leakage of water around the pistons becomes relatively high compared to the leakage at higher pump speeds, resulting to the significant decrease of the recovery ratio (Heijman, et al., 2010).

5.5.5. Cost analysis

The cost of the piston pump is estimated:

Qf (m^3/h)	20.83	10.42	1.04	10.42	5.21	0.52
Cost (€)	-	7,000	3,500	7,000	5,700	3,500

Table 87: Grundfos BMPE piston pump cost (HYDROLOGY, 2013)

The cost of the APM is estimated:

Qb (m^3/h)	16.67	8.33	0.83	6.25	3.13	0.31
Cost (€)	-	-	1,800	-	7,000	1,600

Table 88: Danfoss APM price (Big Brand Water Filter, 2013)

The cost of the gearbox for the case of $\mathrm{Q_f} = 5.21\ \mathrm{m^3/h}$ is assumed to be 200 €. Therefore, the total cost of the APM-driven piston pump (with gearbox in the case of $\mathrm{Q_f} = 5.21\ \mathrm{m^3/h}$) is estimated:

RR (%)	20			40		
Qf (m^3/h)	20.83	10.42	1.04	10.42	5.21	0.52
Qb (m^3/h)	16.67	8.33	0.83	6.25	3.13	0.31
Cost (€)	-	-	5,300	-	12,700	5,100

Table 89: Cost of the APM-driven piston pump for the examined flow rates

5.5.6. Manufacturing complexity

For the APM-driven piston pump the APM has to be coupled to the shaft of the piston pump. In the case of $\mathrm{Q_f} = 5.21\,\mathrm{m^3/h}$ a gearbox has to be interposed.

6. Selection of energy recovery concept

In this chapter the comparison between the energy recovery concepts is performed based on the criteria evaluated in the previous chapter. The energy recovery concept that fulfils most adequately the criteria is selected and further specifications required for the development of this ERD are provided.

In order to perform a clear comparison between the five energy recovery concepts, the cases of brackish water with RO pressure of 12 bar and seawater of RO pressure of 40 bar are outlined for recovery ratio of 20% and 40% and all examined flow rates.

6.1. Energy efficiency

6.1.1. Pelton-driven generator

This ERD consists of a Pelton turbine coupled to a generator that is connected to the motor of a centrifugal or a piston pump. The efficiency of the Pelton turbine is estimated at $\eta_0 = 81\%$ with nozzle efficiency $\eta_N = 96\%$, runner efficiency of $\eta_R = 93\%$ and mechanical efficiency $\eta_m = 91\%$. The generator efficiency is estimated:

ne (%)	Qf (m^3/h)					
	20.83	10.42	1.04	10.42	5.21	0.52
BW (12 bar)	82	78	48	75	66	41
SW (40 bar)	88	85	69	84	80	53

Table 90: Generator efficiency, ne (%)

The motor efficiency is estimated:

nm (%)	Qf (m^3/h)					
	20.83	10.42	1.04	10.42	5.21	0.52
BW (12 bar)	87	84	55	82	70	46
SW (40 bar)	92	89	72	88	85	58

Table 91: Motor efficiency, nm (%)

The efficiency of the multistage centrifugal pump and piston pump is estimated:

Qf (m^3/h)	20.83	10.42	1.04	10.42	5.21	0.52
n1 (%)	71	67	34	67	60	25

Table 92: Multistage centrifugal pump efficiency (Duijvelaar Pompen, 2013)

Qf (m^3/h)	20.83	10.42	1.04	10.42	5.21	0.52
n1 (%)	-	81	89	81	84	76

Table 93: Piston pump efficiency (Grundfos A/S, 2013)

The overall efficiency of Pelton-driven generator with motorized pump is estimated:

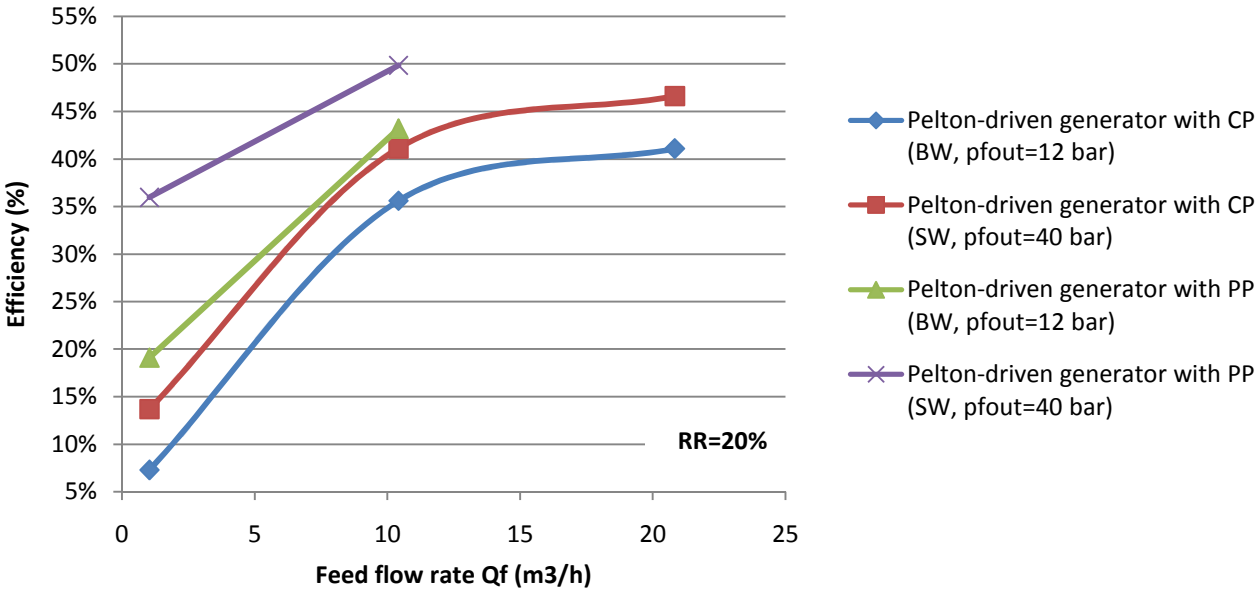

Figure 94: Efficiency of Pelton-driven generator with CP and PP respectively for selected flow rates (RR=20%)

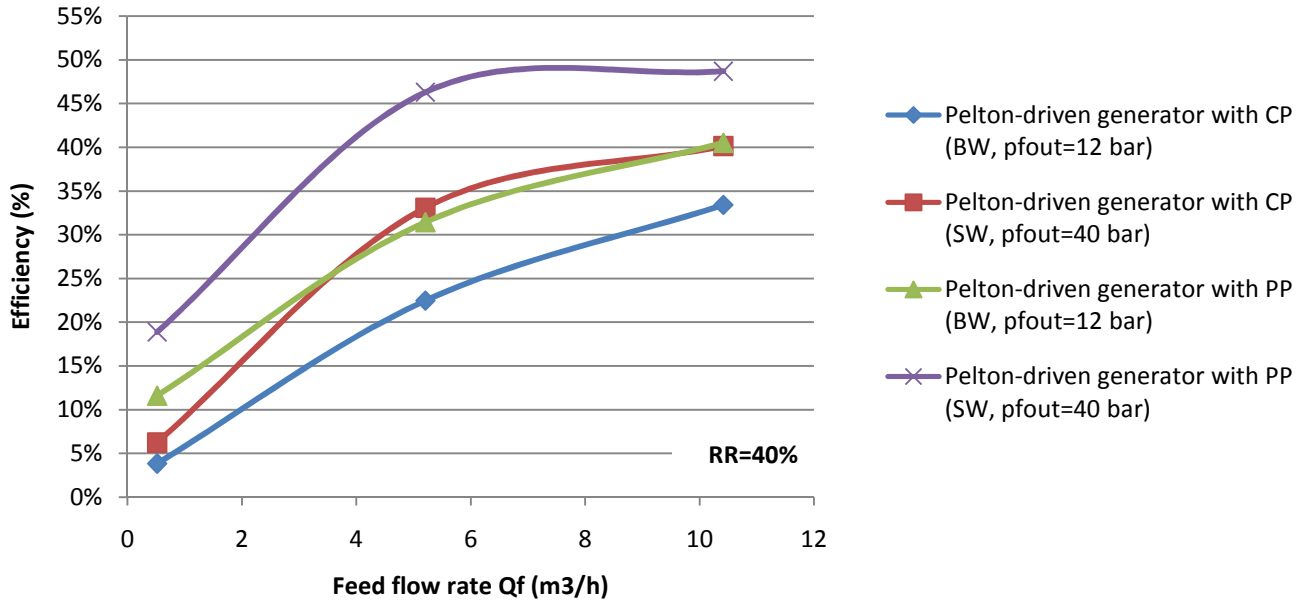

Figure 95: Efficiency of Pelton-driven generator with CP and PP respectively for selected flow rates (RR=40%)

6.1.2. Pelton-driven pump

The efficiency of the increaser spur gearbox is estimated at 95%. The overall efficiency of the Pelton-driven centrifugal pump or piston pump with gearbox is estimated:

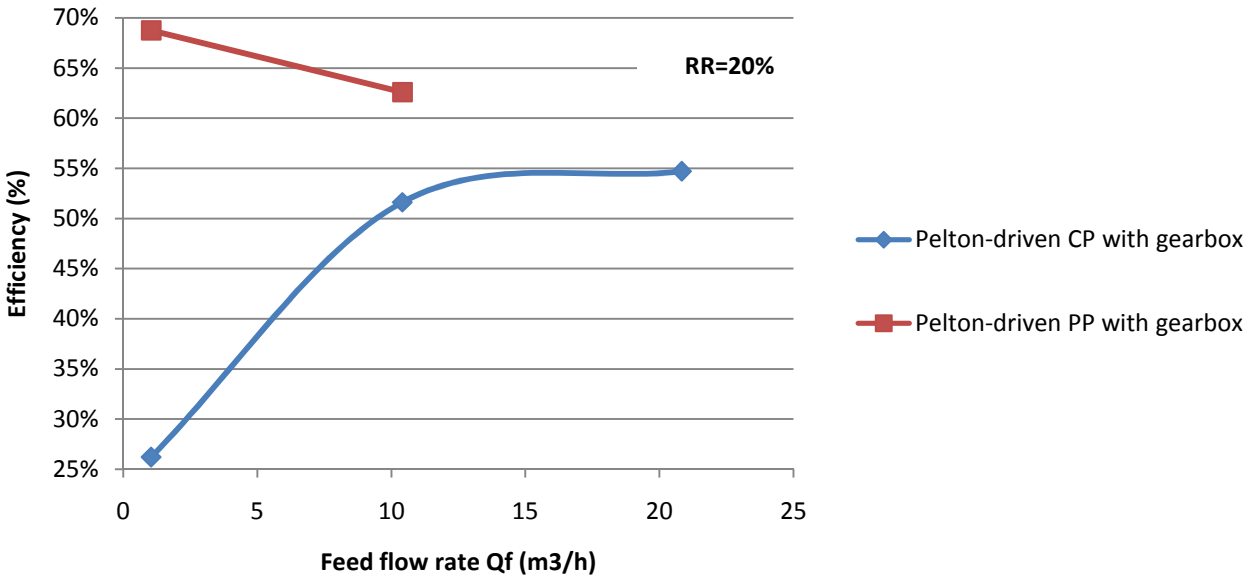

Figure 96: Efficiency of Pelton-driven CP and PP (RR=20%)

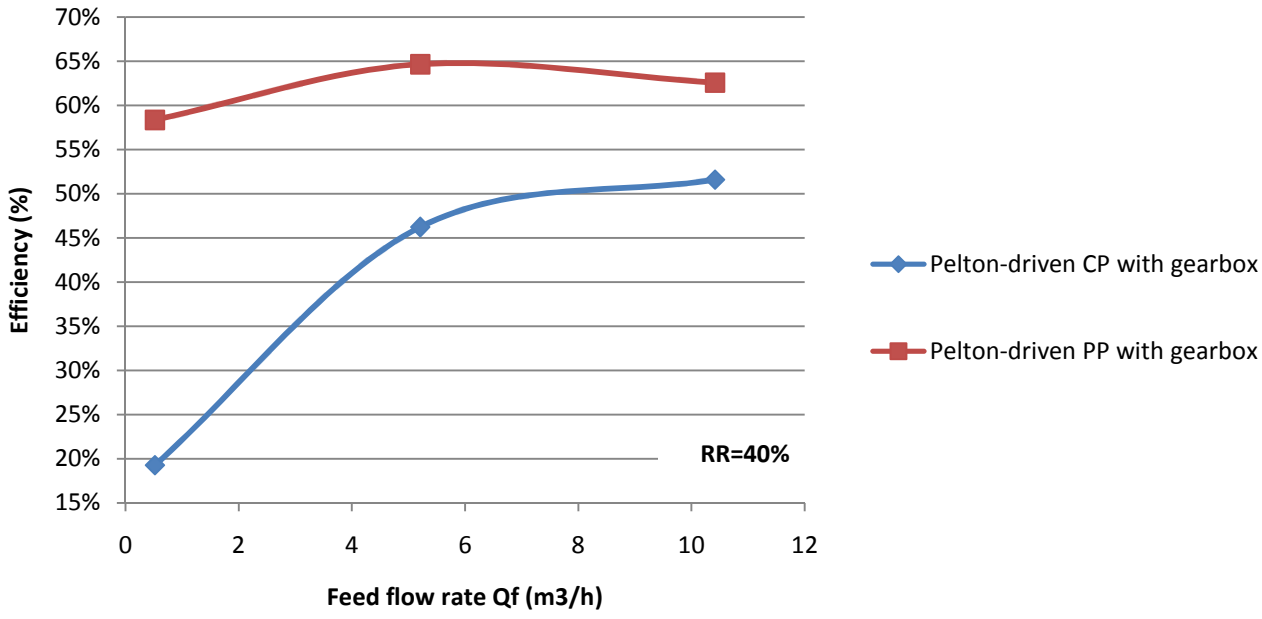

Figure 97: Efficiency of Pelton-driven CP and PP (RR=40%)

6.1.3. Pressure exchanger with two combined double-acting cylinders

The efficiency of pressure exchanger with two double-acting cylinders and the scale factor for the pistons of the ERD are estimated:

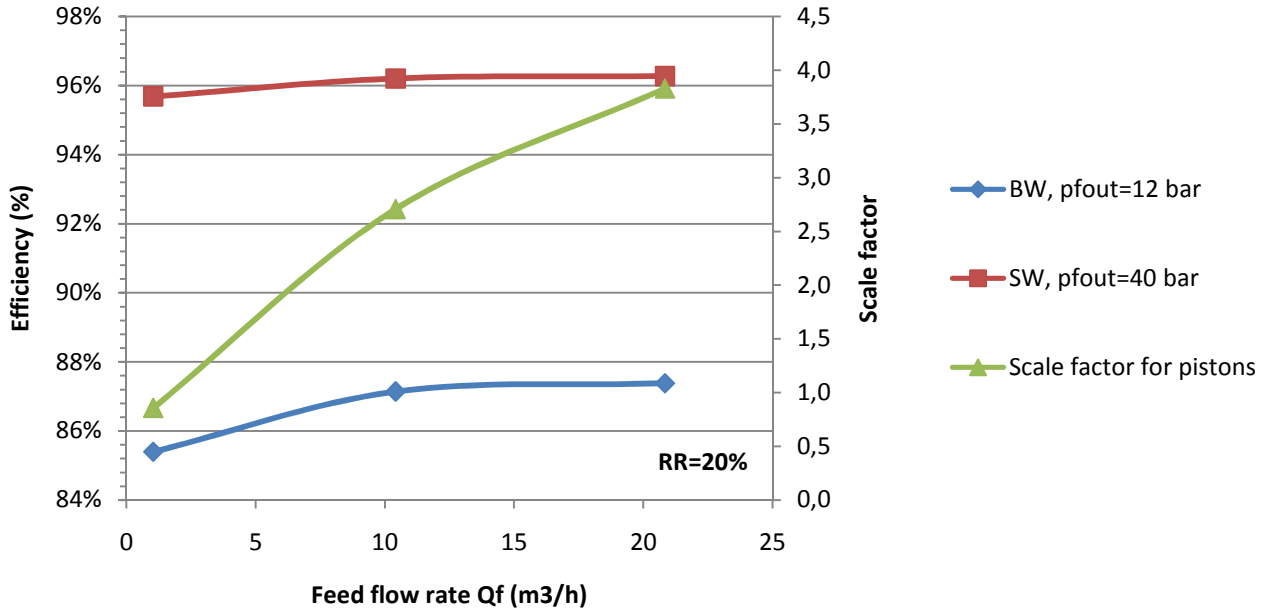

Figure 98: Efficiency of the ERD for BW and SW (RR=20%)

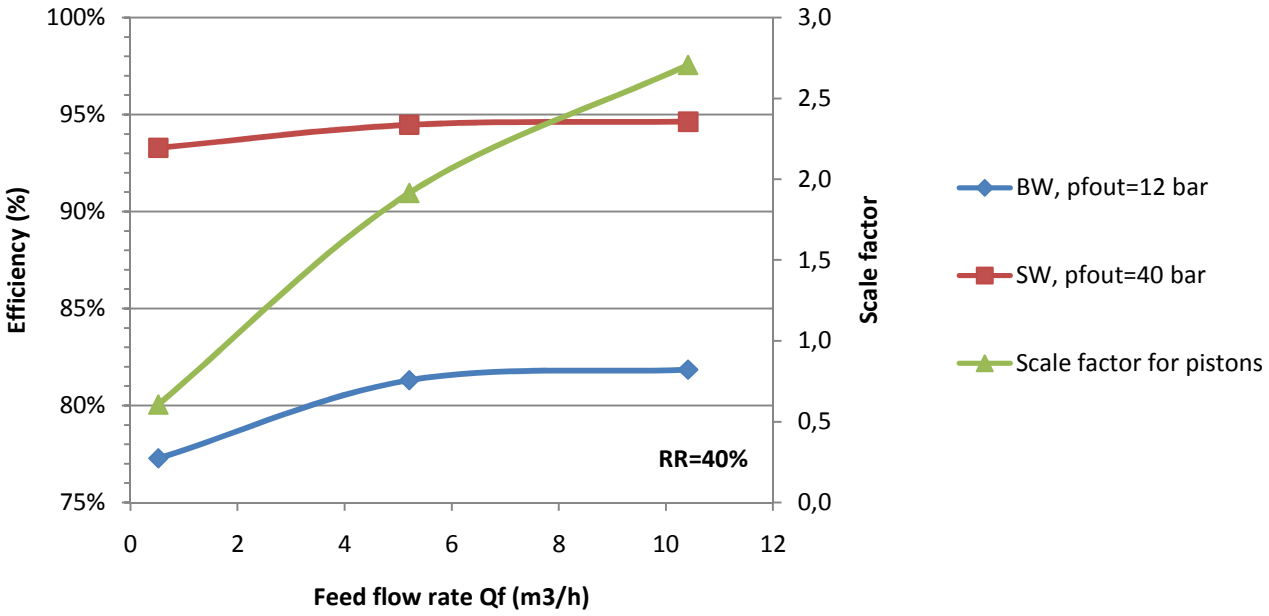

Figure 99: Efficiency of the ERD for BW and SW (RR=40%)

6.1.4. Pressure exchanger with three double-acting cylinders

The efficiency and the scale factor for the pistons of the pressure exchanger with three combined double-acting cylinders without motor are estimated:

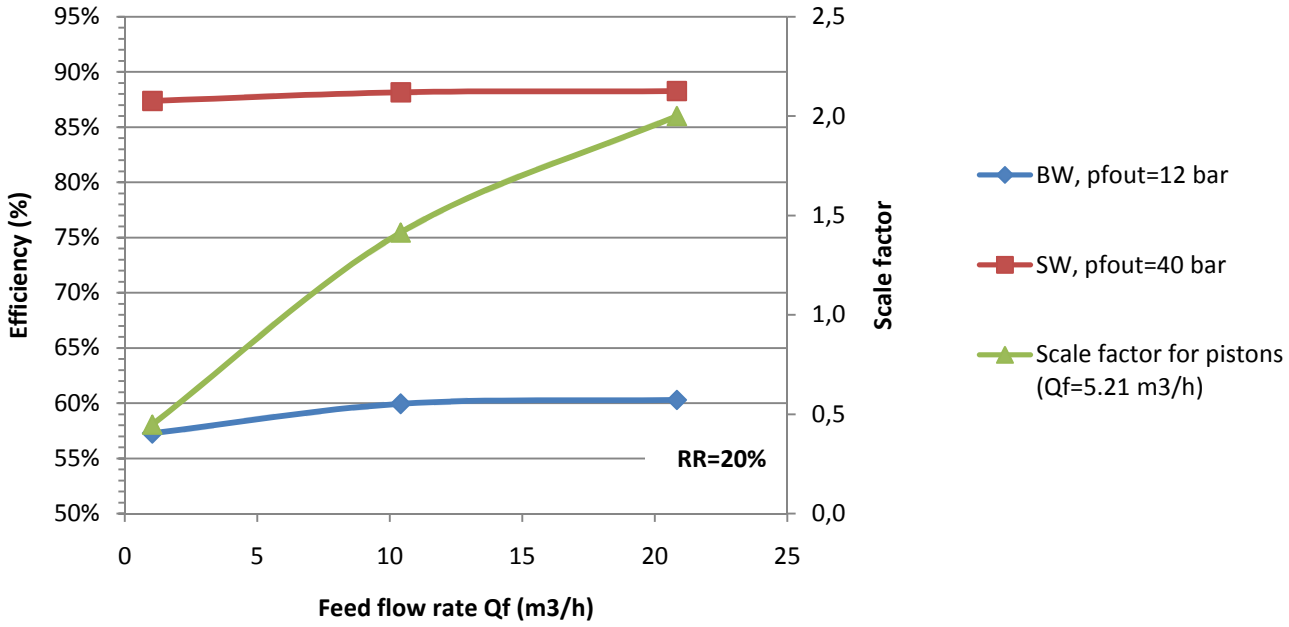

Figure 100: Efficiency and scale factor of pressure exchanger with three double-acting cylinders (RR=20%)

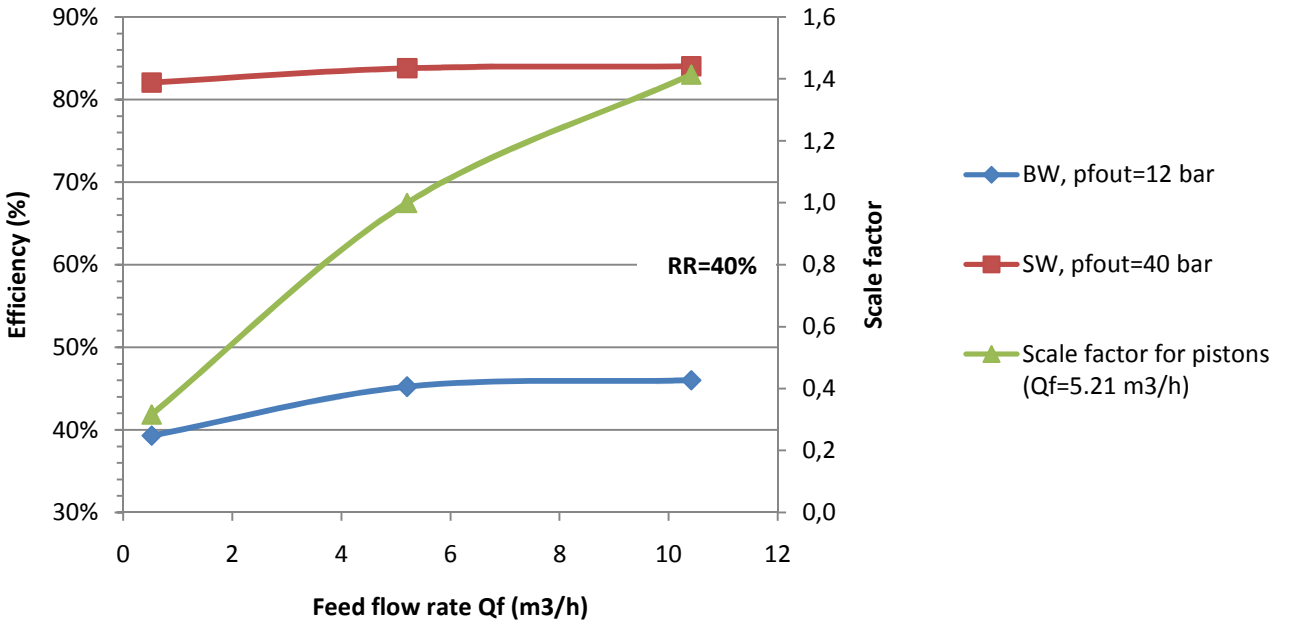

Figure 101: Efficiency and scale factor of pressure exchanger with three double-acting cylinders (RR=40%)

6.1.5. Inverse positive displacement pump

The efficiency of the APM-driven pump is estimated.

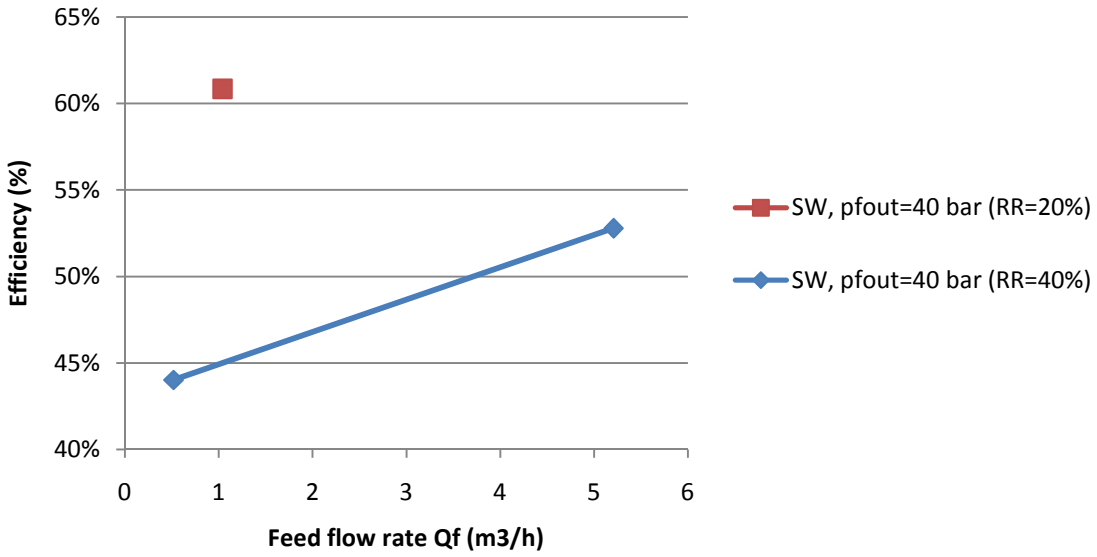

Figure 102: APM-driven piston pump efficiency

6.1.6. Comparison

Thus, the Pelton-driven piston pump with gearbox has the highest overall efficiency (up to 69%) among the examined Pelton-driven energy recovery concepts reaching 69% for $\mathrm{RR} = 20\%$ and $\mathrm{Q_f} = 1.04\,\mathrm{m^3/h}$. The efficiency of the Pelton-driven ERDs that include a centrifugal pump drops with lower flow rate, while in the case a piston pump is included the efficiency is not directly related to flow rate. The overall efficiency of the pressure exchanger with three combined double-acting cylinders reaches 88% for seawater desalination of $\mathrm{p_f^{out}} = 40\,\mathrm{bar}$ and $\mathrm{RR} = 20\%$, while the efficiency of the device for brackish water desalination is significantly lower, around 60% for $\mathrm{RR} = 20\%$ and around 40% for $\mathrm{RR} = 40\%$. The efficiency of the APM-driven piston pump is 61% for $\mathrm{Q_f} = 1.04\,\mathrm{m^3/h}$ and $\mathrm{p_f^{out}} = 60\,\mathrm{bar}$. The most efficient energy recovery concept, for both brackish and seawater desalination and for all examined flow rates, is the optimised pressure exchanger with two combined double-acting cylinders reaching the overall efficiency of 96% for $\mathrm{RR} = 20\%$ and $\mathrm{p_f^{out}} = 40\,\mathrm{bar}$ and 87% for $\mathrm{RR} = 20\%$ and $\mathrm{p_f^{out}} = 12\,\mathrm{bar}$.

6.2. Pressure requirements

As a result of the high efficiency provided, the optimised pressure exchanger with two combined double-acting cylinders also requires the lowest inlet feed pressure for both brackish and seawater desalination and all examined flow rates.

6.2.1. Pelton-driven generator

The required inlet feed pressure is estimated:

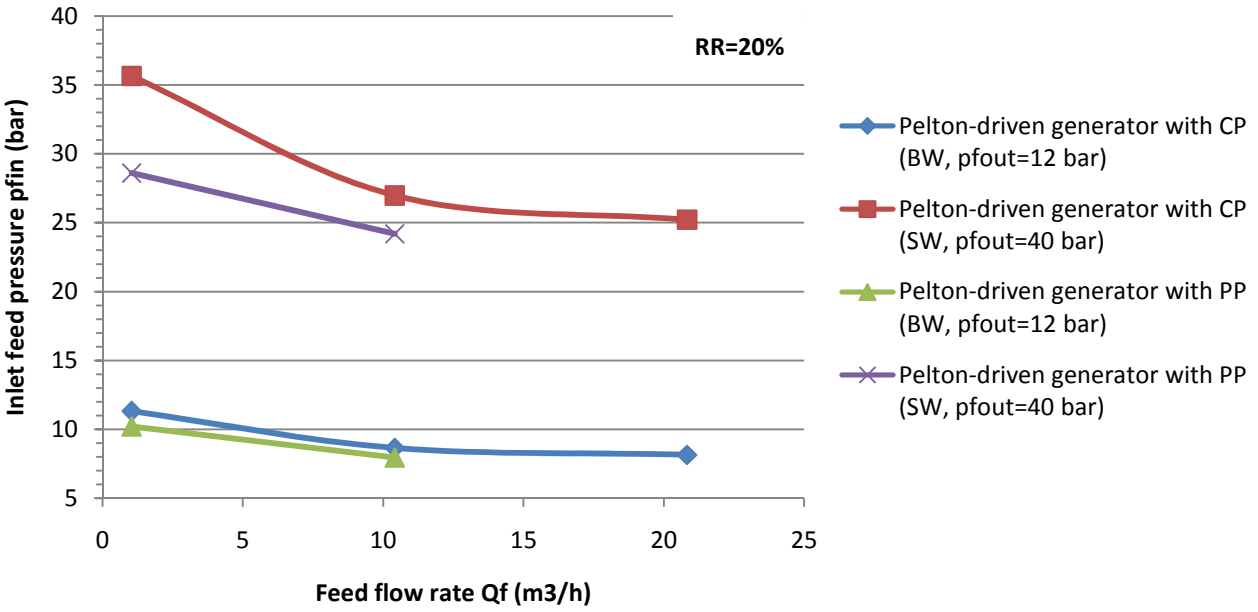

Figure 103: Inlet feed pressure for Pelton-driven generator with CP and PP (RR=20%)

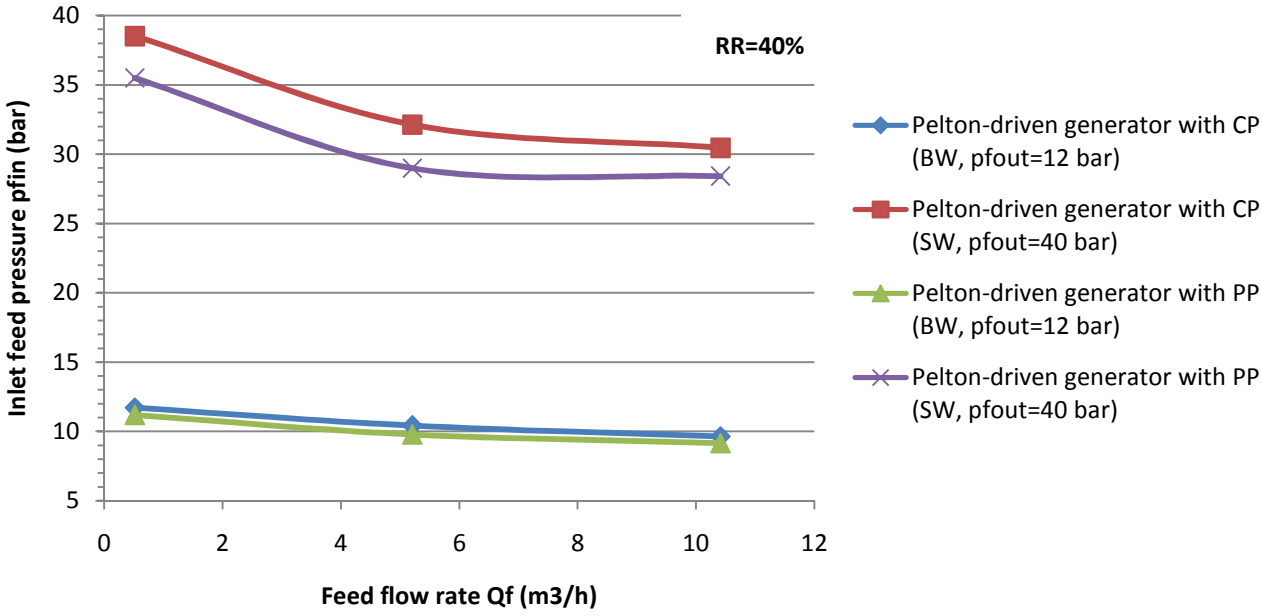

Figure 104: Inlet feed pressure for Pelton-driven generator with CP and PP (RR=40%)

6.2.2. Pelton-driven pump

The required inlet feed pressure for is estimated:

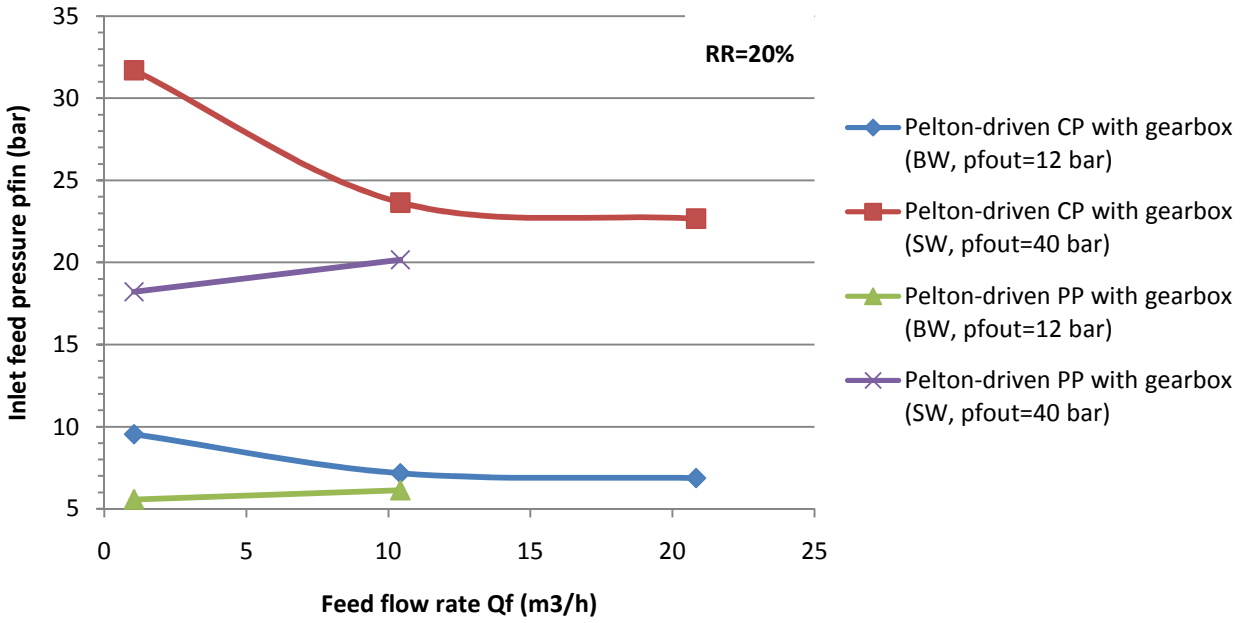

Figure 105: Inlet feed pressure for Pelton-driven CP and PP (RR=20%)

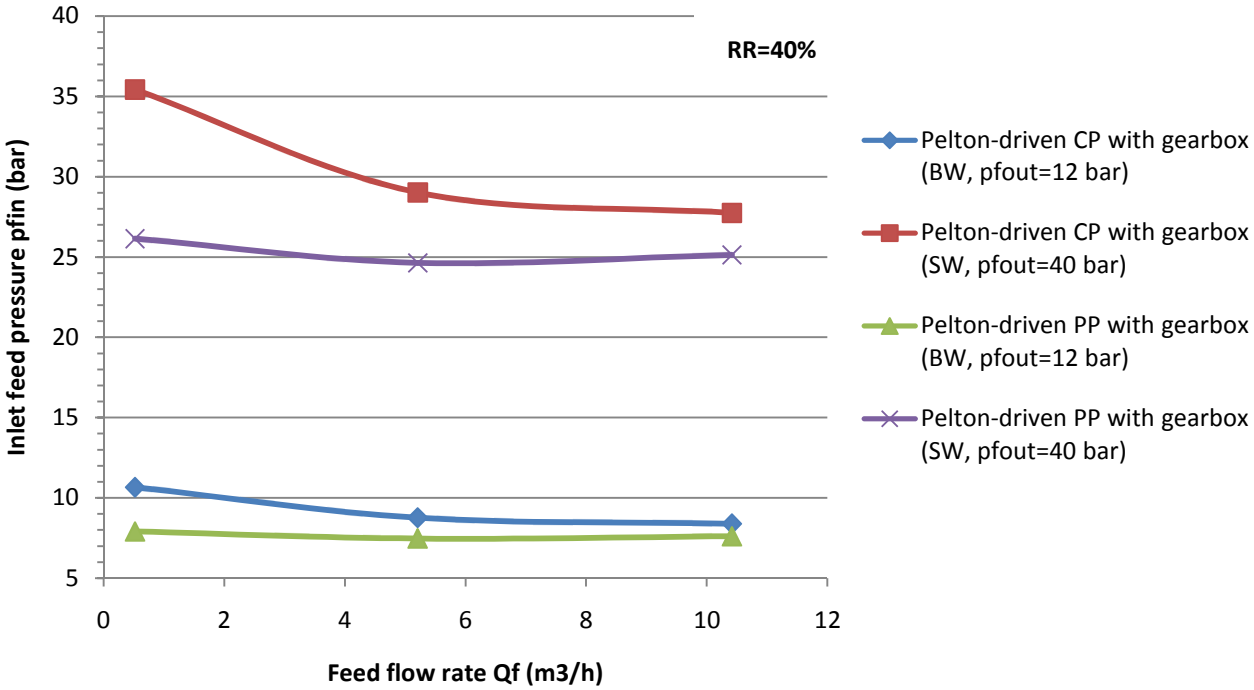

Figure 106: Inlet feed pressure for Pelton-driven CP and PP (RR=40%)

6.2.3. Pressure exchanger with two combined double-acting cylinders

The required inlet feed pressure and the pressure losses due to friction are estimated:

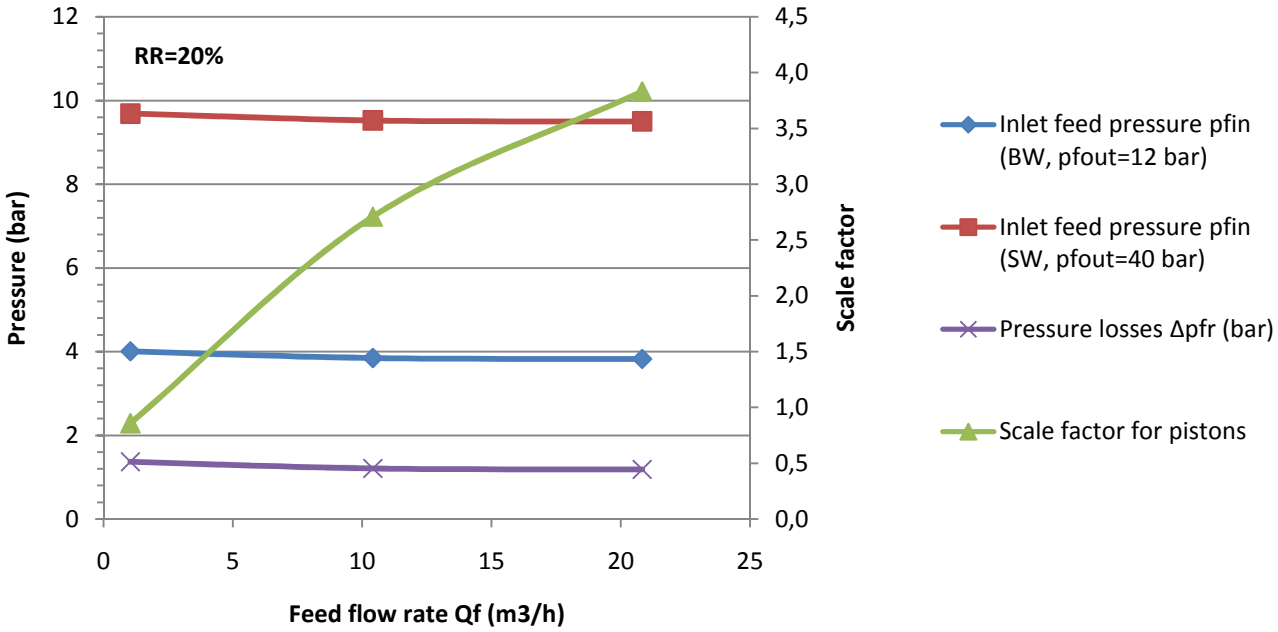

Figure 107: Inlet feed pressure required for BW and SW (RR=20%)

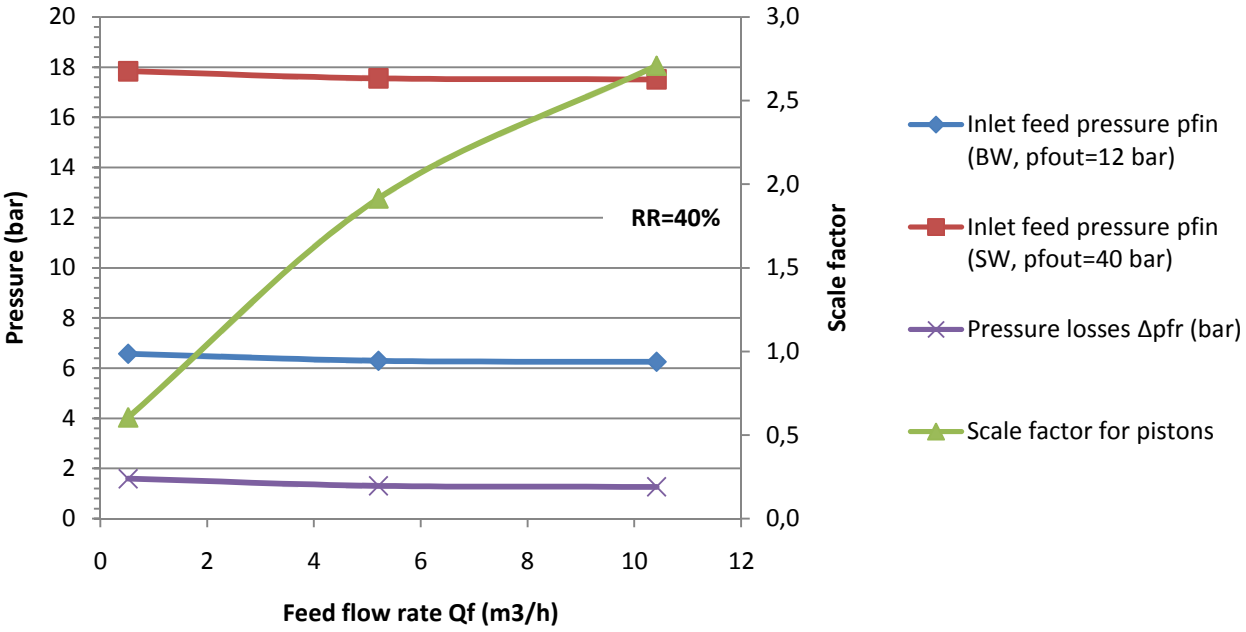

Figure 108: Inlet feed pressure required for BW and SW (RR=40%)

6.2.4. Pressure exchanger with three double-acting cylinders

The required inlet feed pressure and pressure losses due to friction are estimated:

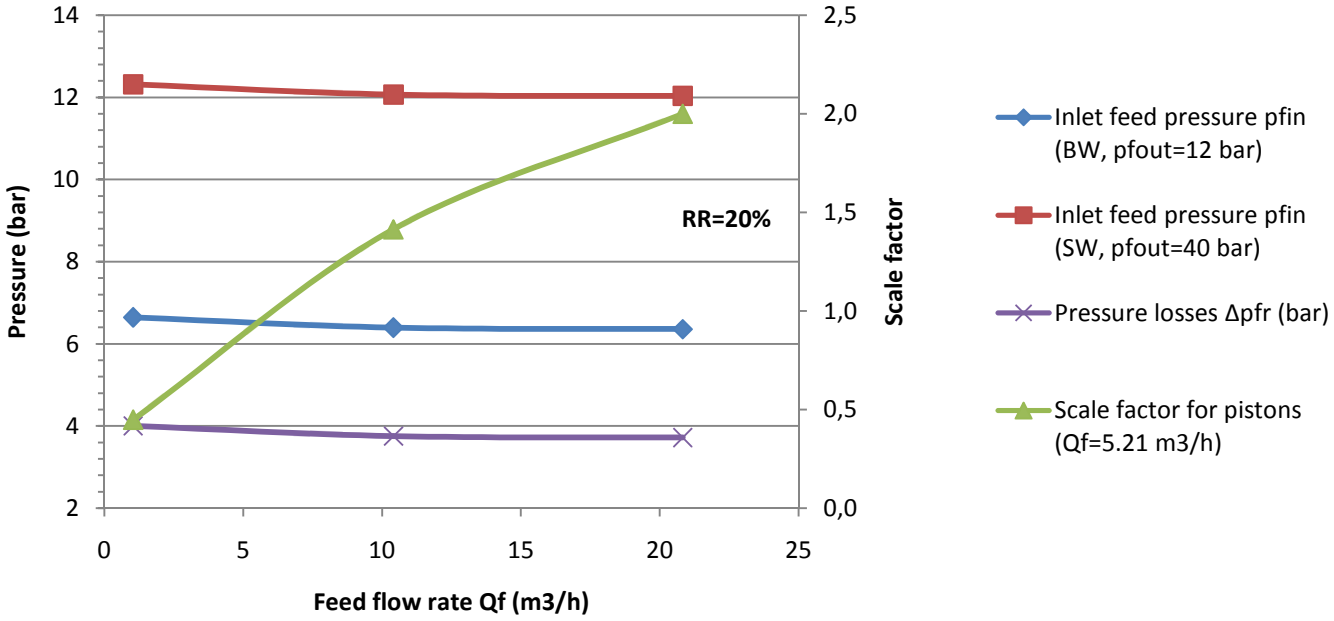

Figure 109: Inlet feed pressure for pressure exchanger with three combined double-acting cylinders (RR=20%)

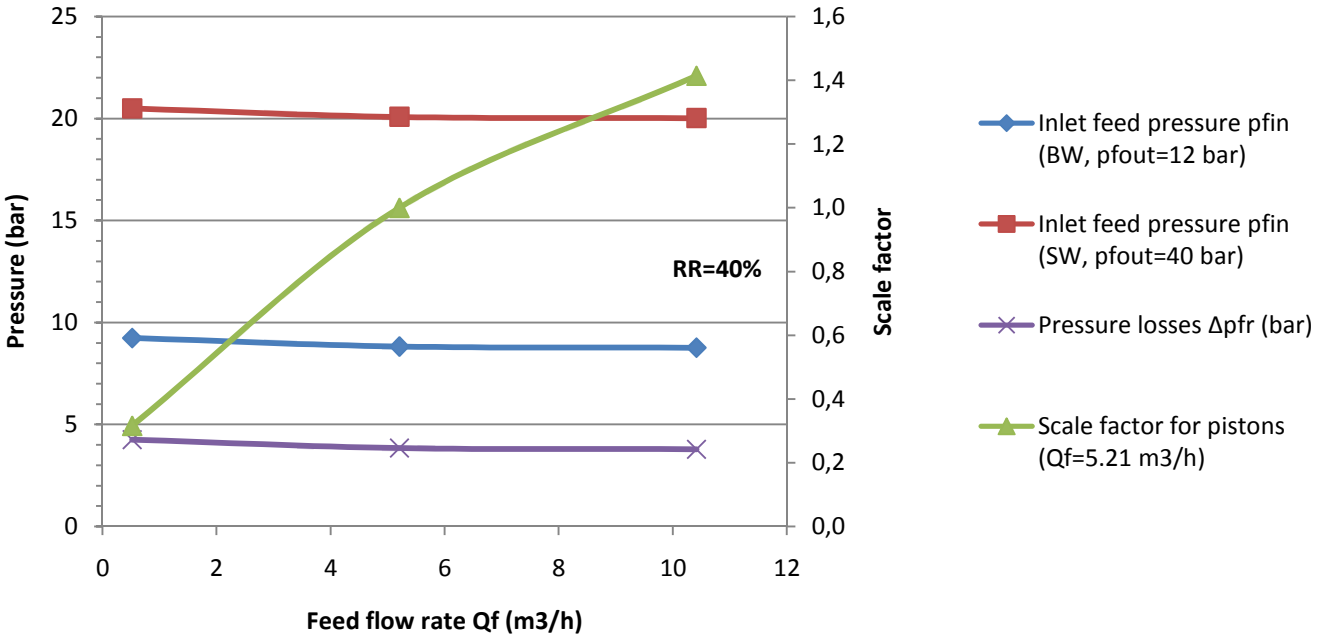

Figure 110: Inlet feed pressure for pressure exchanger with three combined double-acting cylinders (RR=40%)

6.2.5. Inverse positive displacement pump

The required inlet feed pressure is estimated:

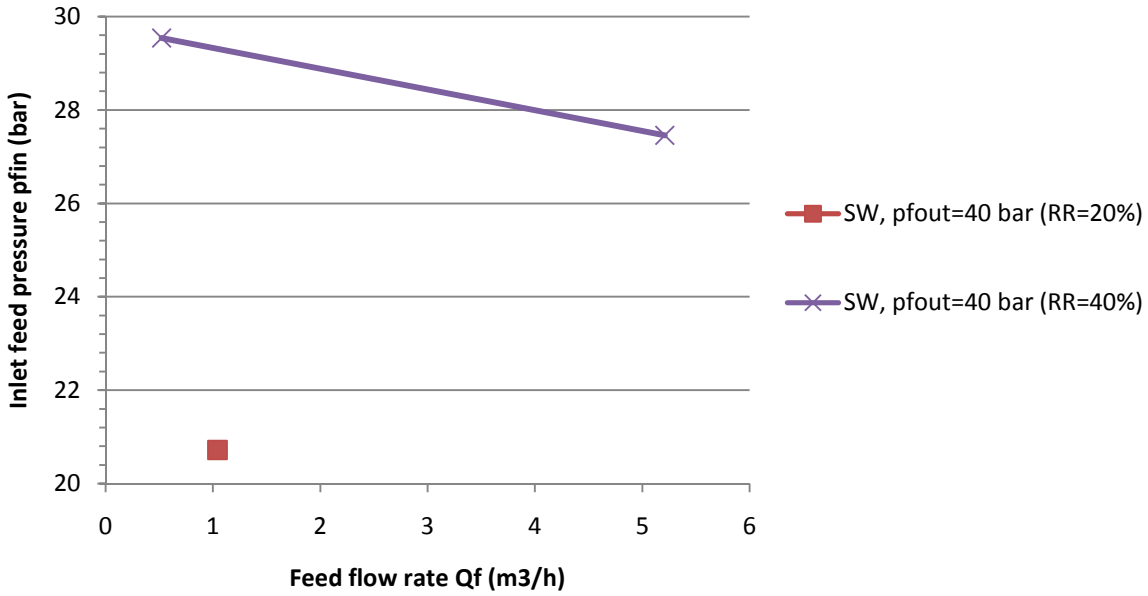

Figure 111: Inlet feed pressure for APM-driven piston pump for BW and SW

6.3. Energy autonomy

For the case of Pelton-driven ERDs the recovery ratio may need to be fixed, especially in the case of Pelton-driven generator where the pump and the Pelton turbine are not directly connected. In order to maintain the permeate flow rate at a specific value an electronically controlled valve that will direct the brine stream through an additional nozzle may be used, so additional energy will be required.

Pressure exchangers both with two and three cylinders rely on the principle of positive displacement and therefore provide constant recovery ratio and do not require additional energy. However, additional power supply may be required in order to control electronically the switching of the ERD in case the suggested mechanical switching proves to be inefficient. In the case of pressure exchanger with three cylinders the switching of the operation is supported by the interconnecting shaft of the cylinders.

In the case of the APM-driven piston pump the piston motor is directly coupled to the piston pump and since both components work on the principle of positive displacement the recovery ratio is constant and, hence, no additional power supply is required.

6.4. Operational stability

In the case of Pelton-driven ERDs external control of the operation may be required in order to fix the recovery ratio and therefore additional power supply may be needed.

In the case of pressure exchangers and the APM-driven pump, the recovery ratio is fixed and the operation of the ERD is self-regulated. For pressure exchangers only in case leakage or

switching problems occur external steering of the operation and, hence, additional power supply may be needed.

6.5. Cost analysis

The estimated costs of the examined energy recovery concepts are presented at the following table.

RR (%)	20			40		
Qf (m^3/h)	20.83	10.42	1.04	10.42	5.21	0.52
Pelton-driven gen. with CP	4,000	3,500	3,000	3,500	3,000	3,000
Pelton-driven gen. with PP	-	8,000	4,500	8,000	6,700	4,500
Pelton-driven CP with gearbox	3,200	2,700	2,200	2,700	2,200	2,200
Pelton-driven PP with gearbox	-	7,200	3,700	7,200	5,900	3,700
PX with two cylinders (BW)	7,992	5,278	1,568	5,113	3,471	1,059
PX with two cylinders (SW)	12,788	8,445	2,509	8,181	5,554	1,694
PX with three cylinders (BW)	5,000	3,536	1,118	3,536	2,500	791
PX with three cylinders (SW)	8,000	5,657	1,789	5,657	4,000	1,265
APM-driven pump	-	-	5,300	-	12,700	5,100

Table 94: Cost of the energy recovery concepts (€)

Due to the scale up of the optimised pressure exchanger with two combined double-acting cylinders required for high feed flow rates its price exceeds the price of other ERDs, especially for seawater desalination. For brackish water desalination and especially for low flow rate it remains competitive. Pelton-driven ERDs that include centrifugal pump are the cheapest options, while for low flow rate the pressure exchanger with three cylinders also maintains low cost. Pelton-driven ERDs that include piston pump are among the most expensive options together with the APM-driven pump due to the high estimated cost of piston pumps (and piston motors).

6.6. Manufacturing complexity

The optimised pressure exchangers require the manufacturing and assembly of resized components which may be more complex and time consuming than the assembly of the main components required for the other ERDs. However, Pelton-driven ERDs may require additional effort in order to regulate their operation while the operation of pressure exchangers and APM-driven pump is already regulated.

6.7. Proposed energy recovery concept

Consequently, the energy recovery concept that complies most efficiently with the above criteria is optimised pressure exchanger with two combined double-acting cylinders.

The operation of the optimised pressure exchanger with two combined double-acting cylinders relies on the principle of positive displacement. The ERD consists of two opposing cylinders with pistons connected on a single rod that passes through a centre block. A switching mechanism allows the cylinders to alternate between driving and pressurising. As

pressure in the driving cylinder is lower than the inlet feed pressure the non return valve opens and feed water enters in the driving cylinder. In the pressurising cylinder the non return valve opens when the pressure in the cylinder is higher than the pressure in the membranes. Pressure rise is achieved by directing the high pressure brine stream at the pressurising cylinder between the piston and the centre block. Permeate water is produced when the pressure is enough for RO to occur in the membranes. At the same time the low pressure brine stream, present in the other cylinder is discharged.

The proposed switching mechanism involves the use the feed stream through grooves within the rod and the centre block of the ERD in order to direct the brine stream to the required cylinder. As shown in the following figure, when the driving piston reaches the centre block the grooves on the rod align with the grooves of the centre block, allowing the feed stream to flow towards the valve that provides the required direction to the brine steam and enabling the discharge of the water present on the other side of the valve chamber.

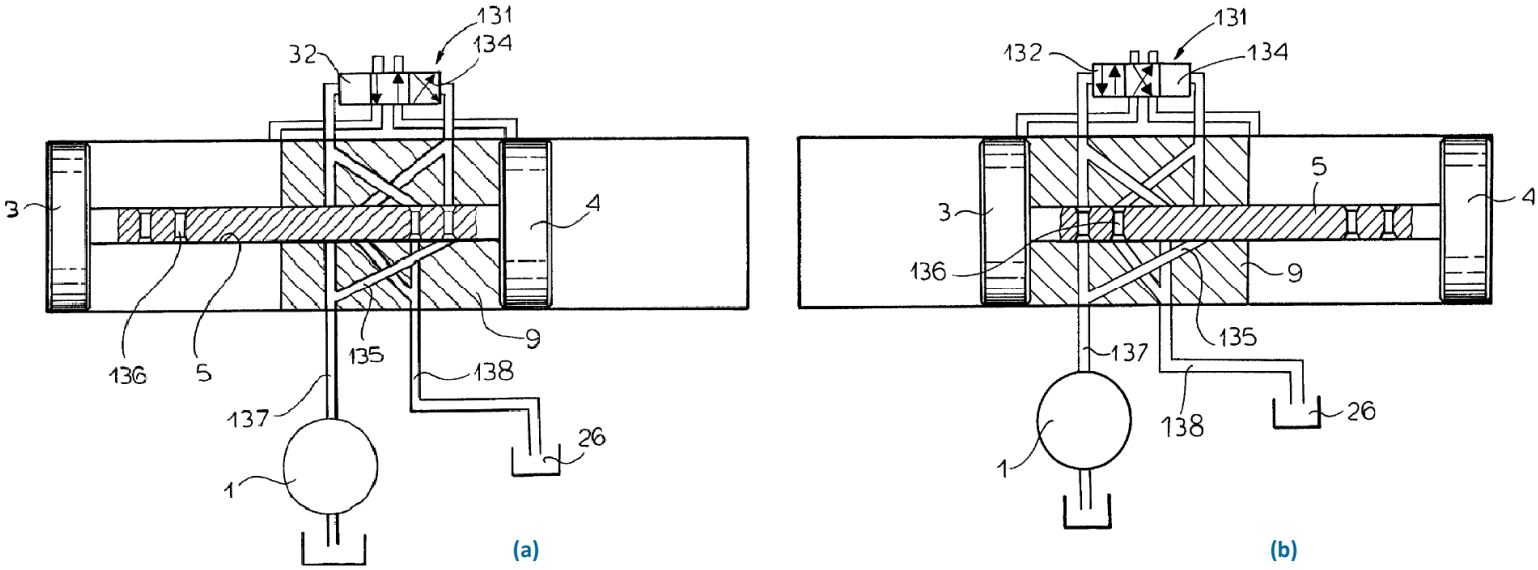

Figure 112: Schenker ERD switching mechanism (Schenker Italia S.R.L., 2001)

In order to deliver the required power output this energy recovery concept is scaled accordingly for the examined flow rates. Since the Schenker ERD is used as reference for the dimensions of the drawings, provided below, scale factor f1 is converted in order to refer to Schenker ERD. Scale factor f1 for the tubing, the switching mechanism and the check valves of the device and scale factor f2 for the pistons of the device (both with reference to the Schenker ERD) are presented subsequently, along with the derived piston diameter and the rod diameter.

Qp (m^3/h)	4.17	2.08	0.21	4.17	2.08	0.21
RR (%)	20%			40%		
Qf (m^3/h)	20.83	10.42	1.04	10.42	5.21	0.52
Scale factor f1	4.91	3.02	0.83	2.82	1.82	0.53
Scale factor f2	3.83	2.71	0.86	2.71	1.92	0.61
d (mm)	360	255	81	255	180	57
drod (mm)	161	114	36	161	114	36

Table 95: Scale factors and diameters of the optimised pressure exchanger with two double-acting cylinders

At the following table the characteristics of the Schenker ERD are presented.

Qp (m^3/h)	0.42
RR (%)	14.67
Qf (m^3/h)	1.42
d (mm)	94
drod (mm)	36

Table 96: Characteristics of the Schenker ERD

At the following figure the dimensions (mm) of the Schenker ERD are shown as a reference value for the size of the pistons of the optimised pressure exchanger with two combined double-acting cylinders.

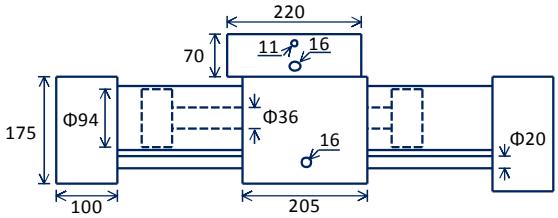

Figure 113: Schenker ERD

At the following figure the dimensions (mm) of the optimised pressure exchanger with two combined double-acting cylinders for $\mathrm{RR} = 20\%$ and $\mathrm{Q_f} = 10.42\,\mathrm{m^3/h}$ are presented.

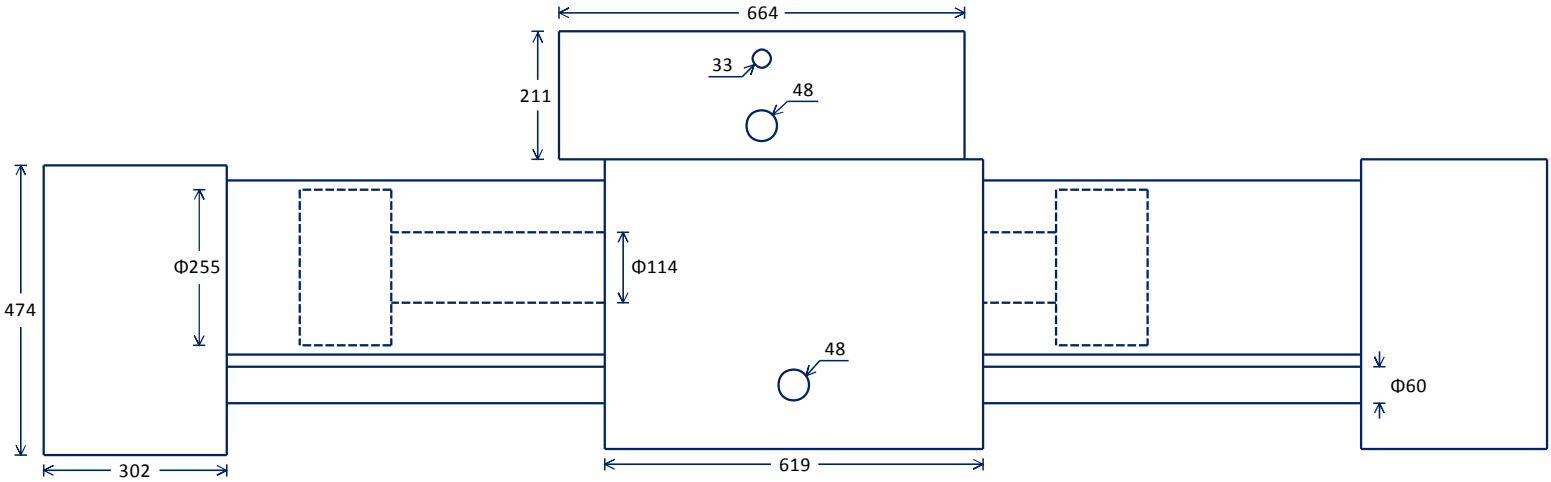

Figure 114: Optimised pressure exchanger with two combined double-acting cylinders (RR=20%)

At the following figure the dimensions (mm) of the optimised pressure exchanger with two combined double-acting cylinders for $\mathrm{RR} = 40\%$ and $\mathrm{Q_f} = 5.21\,\mathrm{m^3/h}$ are shown.

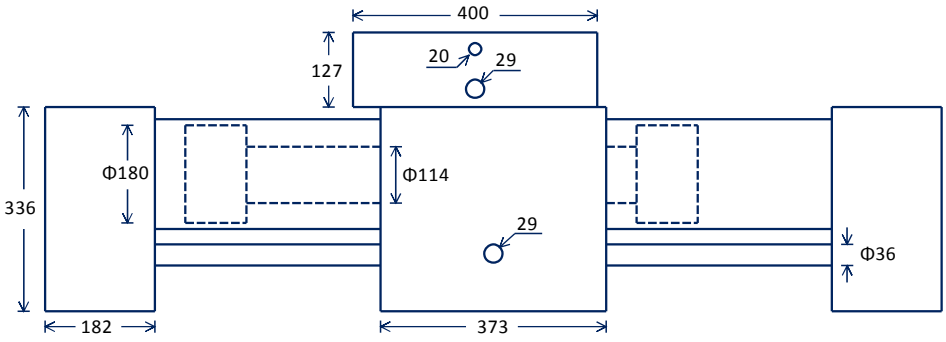

Figure 115: Optimised pressure exchanger with two combined double-acting cylinders (RR=40%)

7. Conclusions

The conclusions can be formulated as an answer to the main research question:

Which is the most efficient energy recovery concept for a small-scale autonomous renewable-driven reverse osmosis desalination system?

In order to tackle this problem the suggested subquestions have been examined:

Which are the energy recovery technologies currently available and what are their characteristics?

Both hydraulic to mechanical-assisted pumping and hydraulically driven pumping in series (turbochargers) include turbine-driven pumps and therefore are classified as centrifugal ERDs. Pelton turbines (impulse turbines) are more efficient than Francis turbines (reaction turbines). However, turbochargers include a reaction turbine. Turbochargers are more efficient than mechanical-assisted pumping since they do not include the turbine generator and the pump motor.

Pressure exchangers consist of piston isobaric ERDs and rotary isobaric ERDs. Piston isobaric ERDs are classified, according to their working principle, to single double-acting cylinder, two double-acting cylinders, three double-acting cylinders and two valve controlled cylinders ERDs. Piston isobaric ERDs deliver constant recovery ratio.

Pressure exchangers with a single double-acting cylinder, such as the PowerSurvivor (Katadyn), have capacity of 0.006-0.013 m^3/h and claimed efficiency of 96-98.4%.

Pressure exchangers with two combined double-acting cylinders, such as the Clark Pump (Spectra Watermakers) and the Schenker Energy Recovery System (Schenker), are claimed to reach efficiency of 97% and deliver permeate flow rate between 0.02-0.20 m^3/h.

Pressure exchangers with three combined double-acting cylinders, such as the Pearson Pump (Spectra Watermakers), require inlet feed pressure between 0.69-1.72 bar and capacity of 0.16-0.79 m^3/h. The power consumption of the motor required for the operation of the Pearson Pump ranges from 0.46-2.29 kW.

Pressure exchangers with two valve-controlled cylinders, such as Dual Work Exchanger Energy Recovery (Calder), require electronically operated valves and a booster pump while they are claimed to reach efficiency of 98%.

Rotary isobaric ERDs, such as PX Pressure Exchanger (ERI, 2013) and iSave pressure exchanger (Danfoss, 2013), require the use of a booster pump deliver permeate flow rate in the range of 5-45 m^3/h and are claimed to reach efficiency higher than 90%.

Seawater pump with energy recovery device (SWPE) consists of an Axial Piston Pump (APP) and an Axial Piston Motor (APM), both connected to a double shafted electric motor (Danfoss, 2013). As both the APM and the APP have fixed volumetric displacement, the recovery ratio is fixed and the flow rate increases with higher rotational speed of the shaft. The SWPE requires inlet feed pressure between 0.5-5 bar and delivers permeate flow rate of 0.14-0.82 m^3/h. The power required by the electric motor ranges from 1.1 to 3 kW.

An overview of the characteristics of the aforementioned energy recovery technologies is provided at Table 3.

Which are the constraints set by the examined renewable-driven RO desalination system and which energy recovery technologies meet these requirements?

The constraints deriving from the examined renewable-driven RO desalination system are:

- Permeate flow rate in the range of 0.04-4.17 m^3/h
- Feed pressure between 8-60 bar
- Recovery ratio between 15-50%
- No additional power supply required

Turbine-driven generators, turbochargers and pressure exchangers with two combined double-acting cylinders comply with the examined system characteristics. Since the Pelton turbine efficiency is higher than the efficiency of the Francis turbine, the Pelton-driven generator and the Pelton-driven pump are further evaluated. In addition, the Pearson Pump and the Seawater pump with energy recovery device also meet the system requirements and they may have such working characteristics that in principle zero power consumption can be accomplished. Thus, both the pressure exchanger with three combined double-acting cylinders and the use of inverse positive displacement pump as a motor are further investigated.

Which energy recovery concepts are suggested for these requirements and how do they comply with the criteria set?

The proposed energy recovery concepts are:

- Pelton-driven generator with centrifugal pump or piston pump
- Pelton-driven centrifugal pump or piston pump with gearbox
- Pressure exchanger with two combined double-acting cylinders
- Pressure exchanger with three combined double-acting cylinders
- APM-driven piston pump

Their evaluation was based on energy efficiency, power and pressure requirements, energy autonomy, operational stability, cost effectiveness and manufacturing complexity for the examined operating range.

In more detail, the Pelton-driven piston pump with gearbox has the highest overall efficiency among the examined Pelton-driven energy recovery concepts. The efficiency of the Pelton-driven ERDs that include a centrifugal pump drops with lower flow rate, while in the case a piston pump is included the efficiency is not directly related to flow rate. The overall efficiency of the pressure exchanger with three combined double-acting cylinders is high for seawater desalination, while the efficiency of the device for brackish water desalination is significantly lower. The efficiency of the APM-driven piston pump is lower than the efficiency of pressure exchangers but still higher than Pelton-driven concepts. The most efficient energy recovery concept, for both brackish and seawater desalination and for all examined flow rates, is the optimised pressure exchanger with two combined double-acting cylinders.

As a result of the high efficiency provided, the optimised pressure exchanger with two combined double-acting cylinders requires the lowest inlet feed pressure for both brackish and seawater desalination and all examined flow rates.

In terms of energy autonomy, for the case of Pelton-driven ERDs the recovery ratio may need to be fixed, especially in the case of Pelton-driven generator where the pump and the

Pelton turbine are not directly connected. In order to maintain the permeate flow rate at a specific value an electronically controlled valve that will direct the brine stream through an additional nozzle may be used, so additional energy will be required.

Pressure exchangers both with two and three cylinders rely on the principle of positive displacement and therefore provide constant recovery ratio and do not require additional energy. However, additional power supply may be required in order to control electronically the switching of the ERD in case the suggested mechanical switching proves to be inefficient. In the case of pressure exchanger with three cylinders the switching of the operation is supported by the interconnecting shaft of the cylinders.

In the case of the APM-driven piston pump the piston motor is directly coupled to the piston pump and since both components work on the principle of positive displacement the recovery ratio is constant and, hence, no additional power supply is required.

Regarding the operational stability, in the case of Pelton-driven ERDs external control of the operation may be required in order to fix the recovery ratio and therefore additional power supply may be needed.

In the case of pressure exchangers and the APM-driven pump, the recovery ratio is fixed and the operation of the ERD is self-regulated. For pressure exchangers only in case leakage or switching problems occur external steering of the operation and, hence, additional power supply may be needed.

Due to the scale up of the optimised pressure exchanger with two combined double-acting cylinders required for high feed flow rates its price exceeds the price of other ERDs, especially for seawater desalination. For brackish water desalination and especially for low flow rate it remains competitive. Pelton-driven ERDs that include centrifugal pump are the cheapest options, while for low flow rate the pressure exchanger with three cylinders also maintains low cost. Pelton-driven ERDs that include a piston pump are among the most expensive options together with the APM-driven pump due to the high estimated cost of piston pumps (and piston motors).

Finally, the optimised pressure exchangers require the manufacturing and assembly of resized components which may be more complex and time consuming than the assembly of the main components required for the other ERDs.

Which is the most applicable energy recovery concept according to the criteria set?

Consequently, the optimised pressure exchanger with two combined double-acting cylinders fulfils most adequately the criteria set. In order to deliver the required power output this energy recovery concept is scaled accordingly for the examined flow rates. The proposed switching mechanism involves the use the feed stream through grooves within the rod and the centre block of the ERD in order to direct the brine stream to the required cylinder.

8. Recommendations

Regarding the optimised pressure exchanger with two combined double-acting cylinders it is possible that the proposed switching mechanism may result to high hydraulic pressure losses due to the narrow grooves required and therefore another switching principle may be considered. In this context, the switching mechanism may include a reversing valve as the one used in the Clark Pump (Paragraph 3.2.1.2). In this case, when the inner surface of the driving piston reaches the centre block, a pilot valve gets mechanically actuated and inverses the process instantly by moving the reversing valve. If high hydraulic losses are estimated also using this mechanism, it is suggested that the direction of the pistons is inversed electronically. Therefore, hydraulic losses due to switching are avoided and minor additional power consumption is required.

Furthermore, in the case of the optimised pressure exchanger with three combined double-acting cylinders it has been assumed that hydraulic pressure losses are 3.58 bar for all examined flow rates and the required scale factor for the tubing, the switching mechanism and the valves of the ERD has not been estimated. Thus, it is suggested that a model describing the hydraulic pressure losses of the pressure exchanger with three combined double-acting cylinders is developed so that the required scaling of the ERD for hydraulic pressure losses of 3.58 bar is estimated. In this sense, it can be assessed what are the lowest hydraulic losses achieved within feasible scaling of the ERD for the examined flow rates.

Finally, in the case of both optimised pressure exchangers it has been proposed that the devices scale accordingly in order to respond to the examined flow rates. This suggestion aims to further reduce the pressure losses of the device and hence deliver high efficiency at high flow rates as well as maintaining as low as possible the cost of the device. In case the resizing of the device is considered a complex procedure, multiple pressure exchangers can be connected in parallel in order to respond to high flow rates. However, significantly higher costs will occur, the efficiency of the energy recovery system will remain the same for all flow rates while the recovery ratio and the flow rate of the process will be restricted to the values of the used pressure exchanger.

9. Appendix

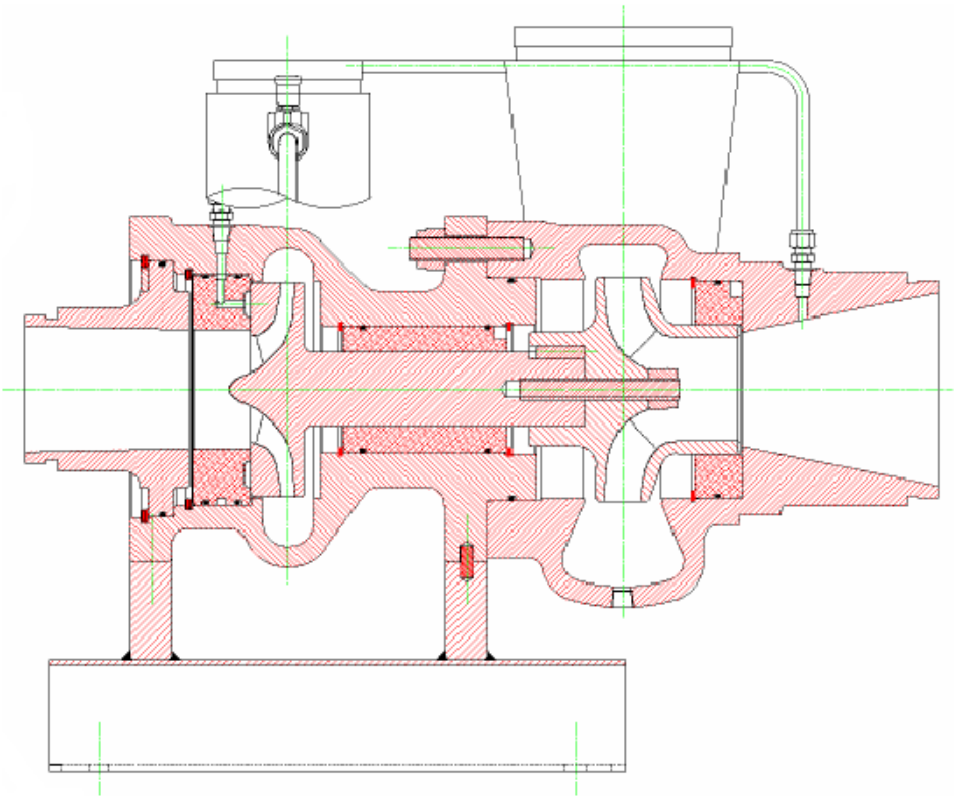

Figure 116: ERI Turbocharger LPT-1000 drawing

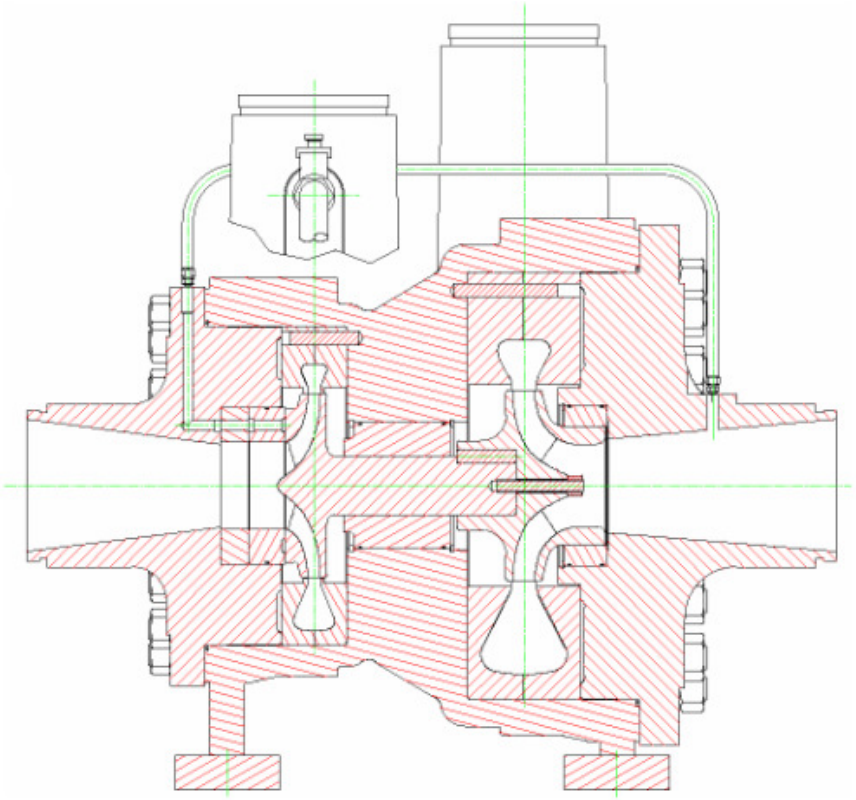

Figure 117: ERI Turbocharger AT-4800 drawing

10. References

Eco-Sistems Watermarkers S.L. 2013. [Online] 2013. http://www.eco-sistems.com/.

Agar, D. and Rasi, M. 2008. On the use of a laboratory-scale Pelton wheel water turbine in renewable energy education. *Renewable Energy.* 2008, 33, pp. 1517-1522.

Al-Karaghouli, A., Renne, D. and Kazmerski, L.L. 2009. Solar and wind opportunities for water desalination in the Arab regions. *Renewable & Sustainable Energy Reviews.* 2009, Vol. 13, 9, pp. 2397-2407.

Aqualyng. 2009. *http://www.aqualyng.com/en/Home.aspx.* [Online] 2009.

B., Ibbotson. 2010. *The Effects of Fluctuating Operation on Reverse Osmosis Membranes.* Delft : Delft University of Technology & University of South Australia, 2010.

Beerens, Jeroen. 2012. *Dynamic model of an energy recovery device.* 2012.

Bermudez-Contreras, A. and Thomson, M. 2009. Modified operation of a small scale energy recovery device for seawater reverse osmosis. *European Desalination Conference: Desalination for the Environment - Clean Water and Energy.* 2009.

Big Brand Water Filter. 2013. [Online] 2013. http://www.bigbrandwater.com/danfoss9.html.

Bradfield, Mike. 2008. *Improving Alternator Efficiency Measurably Reduces Fuel Costs.* s.l. : Remy, Inc, 2008.

Brook Crompton. 2013. Brook Crompton AC Motors. [Online] 2013. http://www.brookcrompton.com/pages/products.html.

Calder. 2013. *www.flowserve.com.* [Online] 2013.

Charcosset, C. 2009. A review of membrane processes and renewable energies for desalination. *Desalination.* 2009, 245, pp. 213-214.

Childs, W. D., et al. 1999. VARI-RO solar-powered desalting technology. *Desalination.* 125, 1999, pp. 155-166.

Contreras, Alfredo Sergio Bermudez. 2009. *An energy recovery device for small-scale seawater reverse osmosis desalination.* s.l. : Loughborough University, 2009. Doctoral Thesis.

Danfoss. 2013. [Online] 2013. http://www.danfoss.com/Solutions/Reverse+Osmosis/.

Dixon, S.L. 2005. *Fluid Mechanics and Thermodynamics of Turbomachinery.* Fifth Edition. Burlington : Elsevier Butterworth-Heinemann, 2005.

Duijvelaar Pompen. 2013. [Online] Duijvelaar Pompen, 2013. http://www.dppumps.com/.

El-Dessouky, H.T. and Ettouney, H.M. 2002. Fundamentals of Salt Water Desalination. *Elsevier.* 2002.

Eltawil, M.A., Zhengming, Z. and Yuan, L.Q. 2009. A review of renewable energy technologies integrated with desalination systems. *Renewable & Sustainable Energy Reviews.* 2009, Vol. 13, 9, pp. 2245-2262.

ERI. 2013. *www.energyrecovery.com.* [Online] Energy Recovery Inc., 2013.

ERIKS. 2013. [Online] 2013. http://eriks.nl/nl/home/.

Farooque, A.M., Jamaluddin, A.T.M. and Al-Reweli, A.R. 2008. Comparative Study of Various Energy Recovery Devices used in SWRO process. *Saline Water Desalination Research Institute.* 2008.

Faulhaber, Fritz. 2002. A second look at Gearbox efficiencies. [Online] 2002. http://machinedesign.com/.

FEDCO. 2013. [Online] Fluid Equipment Development Company, 2013. http://www.fedco-usa.com/.

Feenstra, R. and Vollebregt, S. 2012. *Autonomous Photovoltaic Powered Continuous Desalination using Reverse Osmosis including Energy Recovery Device.* 2012.

Gkeredaki, Evangelia. 2011. *Autonomous photovoltaic powered seawater reverse osmosis forremote coastal areas.* 2011. MSc. Thesis.

Grundfos A/S. 2013. *www.grundfos.com.* [Online] 2013.

Guirguis, Mageed Jean. 2011. *Energy Recovery Devices in Seawater Reverse Osmosis Desalination Plants with Emphasis on Efficiency and Economical Analysis of Isobaric versus Centrifugal Devices.* University of South Florida. 2011. Graduate School Theses and Dissertations.

Heijman, S.G.J., et al. 2010. Sustainable seawater desalination: Stand-alone small scale windmill and reverse osmosis system. *Desalination.* 2010, 251, pp. 114-117.

HYDROLOGY. 2013. [Online] 2013. http://www.hydrology-shop.gr/grundfos-en/pumps-grundfos/piston-pumps-grundfos.html.

IDA. 2012. Desalination Overview. [Online] International Desalination Association, 2012. http://www.idadesal.org/.

Karassik, I.J., et al. 2008. *Pump Handbook, Fourth Edition.* 2008.

Katadyn. 2013. [Online] 2013. http://www.katadyn.com/en/katadyn-products/products/katadynshopconnect/katadyn-entsalzer-powersurvivors/.

KSB. 2013. *http://www.ksb.com/.* [Online] KSB Aktiengesellschaft, 2013.

Lattemann, S., et al. 2010. Chapter 2 Global Desalination Situation. *Sustainability Science and Engineering.* 2010, Vol. 2, pp. 7-39.

Liberman, Boris. 2010. *The importance of energy recovery devices in reverse osmosis desalination.* s.l. : IDE Technologies Ltd., 2010.

LyngAgua, S.L. and Barranco del Lechugal, A.T. 2001. Aqualyng a new system for SWRO with pressure. *Desalination.* 139, 2001.

MacHarg, J.P. 2002. The Evolution of SWRO Energy-Recovery Systems. *Desalination & Water Reuse.* 2002, Vol. 11, 3, p. 48.

Rodriguez, Luis and Sanchez, Teodoro. 2011. *Designing and Building Mini and Micro Hydropower Schemes: A Practical Guide.* s.l. : Practical Action Publishing, 2011.

Schenker. 2012. [Online] 2012. http://www.schenker.it/en/home.php.

Schenker Italia S.R.L. 2001. *Equipment for desalination of water by reverse osmosis with energy recovery.* 2001. Patent Publication No. US2001/0017278 A1.

Sea Recovery Corp. 2013. [Online] 2013. http://www.searecovery.com/marine/.

Shaligram, Satish. 2011. Brackish water: Energy, costs and the use of energy recovery devices. *Filtration and Separation.* 2011, pp. 28-30.

Smith, Nigel. 2008. *Motors as Generators for Micro-Hydro Power.* s.l. : Intermediate Technology Publication, 2008.

Snieder, J. and Stubbé, S. 2013. *Reverse Osmosis Desalination with Energy Recovery Device for Brackish Water.* 2013.

Spectra Watermakers, Inc. 2013. *http://www.spectrawatermakers.com/.* [Online] 2013.

Spellman, F.R. and J., Drinan. 2001. *Pumping.* s.l. : Technomic, 2001.

Stover, R. 2007. Seawater reverse osmosis with isobaric energy recovery devices. *Desalination.* 203, 2007, pp. 168-175.

Stover, R.L. 2006. Energy Recovery Devices for Seawater Reverse Osmosis. *Everything About Water.* 2006.

Sulzer Ltd. 2013. *http://www.sulzer.com/.* [Online] 2013.

Tamar. 2012. *http://www.southerncross.pentair.com/.* [Online] 2012.

Thake, J. 2000. *The Micro-hydro Pelton Turbine Manual: Design, Manufacture and Installation for Small-scale Hydropower.* s.l. : ITDG Publishing, 2000.

Verberk, J.Q.J.C., et al. 2009. Drinking water treatment. *Sanitary Engineering Department, Civil Engineering and Geosciences, TUDelft.* 2009, p. 14.

Walvoort, D.F. 2013. *New design for an ERD.* 2013.

Wasserkraft Volk AG. 2010. *http://www.wkv-ag.com/index.php.* [Online] 2010.

Went, J., et al. 2010. The energy demand for desalination with solar powered reverse osmosis units. *Desalination and Water Treatment.* 2010.